5-1978

Engineering Properties, and Slope Stability and Settlement Analysis Related to Phosphate Mine Spoil Dumps in Southeastern Idaho

Richard Ellsworth Riker
Utah State University

ENGINEERING PROPERTIES, AND SLOPE STABILITY AND SETTLEMENT ANALYSIS RELATED TO PHOSPHATE MINE SPOIL DUMPS IN SOUTHEASTERN IDAHO

by

Richard Ellsworth Riker

A thesis submitted in partial fulfillment
of the requirements for the degree

of

MASTER OF SCIENCE

in

Engineering

UTAH STATE UNIVERSITY
Logan, Utah

1978

ENGINEERING PROPERTIES, AND SLOPE STABILITY AND

SETTLEMENT ANALYSIS RELATED TO PHOSPHATE MINE SPOIL DUMPS

IN SOUTHEASTERN IDAHO

by

Richard Ellsworth Riker, Master of Science

Utah State University, 1978

Major Professor: Dr. Loren R. Anderson
Department: Civil and Environmental Engineering

ACKNOWLEDGEMENTS: The work carried out during this study was initiated under a cooperative agreement between the U.S. Forest Service and the Utah Water Research Laboratory and constitutes a contribution to the efforts of SEAM (Surface Environment and Mining).

The writer would like to express appreciation to Dr. Loren R. Anderson who served as a major professor and as a co-principal investigator. His patience and guidance deserves a special thank you.

The writer would also like to thank Dr. Roland W. Jeppson who served as Project Director and committee member. Appreciation is also extended to Dr. Fred Kiefer, for his support and guidance and to Mr. Rene Winward, for his help and skill with building the necessary laboratory equipment.

Finally, I wish to extend appreciation to both my wife, Debbie, and my parents to whom I owe many thanks for their support throughout this endeavor.

Richard Ellsworth Riker

ABSTRACT: The engineering properties of waste spoil from phosphate mines in Southeastern Idaho were determined through field and laboratory testing. The testing included compaction tests, grain size analysis, powder x-ray defraction tests, permeability tests, compression tests, triaxial and direct shear strength tests, and nutrient analyses. Based on these tests, the slope stability and settlement characteristics of phosphate spoil dumps were investigated.

The study showed that the foundation is an important component of the stability of a spoil dump. Hypothetical examples were used to illustrate possible modes of foundation failures. Such failures might occur when weak foundation soils exist or when there is a lack of embankment-foundation preparation prior to the disposal of waste material. When considering failures through only the middle waste shale embankment material, the study showed that dumps constructed by end-dumping the spoil material over angle of repose embankments or by scraper filling the material in horizontal lifts will be adequately safe against slope failure if:

- o Embankment slopes are graded to 2½ horizontal to 1 vertical or flatter.
- o Proper precautions are taken to prevent the build-up of a phreatic surface near the top of the embankment.

The study also showed that post construction settlement in spoil dumps can be attributed to:

- o A slow continuing settlement which is linear with the log of time.
- o Saturation collapse settlement which occurs with increases in the moisture contents.

Post construction settlement in spoil dumps is caused principally by increases in the moisture content in layers of middle waste shales and soft cherts.

A rationale method for predicting magnitudes of post construction settlement in spoil dumps was also developed as part of this study.

(117 pages)

TABLE OF CONTENTS

Chapter		Page
I	INTRODUCTION	1
	Importance of the Western Phosphate Fields	1
	History of the Southeast Idaho Phosphate Mines	1
	Scope of this Investigation	1
	Spoil Dump Construction Methods	2
	Geologic Setting	2
II	REVIEW OF LITERATURE	9
	Methods for Disposing of Mining Wastes	9
	Current coal waste disposal practices	9
	Current phosphate waste disposal practices in Southeast Idaho	11
	Compaction and Soil Properties	11
	Properties of compacted cohesionless soils	11
	Properties of compacted cohesive soils	12
	Methods of Stability Analysis	13
	Limiting equilibrium methods	13
	Total and effective stress methods	14
	General Considerations Regarding Settlement of Earth and Rockfill Structures	15
	Stability of Coal Waste Embankments	15
III	FIELD AND LABORATORY TESTING	17
	Purpose and Types of Tests	17
	Sampling	17
	Description and Use of Tests	17
	Classification tests	17
	Compaction tests	21
	Permeability tests	22
	Compression tests	23
	Shear strength tests	23
	Nutrient tests	27
	Results of the Field and Laboratory Tests	27
	Classification tests	27
	Relative compaction tests	27
	Permeability tests	36
	Compression tests	38
	Shear Strength tests	44
	Nutrient tests	66
IV	SLOPE STABILITY	69
	Identification of Problem	69
	General Foundation Considerations	69

TABLE OF CONTENTS (Continued)

Chapter		Page
	Field investigations	69
	Weak foundations	70
	Foundation preparation	71
	Summary of foundation considerations	73
		7
	Embankment Considerations	73
	Acceptable factors of safety	73
	Short-term stability	74
	Long-term stability	74
	Results for phreatic surface condition	78
	The South Maybe Dump Landslide	79
V	POST CONSTRUCTION SETTLEMENT	80
	Identification of the Problem	80
	Settlement in Spoil Dumps	80
	Compression from added fill weight	80
	Saturation collapse settlement	80
	Predicting Post Construction Settlement	81
	Creep settlement	81
	Saturation collapse settlement	81
	Example problem	84
	Summary of Post Construction Settlement	87
VI	CONCLUSIONS AND RECOMMENDATIONS	88
	Classification and Engineering Properties	88
	Spoil classification	88
	Engineering properties	88
	Slope Stability	89
	Post Construction Settlement	89
LITERATURE CITED		93
APPENDIX A:	STRAIN LOG TIME CURVES FOR CHERT AND WASTE SHALE MATERIAL	95

LIST OF FIGURES

Figure		Page
I-1	Illustration of free flowing method of construction	2
I-2	Illustration of scraper filled method of construction	2
I-3	Phosphate region of southeast Idaho (excluding the Fort Hall Indian Reservoir)	3
I-4	Principal phosphate deposts of Southeastern Idaho	4
I-5	Location of Wooley Valley and Maybe Canyon Mines	5
I-6	Typical folding of beds in the Phosphoria Formation	6
I-7	Geologic sequence at Maybe Canyon	7
I-8	Section of the Meade Peak Phosphatic Shale member of the Phosphoria Formation at Maybe Canyon	8
II-1	Plan and section views of A B-E 1950-B pit (after Stefanko et al. 1973)	10
II-2	Relative density vs. tangent ϕ for cohesionless soils (after USBR, 1974)	12
II-3	Unconfined compressive strength and unconsolidated undrained strength characteristics of Higgins Clay (after Lee and Haley, 1968)	13
II-4	Various methods of slope stability analysis (after Whitman and Baily, 1966)	14
III-1	Sampling location North Maybe Canyon Dump	18
III-2	Sampling locations Wooley Valley Dump No. 6	18
III-3	Unified soil classification chart (after Bureau of Reclamation, 1960)	20
III-4	Engineering use chart for soils (after Department of Interior, Bureau of Reclamation, 1960)	21
III-5	Proctor cylinder (1/30 ft^3 volume (9.40 x 10^{-4} m^3)) and 5.5 lb (24.47 N) hammer	24
III-6	Moisture density relationship typical of cohesive soils also showing the effect of increased compaction effort	22
III-7	Moisture density relationship typical of clean cohesionless soils	22
III-8	Sand cone apparatus for determining the in-place dry unit weight	24
III-9	Constant head permeameters	24
III-10	Schematic diagram of compression test	23
III-11	4.4 in (1.12 x 10^{-1} m) diameter fixed ring consolidometer and loading frame	24
III-12	Triaxial testing apparatus also showing back pressure device	25
III-13	Direct shear testing apparatus	25
III-14	Illustration of the direct shear test (after Dunn, Anderson and Kiefer, 1976)	25
III-15	Failure envelope established from direct shear testing (after Dunn, Anderson, and Kiefer, 1976)	25

LIST OF FIGURES (Continued)

Figure		Page
III-16	Failure envelope shown tangent to Mohr's circles from three triaxial shear tests (after Dunn, Anderson and Kiefer, 1976)	26
III-17	Total and effective strength envelopes from CU triaxial shear tests on a normally consolidated clay (after Dunn, Anderson, and Kiefer, 1976)	26
III-18	Grain size curves for top soil material obtained from the Wooley Valley erosion study plots, October 1975	28
III-19	Grain size curves for waste shale material obtained from the Wooley Valley erosion study plots, October 1975	29
III-20	Grain size curves for material obtained from the North Maybe Dump, April 13, 1976, and sample T-8a	30
III-21	Plasticity chart	32
III-22	Typical unit weight moisture content relationship for waste shale material (sample S-1a) as determined by ASTM-D 698-64T, Method C (1 lb/ft^3 = 0.157 kN/m^3)	34
III-23	Illustration of percent area receiving wheel compaction assuming drivers use same tracks for every dumping pass (1 ft = 0.305 m)	34
III-24	Time versus compression characteristics of soft chert showing effect of saturation after reaching a stress level of 32,000 lb/ft^2 (lb/ft^2 = .0479 kPa)	39
III-25	Strain log pressure relationship for soft chert showing effects of saturation at a stress level of 32,000 lb/ft^2 (1 lb/ft^2 = .0479 kPa)	40
III-26	Strain versus log pressure relationship for soft chert subjected to cycles of wetting and drying (1 lb/ft^2 = .0479 kPa)	40
III-27	Strain versus log pressure relationships for soft chert showing effects of saturation at a stress level of 32,000 lb/ft^2 (1 lb/ft^2 = .0479 kPa)	41
III-28	Strain versus log pressure relationship for soft chert subjected to cycles of wetting and drying (1 lb/ft^2 = .0479 kPa)	41
III-29	Strain versus log pressure relationships for soft chert (1 lb/ft^2 = .0479 kPa)	42
III-30	Strain versus log pressure relationship for soft chert showing effect of saturation at a stress level of 16,000 lb/ft^2 (1 lb/ft^2 = .0479 kPa)	42
III-31	Strain versus log pressure relationship for hard chert material subjected to cycles of wetting and drying (1 lb/ft^2 = .0479 kPa)	43
III-32	Strain versus log pressure relationship for hard chert showing effect of saturation at a stress level of 32,000 lb/ft^2 (1 lb/ft^2 = .0479 kPa)	43
III-33	Strain versus log pressure relationships for soft chert showing effects of moisture treatments (1 lb/ft^2 = .0479 kPa)	44
III-34	Time-compression characteristics of waste shale material compacted to 82.4% R.C.	45
III-35	Strain versus log pressure relationship for waste shale showing effect of saturation at a stress level of 500 lb/ft^2 (1 lb/ft^2 = .0479 kPa)	45

LIST OF FIGURES (Continued)

Figure		Page
III-36	Strain versus log pressure relationship for waste shale showing effect of saturation at a stress level of 2000 lb/ft^2 (1 lb/ft^2 = .0479 kPa)	45
III-37	Strain versus log pressure relationship for waste shale material showing effect of increasing the moisture content at low pressures (1 lb/ft^2 = .0479 kPa)	46
III-38	Strain versus log pressure relationship for waste shale showing effect of increasing the moisture content at low pressures (1 lb/ft^2 = .0479 kPa)	47
III-39	Strain versus log pressure relationship for top soil material compacted at 83.6% RC (1 lb/ft^2 = .0479 kPa)	48
III-40	Strain versus log pressure relationship for waste shale material compacted at 82.4% RC (1 lb/ft^2 = .0479 kPa)	49
III-41	Strain versus log pressure relationship for waste shale compacted at 96.4% RC (1 lb/ft^2 = .0479 kPa)	49
III-42	Load versus deflection curves from direct shear tests on hard chert (1 lb = 4.45 N)	51
III-43	Mohr's failure envelope from direct shear tests on hard chert (1 lb/in^2 = 6.9 kPa)	51
III-44	Load versus deflection curves from direct shear tests on hard chert (1 lb = 4.45 N)	52
III-45	Mohr's failure envelope from direct shear tests on hard chert (1 lb/in^2 = 6.9 kPa)	52
III-46	Load versus deflection curves from direct shear tests on soft chert 1 lb = 4.45 N)	53
III-47	Mohr's failure envelope from direct shear tests on soft chert (1 lb/in^2 = 6.9 kPa)	53
III-48	Load versus deflection curves from direct shear tests on soft chert (1 lb = 4.45 N)	54
III-49	Mohr's failure envelope from direct shear tests on soft chert (1 lb/in^2 = 6.9 kPa)	54
III-50	Load versus deflection curves from direct shear tests on saturated samples of hard and soft cherts (1 lb = 4.45 N)	55
III-51	Mohr's failure envelope from direct shear tests on saturated samples of hard and soft cherts (1 lb/in^2 = 6.9 kPa)	55
III-52	Consolidated-undrained triaxial shear test stress-strain curves for partially saturated samples (1 lb/in^2 = 6.9 kPa)	56
III-53	Mohr's total stress failure envelope from consolidated-undrained triaxial shear tests on partially saturated samples (1 lb/in^2 = 6.9 kPa)	56
III-54	Consolidated-undrained triaxial shear test stress-strain curves for partially saturated samples (1 lb/in^2 = 6.9 kPa)	57
III-55	Mohr's total stress failure envelope from consolidated-undrained triaxial shear tests on partially saturated samples (1 lb/in^2 = 6.9 kPa)	57
III-56	Consolidated-undrained triaxial shear test stress-strain curves for partially saturated samples (1 lb/in^2 = 6.9 kPa)	58
III-57	Mohr's total stress failure envelope from consolidated-undrained triaxial shear tests on partially saturated samples (1 lb/in^2 = 6.9 kPa)	59

LIST OF FIGURES (Continued)

Figure		Page
III-58	Consolidated-undrained triaxial shear test stress-strain curves with pore pressure measurements (1 lb/in^2 = 6.9 kPa)	59
III-59	Consolidated-undrained triaxial shear test stress-strain curves with pore pressure measurements (1 lb/in^2 = 6.9 kPa)	60
III-60	Mohr's total stress failure envelope from consolidated-undrained triaxial shear tests with pore pressure measurements (1 lb/in^2 = 6.9 kPa)	61
III-61	Mohr's effective stress failure envelope from consolidated-undrained triaxial shear tests with pore pressure measurements (1 lb/in^2 = 6.9 kPa)	61
III-62	Consolidated-undrained triaxial shear test stress-strain curves with pore pressure measurements (1 lb/in^2 = 6.9 kPa)	62
III-63	Mohr's total stress failure envelope from consolidated-undrained triaxial shear tests with pore pressure measurements (1 lb/in^2 = 6.9 kPa)	63
III-64	Mohr's effective stress failure envelope from consolidated-undrained triaxial shear tests with pore pressure measurements (1 lb/in^2 = 6.9 kPa)	63
III-65	Consolidated-undrained triaxial shear test stress-strain curves with pore pressure measurements also showing unloading curve (1 lb/in^2 = 6.9 kPa)	64
III-66	Mohr's total stress failure envelope from consolidated-undrained triaxial shear tests with pore pressure measurements (1 lb/in^2 = 6.9 kPa)	65
III-67	Mohr's effective stress failure envelope from consolidated-undrained triaxial shear tests with pore pressure measurements (1 lb/in^2 = 6.9 kPa)	65
IV-1	Crack patterns associated with ground movement in cohesive material (after Ritchie, 1958)	70
IV-2	Cross-section of example problem illustrating the effect of weak foundation soils (1 ft = 0.305 m)	71
IV-3	Cross-section of example problem (surface foundation preparation) (1 ft = 0.305 m)	72
IV-4	Slope angle, relative compaction, and safety factor relationships for waste shale embankments during and immediately after construction	75
IV-5	Location of phreatic surface used in stability analysis (long-term case 2) for various embankment slopes in waste shales	76
IV-6	Contours of safety factors showing deep and shallow failures in waste shale embankments	77
IV-7	Slope angle, relative compaction and safety factor relationships for waste shale disposal facilities for long-term condition with no phreatic surface in the fill	78
IV-8	Slope angle, relative compaction, and safety factor relationships for waste shale disposal facilities for long-term severe condition with a phreatic surface near the surface of the embankment	79
V-1	Relationships between α_c and vertical stress for dry middle waste shale and top soil material (1 lb/ft^2 = .0479 kPa)	83

LIST OF FIGURES (Continued)

Figure		Page
V-2	Relationships between α_c and vertical stress for chert material (1 lb/ft^2 = .0479 kPa)	83
V-3	Saturation collapse settlement versus vertical stress for middle waste shale material (1 lb/ft^2 = 0.0479 kPa)	84
V-4	Saturation collapse settlement versus vertical stress for soft chert material (1 lb/ft^2 = 0.0479 kPa)	84
V-5	Typical cross-section at spoil dump used as example problem also showing predicted settlement profile (1 ft = 0.305 m)	85
A-1	Time-compression characteristics of soft chert subjected to cycles of wetting and drying (1 lb/ft^2 = .0479 kPa)	95
A-2	Time-compression characteristics of soft chert showing effects of saturation after reaching a stress level of 32,000 lb/ft^2 = .0479 kPa)	97
A-3	Time-compression characteristics of soft chert subjected to cycles of wetting and drying (1 lb/ft^2 = .0479 kPa)	98
A-4	Time-compression characteristics of soft chert (1 lb/ft^2 = .0479 kPa)	99
A-5	Time-compression characteristics of soft chert showing effect of saturation after reaching of stress level of 16,000 lb/ft^2 (1 lb/ft^2 = .0479 kPa)	100
A-6	Time-compression characteristics of hard chert subjected to cycles of wetting and drying (1 lb/ft^2 = .0479 kPa)	101
A-7	Time-compression characteristics of hard chert showing effect of saturation after reaching a stress level of 32,000 lb/ft^2 (1 lb/ft^2 = .0479 kPa)	102
A-8	Time-compression characteristics of waste shale material showing effect of saturation at a stress level of 500 lb/ft^2 (1 lb/ft^2 = .0479 kPa)	103
A-9	Time-compression characteristics of waste shale showing effect of saturation at a stress level of 2000 lb/ft^2 (1 lb/ft^2 = .0479 kPa)	104
A-10	Time-compression characteristics of waste shale showing effect of the addition of minor quantities of water at a stress level of 2000 lb/ft^2 (1 lb/ft^2 = .0479 kPa)	105
A-11	Time-compression characteristics of waste shale showing the effect of the addition of minor quantities of water at a stress level of 2000 lb/ft^2 (1 lb/ft^2 = .0479 kPa).	106
A-12	Time-compression characteristics of waste shale material compacted to 96.4% R.C. (1 lb/ft^2 = .0479 kPa)	107
A-13	Time-compression characteristics of top soil material compacted to 83.6% R.C. (1 lb/ft^2 = .0479 kPa)	108

LIST OF TABLES

Table		Page
II-1	Limiting equilibrium methods and equilibrium conditions (after Duncan; class notes)	15
III-1	Sample numbering system	19
III-2	Common indexes of grain size distributions	31
III-3	Summary of specific gravities	31
III-4	Summary of in-place unit weight tests	33
III-5	Summary of compaction tests (ASTM-D 698-64T, Method C)	35
III-6	Summary of permeabilities	36
III-7	Cross-sectional areas of frech drain for various assumed depths of water	37
III-8	Estimates of flow rate that the french drain might be expected to pass for various depths and hydraulic gradients (i)	37
III-9	Friction angle versus compaction and moisture content for waste shale material	66
III-10	Summary of nutrient analysis	67
IV-1	Results of stability analysis for various hypothetical foundation conditions	72
IV-2	Summary of parameters used in short-term stability analysis of waste shale embankments	75
IV-3	Summary of parameters used in long-term stability analysis of waste shale embankments	77
V-1	Summary of example problem	86

LIST OF SYMBOLS

B - pore pressure coefficient

c - cohesion

D_r - relative density

e - void ratio

e_{max} - maximum void ratio

e_{min} - minimum void ratio

ε - strain

ε_c - creep strain

ε_{ci} - creep strain in layer i

ε_s - saturation strain

F.S. - factor of safety

h_{ci} - creep settlement in layer i

h_{oi} - initial thickness of layer i

h_{si} - saturation collapse settlement in layer i

ΔH - total post construction settlement

ΔH_c - total creep settlement

ΔH_s - total saturation collapse settlement

i - hydraulic gradient

K - permeability

n - number of layers

N - normal force

RC - relative compaction

t_1 - initial time

t_2 - final time

t_o - beginning of construction time

t'_o - reference starting time

T - shearing force

u - pore water pressure

Δu - change in pore water pressure

W - Weight of wedge

$\%\ w$ - percent moisture content

y_i - depth from ground surface to the middle of layer i

β - external slope of embankment (degrees)

σ_i - stress in the middle of layer i

σ_1 - major principal stress

σ_3 - minor principal stress

$\bar{\sigma}$ - effective stress

$\bar{\sigma}_n$ - effective normal stress

$\Delta\sigma$ - change in stress

$\Delta\sigma_3$ - change in the minor principal stress

η - porosity

τ - shearing stress

α - slope of settlement versus log time curve

α_c - slope of creep strain versus log time curve

γ - unit weight of soil

γ_d - dry unit weight of soil

γ_t - total unit weight of soil

ϕ - angle of internal friction, total stress

$\bar{\phi}$ - angle of internal friction, effective stress

Σ - summation

CHAPTER I

INTRODUCTION

Importance of the Western Phosphate Fields

Phosphate rock is used to produce phosphate which is a vital part of our present existence. Southeastern Idaho contains approximately 35 percent of the total United States phosphate reserves (U.S.G.S., 1976). The total reserves in the western fields are estimated at about 12 billion tons (Service and Coffman, 1967). Approximately 80 percent of this lies in Southeastern Idaho. The importance of the western phosphate industry is recognized nationally. Indicators are that the western phosphate fields will continue to grow in importance. Consumption including exports of phosphate rock increased from 20 million short tons in 1961 to over 40 million short tons in 1971, a 100 percent increase. The abundance of resources in a sparsely populated area provide the western phosphate industry with the qualities necessary for future expansion. Even if the geographic distribution of supply and demand does not change from the present pattern, the western mining and processing of phosphate should show greater increases because the west is still showing greater population increases than any part of the country.

History of the Southeast Idaho Phosphate Mines

Phosphate mining in Southeastern Idaho dates back as early as 1906 when phosphate rocks were produced from underground operations at the Waterloo Mine near Montpelier, Idaho (Service and Coffman, 1967). The mine was operated by the San Francisco Chemical Company and closed down in 1929. In 1945, the mine was reactivated as a surface strip-mine and produced phosphate rock until 1958. In 1920, the Conda Mine, owned by the Anaconda Company of Southern California, began underground mining just north of Soda Springs and continued until 1957. Surface strip-mining began at Conda in 1952 as a supplement to underground production (U.S.G.S., 1976). Until 1946, the Waterloo Mine near Montpelier and the Conda Mine were the only phosphate mines in Idaho.

The development of large earth moving equipment as well as economic considerations resulted in a shift from underground to surface strip-mining. Several mining leases were subsequently sold and surface strip-mines founded. The Maybe Canyon Mine currently operated by Beker Industries and the Wooley Valley Mine operated by the Stauffer Chemical Company are the two strip-mines considered herein.

The steady increase in demands for phosphate has increased strip-mining activity in Southeastern Idaho. Larger amounts of overburden material are currently being removed so that greater volumes of ore can be extracted. Currently, this overburden material is being placed in large spoil dumps. Some of these dumps will contain over a million cubic yards of material. A number of engineering considerations are associated with the design and construction of these spoil dumps. Problems can and have resulted from mass failures and improper drainage. The emphasis towards increased environmental standards in recent years has influenced waste disposal. Dumps must be safe from landslides and massive erosion. Currently, efforts are to revegetate the spoil dump as soon as practical.

Scope of this Investigation

The primary objectives of this study are to develop guidelines for the placement of spoil dumps as related to mass stability and also to develop a useful method for estimating magnitudes of post construction settlements. The accomplishment of these objectives entails the following three tasks:

1. Determining the engineering properties of the typical spoil materials through laboratory and field tests.

2. Investigating the stability of mine dumps against mass failure including:

   a. The effects of foundation preparation or lack thereof on the safety factor against mass failure.

   b. Deep foundation failures and conditions that may contribute to such failures.

   c. Establishing relationships between slope angle, relative compaction, and safety factor to be used as guidelines for the construction of disposal fills.

3. Developing a method to predict the post construction settlement of spoil dumps.

This study deals specifically with the Wooley Valley and Maybe Canyon Mines. Different dump construction methods are used at these two mines. Free flowing dumps are constructed at

Maybe Canyon by dumping the overburden from haul trucks over the end of the dump and the material rolls down the face at the angle of response. At Wooley Valley the material is spread on the dump in approximately 1 ft lifts by scrapers. The properties of a dump are significantly effected by the method of construction. Data from field and laboratory tests are used to determine how each of these methods effects the engineering properties of the dump. The typical dump construction methods are discussed in more detail in the following section.

Spoil Dump Construction Methods

Spoil dump construction varies depending on the general terrain at the site and the type of earth moving equipment being used. The different construction methods cause differences in the unit weight and moisture condition of the material and this, in turn, leads to differences in the engineering properties of the dump material.

It is well known that the density and remolding moisture content greatly effects the shear strength and compressibility properties of fine grained soils. Consequently, with all other factors equivalent the stability of the dumps against mass failure will be a function of the method of construction. At Maybe Canyon, where end dump trucks are used, the construction is "free flowing". A free flowing dump is built by end dumping spoil material over angle of repose embankments. The material flows down the side with an angle equal to the angle of repose of the material. Vertical heights of such embankments often exceeds 100 ft and can be as high as 325 ft. The area of the dump is increased as material is continually placed over the edge of the embankment. The photograph shown in Figure I-1 helps illustrate the free flowing method of construction. The free flowing method results in low placement densities because the bulk of the material receives little compaction effort. Segregation of particles also results. The large materials roll to the bottom toe area while the finer materials remain near the top. Finished dumps are terraced and finish slopes are generally graded to 3 horizontal to 1 vertical.

Waste dumps at the Wooley Valley Mine are placed in thin horizontal layers, approximately 1 to 1½ ft thick. Wheel tractor scrapers deposit the material, see Figure I-2. Some compaction is achieved by the scraper wheels passing directly over the material. The densities vary because portions of the fill do not receive direct wheel contact. Finished dumps are also terraced and finish slopes are graded to 3 horizontal to 1 vertical.

Geologic Setting

It is well known that geology is an integral part of every geotechnical investigation.

Figure I-1. Illustration of free flowing method of construction.

Figure I-2. Illustration of scraper filled method of construction.

The nature and behavior of soil depends upon geology and geologic history. A number of reports describing the geology of the western phosphate region are available. The geology of the study area was obtained from such reports and is described below.

Most of the phosphate regions of Southeastern Idaho are located in mountainous terrain of both the Caribou National Forest and private lands, Figure I-3. The area covers approximately 10,000 square miles. The location of the principal phosphate deposits are shown in Figure I-4. The Wooley Valley and Maybe Canyon Mines are situated along north and northwest trending mountain ridges some 20 to 25 miles northeast of Soda Springs, Idaho (see Figure I-5). These mountain ridges are composed primarily of the Phosphoria Formation which is well developed at these sites. Other geologic formations at these sites include the Dinwoody Formation and the Wells Formation. These formations are all of Permian age of the Palezoic Era. Traces of the Park City Formation are also present (U.S.G.S., 1976).

The Phosphoria Formation consists of mainly dark chert, phosphatic and carbonaceous mudstones, phosphorite, and cherty mudstones. The Phosphoria Formation is made up of four members: the Meade Peak Phosphatic Shale, the Rex Chert, the Cherty Shale, and the Retort Phosphatic Shale (McKelvey, et al., 1956). The Retort Phosphate Shale member is absent from the geology sequence at the two mines. The Meade Peak member consists principally of dark carbonaceous, phosphatic, and argillaceous rocks. Mudstones and phosphorites are also common. This member varies in thickness from 125 ft to 225 ft and is approximately 200 ft thick at the Maybe Canyon Mine. It is the bottom most member of the Phosphoria Formation and contains all the phosphate ore. The Rex Chert member which lies above the Meade Peak member ranges from 50 ft thick to 100 ft thick and is composed almost entirely of hard resistant dark chert. Above the Rex Chert member is the Cherty Shale member. The Cherty Shale member can be distinguished from the Rex Chert member by the presence of mudstones. Mudstones and cherty mudstones ranging from 100 to 150 ft in thickness make up the Cherty Shale member. In much of the subsequent discussions the Rex Chert and Cherty Shale will be called chert.

Local geologic events such as folding, faulting, and erosive processes have disrupted the

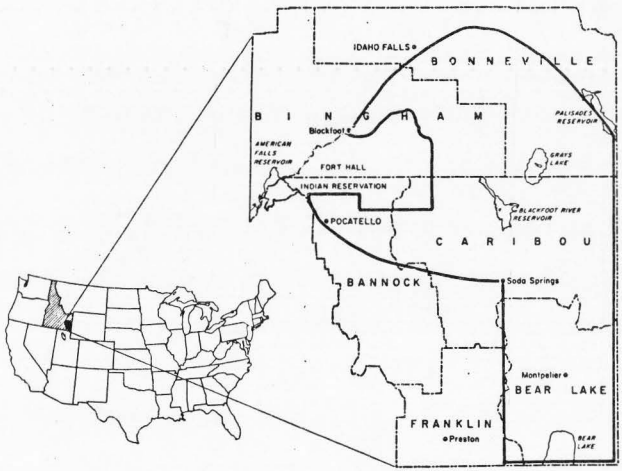

Figure I-3. Phosphate region of southeast Idaho (excluding the Fort Hall Indian Reservoir). (After U.S.G.S., 1976.)

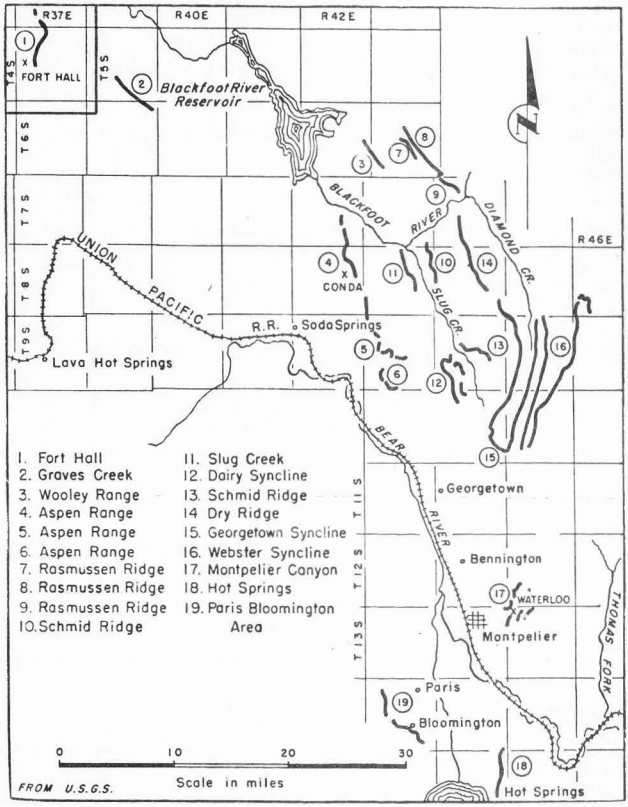

Figure I-4. Principal phosphate deposits of Southeastern Idaho. (After Butner, 1949.)

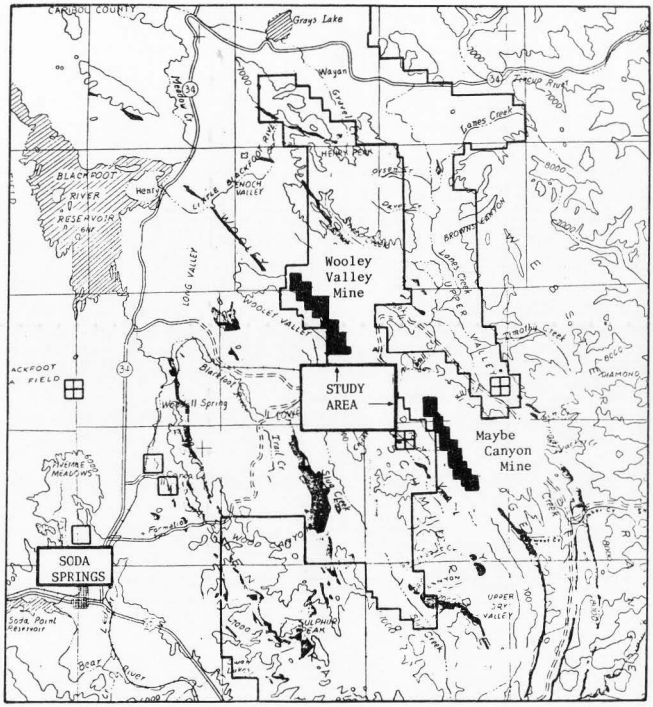

Figure I-5. Location of Wooley Valley and Maybe Canyon Mines. (After draft environmental impact statement, 1976.)

continuity within the Phosphoria Formation. Consequently, surface outcrops of the Meade Peak Phosphatic Shale member have resulted. These outcrops are located between steeply sloping beds of the Rex Chert member of the Phosphoria Formation and the limestones of the Wells Formation, Figure I-6, (McKelvy, et al., 1959). It is in these outcrops that mining operations are being conducted. A typical section of the geologic sequence at the Maybe Canyon Mine is shown in Figure I-7. A detailed section also giving P_2O_5 concentration, of the Meade Peak member at Maybe Canyon is shown in Figure I-8. Only those shown in black are mined for processing to phosphate. This illustration shows that two zones of high grade phosphate ore exist. Typically with present mining operations these zones are approximately 30 and 160 ft below the ground surface, respectively. The upper zone averages 20 ft in thickness and the lower zone averages 30 ft in thickness. The material lying above both these zones is typical of the waste dump spoil.

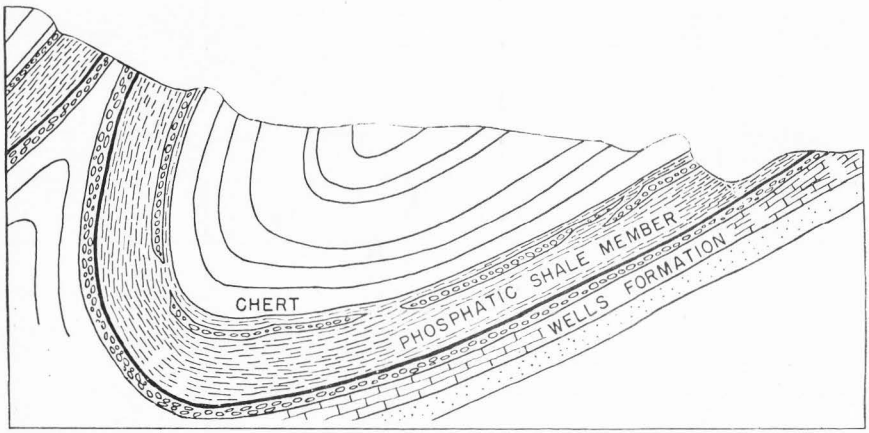

Figure I-6. Typical folding of beds in the Phosphoria Formation. (After D.W. Butner, 1949.)

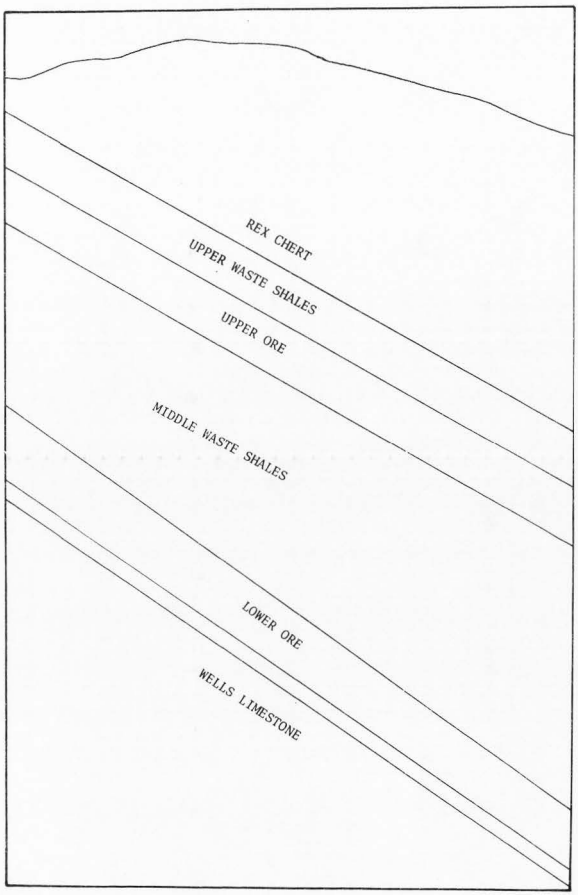

Figure I-7. Geologic sequence at Maybe Canyon. (After discussions with U.S.G.S., 1976.)

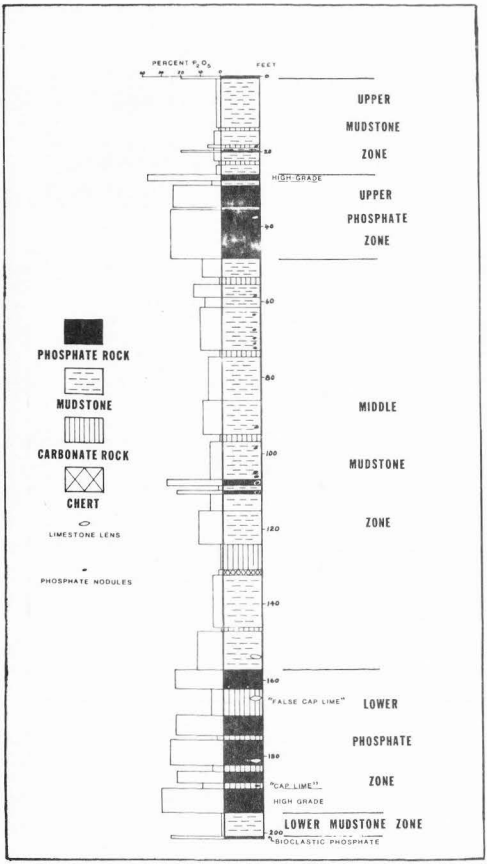

Figure I-8. Section of the Meade Peak Phosphatic Shale member of the Phosphoria Formation at Maybe Canyon. (After draft environmental impact statement, 1976.)

CHAPTER II

REVIEW OF LITERATURE

The material covered in this chapter has been grouped into the following four general categories:

- Generally accepted methods for disposing of surface mining overburden and mining waste material.
- The effect of compaction on the engineering properties of soil.
- Methods of stability analysis.
- Settlement of earth and rock-fill structures.

The state-of-the-art concerning each of these topics is briefly summarized. Detailed discussion on much of this material is presented in subsequent chapters.

Methods for Disposing of Mining Wastes

Concern for detrimental environmental and ecological effects of surface strip mining has significantly increased in recent years and as a consequence strip mining has been accompanied by considerable costs of rehabilitation. While there is little doubt that strip mining does disturb the environment there is reason to believe that with proper planning and design these adverse effects need not be permanent. In an effort to minimize undesirable surface mining effects, the 95th Congress has recently enacted environmental protection standards and regulations regarding the extraction of coal and other mineral resources from the earth (Public Law 95-87, August 3, 1977). These new regulations will undoubtedly effect future waste disposal practices.

Current coal waste disposal practices

The majority of literature concerned with the disposal of strip mining waste materials is in reference to surface coal mining. Obvious similarities exist between coal and phosphate surface mining. Many of the geotechnical considerations regarding coal overburden and waste disposal apply to phosphate spoil disposal. A brief discussion regarding the current practices of coal overburden and waste disposal is, therefore, presented.

Surface strip mining of coal generates wastes materials of two essential types; (1) overburden material, which must be removed in order to expose the coal seam and (2) refuse, which is waste generated during the processing of the raw ore. Two specific types of wastes are associated with the processing of coal ore. They are coarse refuse commonly referred to as coarse discard, spoil, or bony coal; and fine refuse often called tailings, fine discard, or slurry. The discard of fine refuse is a special disposal process that is in no way similar to the disposal of phosphate mining waste and is, therefore, not included in the following discussion. Many details regarding the disposal of fine refuse are presented in the 1977 Geotechnical Engineering Speciality Conference (ASCE, 1977).

The specific methods and equipment used to remove and dispose of overburden waste material during the mining of coal depends on the overburden characteristics as well as local topography and geology. Stofanko, Pamani, and Fuko (1973) present details on specific methods currently used in the United States. Typically, the overburden is removed by large power shovels or draglines operating on the highwall or in the mining pit. The large power shovel or dragline then deposits the overburden in an area which has been previously mined out. This technique is briefly described below. The mining cycle is initiated by the stripping shovel or dragline removing sufficient overburden to expose the coal seam and establishing a workable pit width (100 to 200 ft) by following the contour of the outcrop line. The overburden is cast adjacent to the pit length. Successive cuts are made by the stripping shovel or dragline removing the overburden and placing it into the cut where the exposed coal has been previously loaded out. Figure II-1 shows both plan and section views of a typical surface coal mining operation including overburden removal and disposal. The mined pit area is continually filled with overburden as more coal seam is exposed. The spoil dump is eventually graded by bulldozers to a rolling contour and seeded.

Coarse coal refuse disposal is conducted in a manner very similar to the disposal of phosphate mining wastes. Discussions regarding the disposal of coarse and combined refuse are presented by Cowherd (1977). It is generally transported to nearby disposal sites by conveyor belts where it is spread by trucks, scrapers or sometimes aerial tramways. The material is either end-dumped over angle of repose embankments or spread in horizontal lifts. A number of recommendations are presented by Doyle et al. (1975) in relation to coarse refuse disposal and are listed below:

1. Materials susceptible to weathering should be broken down mechanically (by haul trucks and placing equipment) as much as possible to reduce post construction weathering.

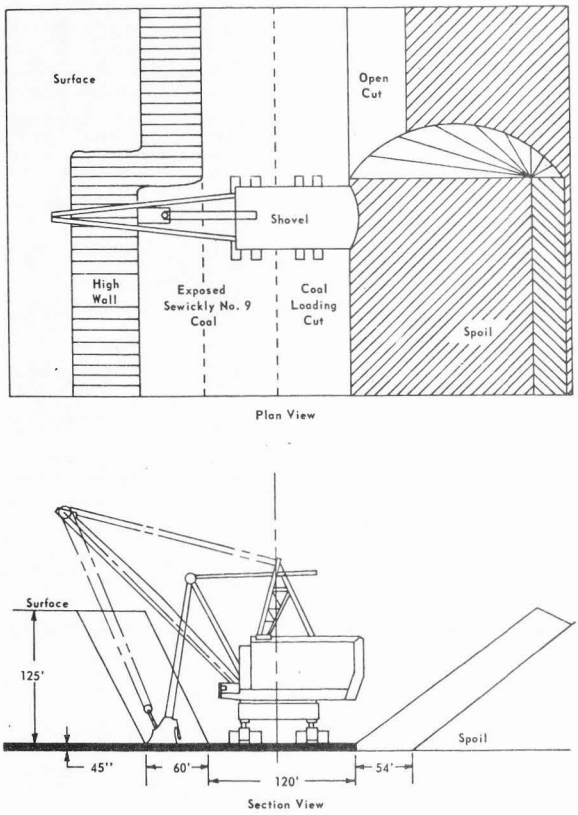

Figure II-1. Plan and section views of A B-E 1950-B pit (after Stefanko et al. 1973).

2. Infiltration of water into the refuse embankment by direct precipitation, storm runoff, stream flow, or from ponded water should be eliminated or minimized.

3. The embankment should be properly zoned with various appropriate materials and compaction efforts to form the most economical and trouble free embankment practical.

4. Proper field inspection should be implemented after construction to detect possible instability.

Coarse refuse is also used to construct embankments for the purpose of impounding slurry from fine refuse disposal. This, in effect, creates an earth dam. Prior to 1972, little technical efforts were devoted to the planning and design of such facilities. However, in February 1972 a coal refuse facility located in West Virginia failed resulting in the loss of over 100 lives. This catastrophic event known as the Buffalo Creek slide has brought increasing attention into the design requirement of coarse refuse disposal facilities to be used as impounding embankments. Current recommendations regarding the planning, design and construction of such facilities are presented by D'Appolonia et al. (undated).

Current phosphate waste disposal practices in Southeast Idaho

Waste material generated from phosphate mining in Southeastern Idaho generally consists of shale and chert materials. The waste is transported by trucks or scrapers to nearby designated disposal sites. At the currently active Wooley Valley Mine waste is transported by scrapers and spread in horizontal lifts one to two ft thick. At the Maybe Canyon Mine waste material is transported by truck and end-dumped over angle of repose embankments. Few geotechnical engineering design considerations are specified.

Compaction and Soil Properties

Compacting soils involves reducing the volume of a soil, water, and air matrix by removing the air and simultaneously reducing the volume of void space. The water content remains constant since the masses of soil and water do not change, however, the degree of saturation is increased because the void ratio is reduced. For cohesive soils the degree of compaction is directly related to the molding water content and compaction effort applied. Cohesionless soil such as clean sand and gravels are not significantly effected by the water content during compaction.

Compaction of earthfill embankments is generally achieved by applying momentary loads to the soil. A number of compaction devices have been developed to accomplish this. The more common compaction devices include sheepfoot rollers, rubber tire rollers, vibratory compactors, smooth drum rollers, and mechanical tampers. These devices are described in detail by the Bureau of Reclamation (1973) and Mitchell (1977). The appropriate type of compaction device depends chiefly on the type of material being compacted.

The effects that compaction has on the physical properties of soils such as permeability, compressibility, and shear strength, are related to the compacted state of the soil, (Bureau of Reclamation, 1960, 1973; Hilf, 1975; Mitchell, 1977; Sherard et al., 1963). Although a number of soil additives (organic and inorganic) have been developed to stabilize soils, mechanical compaction is the most widely used type of stabilization method (Mitchell, 1977). Generally, compaction increases the shear strength and reduces the compressibility and permeability of the soil.

Properties of compacted cohesionless soils

The state of compaction for cohesionless soil is generally defined in terms of relative density;

$$D_r = \frac{e_{max} - e}{e_{max} - e_{min}} (100)$$

where,

e_{max} = void ratio of the soil in its loosest state

e = void ratio of the soil being measured

e_{min} = void ratio of the soil in its densest state

D_r = relative density expressed as a percentage

Relative densities of 100 percent correspond to the maximum dry unit weight of the soil whereas a relative density of 0.0 percent corresponds to the soil in its loosest state. It is generally accepted that the performance of cohesionless soils in terms of engineering application can be improved by increasing the relative density.

The permeability of a cohesionless soil is related to the void ratio, as the void ratio is decreased by compaction the permeability is subsequently decreased.

The compressibility of cohesionless material has been studied by Lee and Seed (1967) and Marachi et al. (1969). Discussions regarding the

compressibility of sands and gravels are also presented by Bureau of Reclamation (1973), Hilf (1975), Lambe and Whitman (1969) and Terzaghi and Peck (1967). Sands and gravels at low relative densities are more compressible than the same material at higher relative densities. Therefore, compaction will generally reduce the compressibility of the material. Under high pressures particle crushing has a significant influence on the compressibility. For cohesionless soil under high loads compressibility is not greatly improved through compaction (Hilf, 1975).

The shearing strength of cohesionless soils depends almost entirely on the angle of internal friction. The angle of internal friction is known to be directly related to the relative density. Loose sands and gravels exhibit less shearing resistance than the same soil in a dense state. Figure II-2 shows typical relationships between relative density and friction angle for various types of cohesionless material. As shown, the particle size, shape and gradation also effect the shearing strength. Further discussion regarding the shear strengths of cohesionless material is presented by Bureau of Reclamation (1973), Dunn, Anderson and Kiefer (1976), Hilf (1975), Lambe and Whitman (1969), and Terzaghi and Peck (1967).

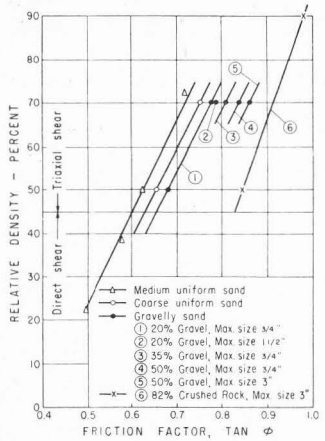

Figure II-2. Relative density vs tangent ϕ for cohesionless soils (after USBR, 1974).

Properties of compacted cohesive soils

Compaction of cohesive soils follows the principles stated by Proctor. The degree of compaction clearly depends on the compaction effort and the molding water content, see Chapter III. Permeability, compressibility, and shear strength are of major concern when discussing compacted cohesive soils.

Permeability. Major factors which effect the saturated permeability of a cohesive soil include soil type, void ratio, and soil structure. As the void ratio is decreased during compaction, the volume of the pore space is reduced. The permeability is subsequently decreased. For a given void ratio and assuming saturated flow, soil structure becomes an important factor. Consider two samples of the same soil compacted to identical densities (i.e., same void ratio), but one compacted wet of optimum moisture content and the other compacted dry of optimum moisture content. It has been shown that the sample compacted wet of optimum will have a lower permeability (Lambe, 1958) and (Mitchell, 1977). This can best be explained by examining the soil structure. Compacting clay soil dry of optimum will generally result in a flocculent structure. However, when compacting cohesive soils wet of optimum a dispersed soil structure results. The flocculent structure tends to have more large pore spaces (Lambe, 1958) and therefore greater permeability.

Compressibility. The compressibility of a soil is the relationship between volumetric strain and effective stress. The compressibility of compacted cohesive soils is discussed by the Bureau of Reclamation (1960, 1973) and Hilf (1975). The compressibility of a cohesive soil is naturally effected by the amount and character of the fines and by the amount and gradation of the coarse particles present (Hilf, 1975). More important, however, is the soil density and moisture content at the time of loading. Tests conducted by the Bureau of Reclamation suggested that the placement moisture affected the compressibility more than the dry density did. Samples compacted wet of optimum are more compressible than similar samples compacted to the same density dry of optimum. Lambe (1958, 1969) suggested that the capillary forces associated with the double layer hold the soil particles such that they resist particle rearrangement. When compacted dry of optimum, more energy is required to rearrange the particles. However, upon saturation, samples compacted dry of optimum experience additional settlement as the capillary forces are reduced. This additional settlement is called "collapse settlement" (Hilf, 1975). Mitchell (1976) describes collapse settlement as a reduction in effective stress in clay particles which coat or "buttress" sand or

silt grains. The clay particles swell, become weaker and fail in shear thus resulting in collapse of the soil and a subsequent decrease in volume.

Shear strength. Shear strength or shearing resistance of cohesive soils can also be improved by compaction. The effect compaction has on the shearing resistance of cohesive soils is discussed by Bureau of Reclamation (1973), Dunn, Anderson, and Kiefer (1976), Hilf (1975), Lambe and Whitman (1969), and Terzaghi and Peck (1967). For a cohesive soil the electrical and molecular forces surrounding the soil particles play a more prominent role in resisting the relative movement between particles as the void ratio becomes smaller (Dunn, Anderson, and Kiefer, 1976). Therefore, the smaller the void ratio, the greater is the shearing resistance. The molding water content at which the soil is compacted may also have a significant effect on shear strength. Samples compacted slightly dry of optimum moisture content, approximately two percent, exhibit greater shearing resistance than samples compacted at or wet of optimum, (Bureau of Reclamation, 1960, 1973; Gibbs, 1960; Hilf, 1975; and Lambe, 1958). This phenomenon can best be explained by the fact that particles are arranged in a flocculent structure thereby offering more resistance to shear and exhibiting greater attraction for one another through capillary forces (i.e., negative pore water pressure). Samples compacted dry of optimum will exhibit a greater loss of strength after saturation than samples compacted wet of optimum. However, because of the flocculent structure associated with the samples compacted dry of optimum the shearing resistance after saturation will still be greater as compared to samples compacted wet of optimum. The degree to which shearing resistance can be improved by controlling the molding water content of a cohesive soil or fine grained nonplastic soil such as the spoil material at both Wooley Valley and Maybe Canyon mines will depend principally on the soil type. Shear strength tests conducted by Lee and Haley (1968) on a commercial Kaolinite (Higgins Clay) showed significant increases in strength for specimens compacted dry of optimum and sheared before saturation, Figure II-3. The samples prepared dry of optimum (flocculent structure) exhibited up to three times the unconfined compressive strength of those compacted wet of optimum. In addition, the unconsolidated undrained strength was also significantly improved by compacting specimens dry of optimum. For any given cohesive soil or nonplastic fine grained material the amount of improvement in strength achieved through compacting dry of optimum is variable and must be determined by laboratory tests.

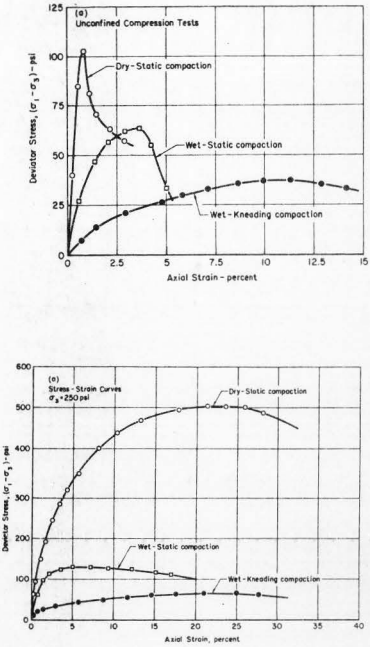

Figure II-3. Unconfined compressive strength and unconsolidated undrained strength characteristics of Higgins Clay (after Lee and Haley, 1968).

Methods of Stability Analysis

Two basic approaches to slope stability analysis exist. The most common of these approaches is the limiting equilibrium method. The second approach is to perform an exact analysis. This approach has just recently been possible with the development of the Finite Element Method and its application to Soil Mechanics problems.

Limiting equilibrium methods

In a Limiting Equilibrium method of analysis a failure surface is assumed and a freebody diagram is developed for the assumed failure mass. An impending failure condition is assumed and the shearing stresses required to maintain equilibrium

are determined. These shearing stresses required to maintain equilibrium are then compared to the shear strength of the soil and a factor of safety is determined. Three general types of limiting equilibrium methods are used and include the following:

- Methods that consider the failure mass as a whole.
- Methods that divide the failure mass into a number of slices.
- Methods that assume failure along one or two failure planes (Wedge methods).

Figure II-4 illustrates each of these methods.

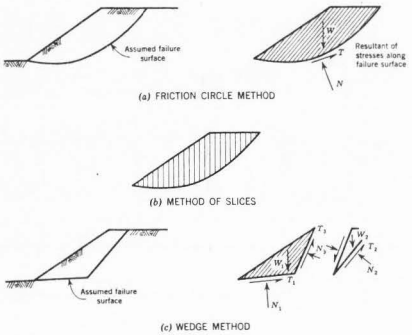

Figure II-4. Various methods of slope stability analysis (after Whitman and Baily, 1966).

The friction circle method is often used when considering the freebody as a whole. This method assumes a circular failure surface. Figure II-4a is an example of this approach. Several versions using the method of slices exist. The most common include the Fellenius method, the Simplified Bishop method, and the Morgenstern-Price method (Whitman and Baily, 1966). The Fellenius and Simplified Bishop methods assume circular failure surfaces while the Morgenstern-Price method will handle non-circular but curved failure surfaces. When using the method of slices the failure mass is divided into a number of vertical slices and the equilibrium of each slice is considered in the analysis.

The basic principles of the above stated methods are discussed in detail in most soil mechanics textbooks such as Lambe and Whitman (1969) and by Whitman and Baily (1966).

All limiting equilibrium methods are statically indeterminate and, therefore, a number of assumptions must be made in order to solve the problem by statics. The number and nature of the assumptions account for the differences in the various limiting equilibrium methods. Table II-1 lists several equilibrium methods and gives some indication as to their basic differences and assumptions.

Total and effective stress methods

Two general methods can be used to specify the strength parameters for a limiting equilibrium analysis. The selection of strength parameters to be used depends on how the excess pore pressures are to be accounted for in the solution. The methods are referred to as effective stress and total stress methods of analysis.

Total stress methods. In a total stress analysis the shear strength parameters are determined from a total strength envelope (see Chapter III). Laboratory tests are conducted on samples that are assumed to develop pore pressures during shear equal to those which will occur in the embankment. The total stress analysis is generally applied to undrained conditions where loads are applied rapidly enough that pore pressures cannot dissipate. For earth dams the end of construction condition and sudden drawdown are generally performed on a total stress basis.

Effective stress methods. An effective strength envelope (Chapter III) also provides the strength parameters needed for a stability analysis. Effective strength parameters are generally determined from a consolidated undrained test with pore pressure measurements. The actual pore pressures which develop in the embankment at the failure surface are estimated and used in the stability computations. The steady-state seepage condition for earth dams is usually performed as an effective stress analysis.

Relationship between both methods. Both the effective and total stress methods of analysis will result in the same factor of safety provided that the pore pressures are accurately accounted for. Problems associated with each method occur when trying to estimate the pore pressures. One advantage of using an effective stress method is that pore pressures in the embankment can be monitored by field instruments and design changes can be implemented as required when excessive pore pressures are measured.

Table II-1. Limiting equilibrium methods and equilibrium conditions (after Duncan; class notes).

Procedure	Equilibrium Conditions Satisfied				Shape of Failure Surface
	Overall Moment	Ind. Slice Moment	Ver.	Hor.	
Ordinary Method of Slices	Yes	No	No	No	Circular
Bishop's Simplified Method	Yes	No	Yes	No	Circular
Janbu's Generalized Procedure of Slices	Yes	Yes	Yes	Yes	Any
Spencer's Procedures	Yes	Yes	Yes	Yes	Any

Further discussion regarding total and effective stress methods is presented by Bishop (1960); Lambe and Whitman (1969); Terzaghi and Peck (1967); and Whitman (1960).

General Considerations Regarding Settlement of Earth and Rockfill Structures

Methods for settlement analysis of natural soil deposits are established, (Dunn, Anderson and Kiefer, 1976; Lambe and Whitman, 1969; Taylor, 1948; Terzaghi and Peck, 1967; and U.S. Army Corp of Engineers, 1953). Procedures to predict the magnitude and rate of settlement of earth and rockfill embankments are not well established. The mechanics of rockfills and the compressibility of rockfills are discussed by Marsal (1973) and Sower et al. (1965). Sowers et al. (1965) studied the compressibility of broken rock and suggested a method to predict the long-term settlement of rockfills. His work is summarized below. The magnitude of settlement of rockfill dams when expressed as a percentage of the fill height is related to the method of construction rather than the dam height, type, or rock type.

The rate of settlement characteristics of several rockfill dams were measured by Sowers et al. (1965). These measurements indicated that settlement versus log of time plots as a straight line. Therefore, settlement can be estimated by

$$\Delta H = \alpha \, (\log t_2 - \log t_1)$$

where α is the slope of the settlement versus log time plot. Values of α for the dams considered by Sowers et al. (1965) ranged from 0.2 to 1.05.

Sowers et al. (1965) also performed compression tests on samples of crushed rocks taken from the dam sites. These tests showed the settlement log time relationships for the crushed rocks were similar to the observed field relationships. Furthermore, rates of settlement were accelerated by applying water to the laboratory samples. Because the laboratory settlement curves were similiar to the field curves, Sowers et al. (1965) indicate that rockfill settlements can be accurately predicted from laboratory tests.

Sowers et al. (1965) suggest that the mechanism of creep settlement involves continual crushing of particle contact points which causes redistributions of stress concentrations.

> "The time dependent compression of the mass can be explained by the local crushing of one point which causes a local redistribution of stress and a slight shifting of the particles which in turn, brings added crushing of a new location. The number of fresh faces and points subject to crushing becomes less as each point in turn is crushed and so the rate decreases, a process which can be expressed by a straight line on a semi log plot". Sowers et al. (1965).

Why water accelerates the rate of settlement is not well understood. Sower et al. (1965) suggested that possible increases in local shear stresses develop at contact points as water enters microfissures near or at contact points. However, additional studies into the causes of accelerated rates of settlements have not verified this hypothesis and the matter is not resolved at present.

Stability of Coal Waste Embankments

Studies related to the stability of coal waste embankments are presented by Cowherd (1977)

and Huang (1977). Huang (1977) describes a procedure for developing design curves for mine spoil banks and hollow fills to be used as construction guidelines so that a factor of safety against failure of 1.5 can be obtained. Two modes of failure are considered and include a cylindrical failure through the fill of the embankment only, and failure along the foundation-embankment interface.

Cowherd (1977) describes three slope stability case studies. The first study describes a disposal facility constructed principally from fine refuse or tailings. The second study describes a slope stability investigation and analysis for a waste disposal facility constructed with combined refuse. The third study involves an end dump constructed or, angle of repose facility containing overburden spoil waste. Because of the obvious similarities between this disposal facility and embankments constructed by using the free flowing method in Southeastern Idaho, a brief discussion of the study is presented below.

The spoil material consisted primarily of rock. Because of the construction method, the large rocks roll down to the valley floor and are located in the lower layers of the fill. The smaller particles are near the top of the fill. To determine strength parameter the cross-section studied was first divided into several layers. The uppermost layer contained maximum particle sizes less than six in in diameter. Triaxial shear strength tests were conducted to determine the angle of internal friction and cohesion of the material in this layer. The lower layers consisted of rock material too large to be tested in the laboratory. Therefore, a review of literature concerning the strength and unit weights of such rockfills was conducted and friction angles as well as unit weights were then estimated based on this literature review. A stability analysis was then performed. The results indicated the facility was adequately safe against slope failure. A stability analysis similar to this could probably provide a reasonable estimate of the factor of safety against failure for end-dumped or angle of repose dumps constructed in Southeastern Idaho.

CHAPTER III

FIELD AND LABORATORY TESTING

Purpose and Types of Tests

Laboratory tests were conducted for the purpose of classifying the spoil dump material and for determining the permeability, compressibility and shear strength characteristics of the spoil material. The laboratory tests included grain size analyses, Atterberg Limits, specific gravity, compaction, permeability, compressibility and shear strength. Nutrient analyses were conducted to determine deficiencies in the fertility of the spoil material, and two x-ray powder diffraction tests were conducted on rock specimens.

Field tests were performed to determine the effect of construction methods on the inplace dry unit weights of the spoil embankments. In-place dry unit weight and field moisture tests were conducted.

The following material in Chapter III is organized into three general sections. The first section describes when and where samples of the mining spoil were obtained. The last two sections constitute the majority of the material presented and include first a description and applications of the types of tests conducted and second a discussion of the test results. The section discussing the description and application of the tests is included for the reader who is not familiar with soils testing and the engineering properties of soils.

Sampling

The laboratory tests were conducted on samples of middle waste shale material taken from the active Wooley Valley and Maybe Canyon Mines. Sixteen samples were obtained from the Wooley Valley erosion study plots in October 1975. Nine samples were taken from the surface of the North Maybe Canyon dump; four of which were obtained on April 13, 1976 and an additional five obtained on July 23, 1976. Ten samples were obtained from the surface of dump number six at Wooley Valley; five of which were obtained July 24, 1976 and an additional five were taken on August 2, 1976. Laboratory tests were also conducted on samples of chert material taken from both the Wooley Valley and Maybe Canyon Mines. The location of all middle waste shale samples and corresponding sample number designations are summarized on Figures III-1, III-2, and in Table III-1.

Description and Use of Tests

Classification tests

Classification tests included: Grain size analysis, Atterberg Limits, specific gravity and x-ray powder diffraction. A grain size analysis gives the distribution of particle sizes that make up a given soil. These analyses included sieve and hydrometer analyses (ASTM D-422-63) and the results were plotted on a grain size distribution curve. Liquid and plastic limits (Atterberg Limits) represent water contents for fine-grained soils which define the boundaries between a liquid state and plastic state and a plastic state and semi solid state respectively. The Atterberg Limits provide tremendous insight as to the general engineering behavior of fine-grained soils. Atterberg Limit tests were performed according to methods ASTM-D 423-61-T and ASTM-D 424-59. Specific gravity is defined as "the ratio of the weight in air of a given volume of material at a stated temperature to the weight in air of an equal volume of distilled water at a stated temperature" (ASTM Committee, 1977). Specific gravity tests were performed according to ASTM-D 854-58. The specific gravity of the solid particles were determined from these tests. X-ray diffraction tests are useful in determining the crystal structure and clay mineralogical composition of both rock and fine-grain soils.

A grain size distribution together with the Atterberg Limits are used as the basis for classifying soils under the Unified Soil Classification System (ASTM-D 422-63). The Unified Soil Classification System groups soils depending on the percentages of coarse and fine particles as well as the nature of the fine particles. The field identification procedure and the laboratory classification criteria are given on Figure III-3.

This classification system serves as a guide for determining the suitability of soils for various engineering purposes. An engineering use chart for soils has been developed and published by the Department of Interior, Bureau of Reclamation (1960). The chart is based on the Unified Soil Classification System and is shown in Figure III-4. The engineering use chart provides an indication of some of the important engineering properties typical of various soil groups.

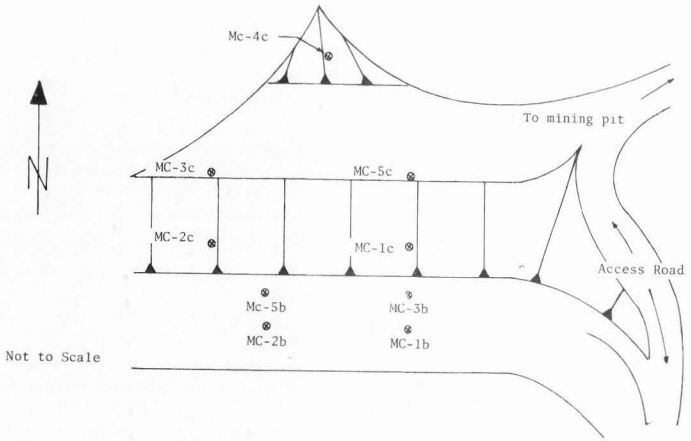

Figure III-1. Sampling location North Maybe Canyon Dump.

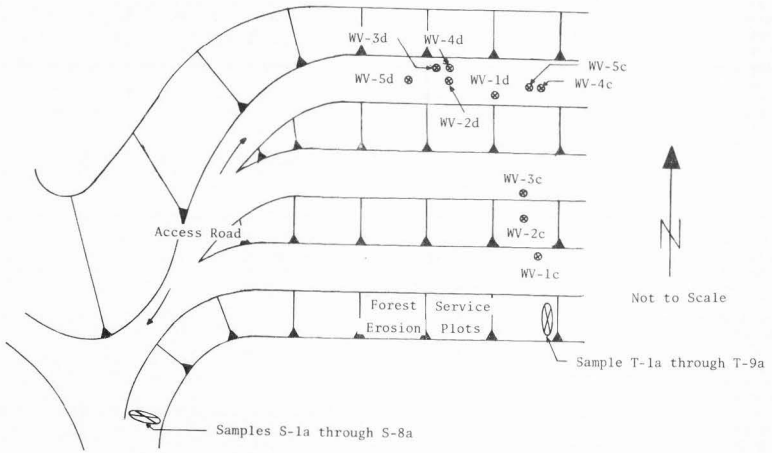

Figure III-2. Sampling locations Wooley Valley Dump No. 6.

Table III-1. Sample numbering system.

Sample Number	Date Obtain	Location Obtained
S-1a	October 1975	Forest Service Plots, Wooley Valley
S-2a	October 1976	Forest Service Plots, Wooley Valley
S-3a	October 1975	Forest Service Plots, Wooley Valley
S-4a	October 1975	Forest Service Plots, Wooley Valley
S-5a	October 1975	Forest Service Plots, Wooley Valley
S-6a	October 1976	Forest Service Plots, Wooley Valley
S-7a	October 1975	Forest Service Plots, Wooley Valley
S-8a	October 1975	Forest Service Plots, Wooley Valley
T-1a	October 1975	Forest Service Plots, Wooley Valley
T-2a	October 1975	Forest Service Plots, Wooley Valley
T-3a	October 1975	Forest Service Plots, Wooley Valley
T-4a	October 1975	Forest Service Plots, Wooley Valley
T-5a	October 1975	Forest Service Plots, Wooley Valley
T-6a	October 1975	Forest Service Plots, Wooley Valley
T-7a	October 1975	Forest Service Plots, Wooley Valley
T-8a	October 1975	Forest Service Plots, Wooley Valley
MC-1b	April 13, 1976	North Maybe Canyon Dump
MC-2b	April 13, 1976	North Maybe Canyon Dump
MC-3b	April 13, 1976	North Maybe Canyon Dump
MC-5b	April 13, 1976	North Maybe Canyon Dump
MC-1c	July 23, 1976	North Maybe Canyon Dump
MC-2c	July 23, 1976	North Maybe Canyon Dump
MC-3c	July 23, 1976	North Maybe Canyon Dump
MC-4c	July 23, 1976	North Maybe Canyon Dump
MC-5c	July 23, 1976	North Maybe Canyon Dump
WV-1c	July 24, 1976	Wooley Valley Dump Six
WV-2c	July 24, 1976	Wooley Valley Dump Six
WV-3c	July 24, 1976	Wooley Valley Dump Six
WV-4c	July 24, 1976	Wooley Valley Dump Six
WV-5c	July 24, 1976	Wooley Valley Dump Six
WV-1d	August 2, 1976	Wooley Valley Dump Six
WV-2d	August 2, 1976	Wooley Valley Dump Six
WV-3d	August 2, 1976	Wooley Valley Dump Six
WV-4d	August 2, 1976	Wooley Valley Dump Six
WV-5d	August 2, 1976	Wooley Valley Dump Six

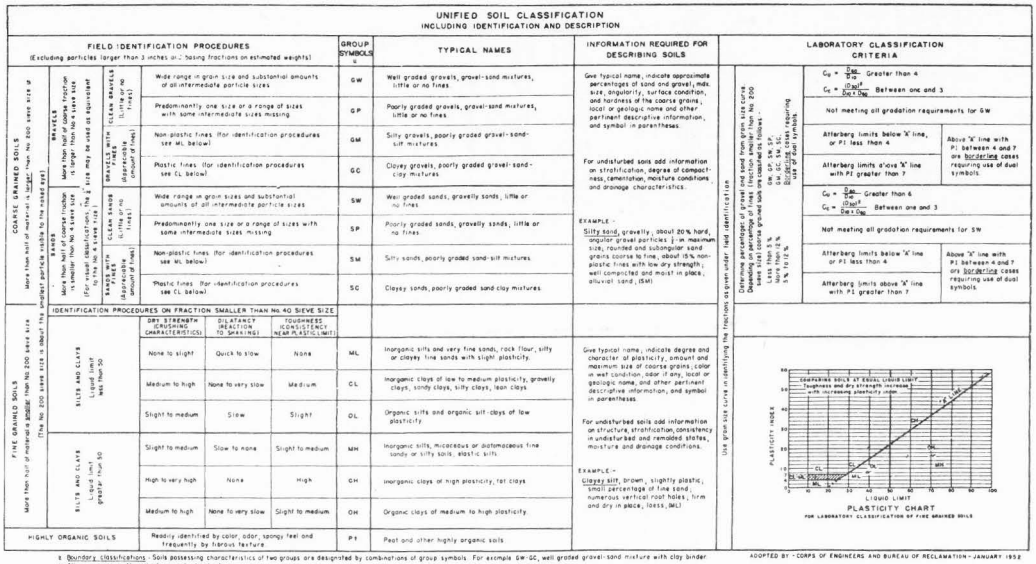

Figure III-3. Unified soil classification chart (after Bureau of Reclamation, 1960).

TYPICAL NAMES OF SOIL GROUPS	GROUP SYMBOLS	IMPORTANT PROPERTIES				RELATIVE DESIRABILITY FOR VARIOUS USES*									
						ROLLED EARTH DAMS			CANAL SECTIONS		FOUNDATIONS		ROADWAYS		
		PERMEABILITY WHEN COMPACTED	SHEARING STRENGTH WHEN COMPACTED AND SATURATED	COMPRESSIBILITY WHEN COMPACTED AND SATURATED	WORKABILITY AS A CONSTRUCTION MATERIAL	HOMOGENEOUS EMBANKMENT	CORE	SHELL	EROSION RESISTANCE	COMPACTED EARTH LINING	SEEPAGE IMPORTANT	SEEPAGE NOT IMPORTANT	FILLS: FROST HEAVE NOT POSSIBLE	FILLS: FROST HEAVE POSSIBLE	SURFACING
WELL GRADED GRAVELS, GRAVEL SAND MIXTURES, LITTLE OR NO FINES	GW	PERVIOUS	EXCELLENT	NEGLIGIBLE	EXCELLENT	—	—	1	1	—	—	1	1	1	3
POORLY GRADED GRAVELS, GRAVEL SAND MIXTURES, LITTLE OR NO FINES	GP	VERY PERVIOUS	GOOD	NEGLIGIBLE	GOOD	—	—	2	2	—	—	3	3	3	—
SILTY GRAVELS, POORLY GRADED GRAVEL SAND SILT MIXTURES	GM	SEMI PERVIOUS TO IMPERVIOUS	GOOD	NEGLIGIBLE	GOOD	2	4	—	4	4	1	4	4	9	5
CLAYEY GRAVELS, POORLY GRADED GRAVEL SAND CLAY MIXTURES	GC	IMPERVIOUS	GOOD TO FAIR	VERY LOW	GOOD	1	1	—	3	1	2	6	5	5	1
WELL GRADED SANDS, GRAVELLY SANDS, LITTLE OR NO FINES	SW	PERVIOUS	EXCELLENT	NEGLIGIBLE	EXCELLENT	—	—	3 If Gravelly	6	—	—	2	2	2	4
POORLY GRADED SANDS, GRAVELLY SANDS, LITTLE OR NO FINES	SP	PERVIOUS	GOOD	VERY LOW	FAIR	—	—	4 If Gravelly	7 If GRAVELLY	—	—	5	6	4	—
SILTY SANDS, POORLY GRADED SAND SILT MIXTURES	SM	SEMI PERVIOUS TO IMPERVIOUS	GOOD	LOW	FAIR	4	5	—	8 If GRAVELLY	5 EROSION CRITICAL	3	7	8	10	6
CLAYEY SANDS, POORLY GRADED SAND CLAY MIXTURES	SC	IMPERVIOUS	GOOD TO FAIR	LOW	GOOD	3	2	—	5	2	4	8	7	6	2
INORGANIC SILTS AND VERY FINE SANDS, ROCK FLOUR, SILTY OR CLAYEY FINE SANDS WITH SLIGHT PLASTICITY	ML	SEMI PERVIOUS TO IMPERVIOUS	FAIR	MEDIUM	FAIR	6	6	—	—	6 EROSION CRITICAL	6	9	10	11	—
INORGANIC CLAYS OF LOW TO MEDIUM PLASTICITY, GRAVELLY CLAYS, SANDY CLAYS, SILTY CLAYS, LEAN CLAYS	CL	IMPERVIOUS	FAIR	MEDIUM	GOOD TO FAIR	5	3	—	9	3	5	10	9	7	7
ORGANIC SILTS AND ORGANIC SILT CLAYS OF LOW PLASTICITY	OL	SEMI PERVIOUS TO IMPERVIOUS	POOR	MEDIUM	FAIR	8	8	—	—	7 EROSION CRITICAL	7	11	11	12	—
INORGANIC SILTS, MICACEOUS OR DIATOMACEOUS FINE SANDY OR SILTY SOILS, ELASTIC SILTS	MH	SEMI PERVIOUS TO IMPERVIOUS	FAIR TO GOOD	HIGH	POOR	9	9	—	—	—	8	12	12	13	—
INORGANIC CLAYS OF HIGH PLASTICITY, FAT CLAYS	CH	IMPERVIOUS	POOR	HIGH	POOR	7	7	—	10	8 VOLUME CHANGE CRITICAL	9	13	13	8	—
ORGANIC CLAYS OF MEDIUM TO HIGH PLASTICITY	OH	IMPERVIOUS	POOR	HIGH	POOR	10	10	—	—	—	10	14	14	14	—
PEAT AND OTHER HIGHLY ORGANIC SOILS	PT	—	—	—	—	—	—	—	—	—	—	—	—	—	—

Low number indicates preferred soil.

Figure III-4. Engineering use chart for soils (after Department of Interior, Bureau of Reclamation, 1960).

Compaction tests

Compaction of material in the spoil dumps results only from the movement of earth hauling and placing equipment. At present no attempts are made to achieve uniform compaction by using compaction devices. The result is a relatively loosely deposited fill with a range of relative compactions and field moisture contents. The initial in-place unit weight of spoil dump material is influenced by the compaction effort and the water content during placement. Compressibility, permeability and shear strength will depend on the initial unit weight of the material and placement moisture content during placement. It was, therefore, important to establish the values of field moisture contents and the relative compaction of the fill material as it was placed in the spoil dumps. The relative compaction is defined as the ratio of the dry unit weight of the fill material to the maximum dry unit weight of the fill material as determined from the standard proctor compaction test (described below) expressed as a percent.

The maximum dry unit weight of the material was determined from the standard proctor compaction test (ASTM 698-64-T Method C). The compaction test relates the compacted dry unit weight to the remolding moisture content for a standard compaction effort. The compaction effort for this study consisted of dropping a 5.5 lb (24.47 N) hammer 25 times through a height of 12.00 in (305 mm) onto each of three successive layers of soil in a proctor cylinder. The proctor cylinder is 4.00 in (102 mm) in diameter, 4.50 in (114 mm) high and contains a volume of 1/30 ft^3 (9.40 x 10^{-4} m^3). The proctor cylinder and hammer are shown on Figure III-5 (see page 24). Several specimens are individually compacted in the proctor cylinder at various moisture contents and the results are plotted as dry unit weight versus moisture content. The moisture content which produces the maximum

dry unit weight is the optimum moisture content for the compaction effort used.

For a cohesive soil this compaction curve will generally indicate that as the moisture content increases the dry unit weight increases to a peak and then decreases as shown on Figure III-6. Also, shown in Figure III-6 is the effect of increasing the compaction effort on cohesive soils. By changing the field moisture content during placement, the relative compaction of cohesive soils can be controlled without changing the compaction effort.

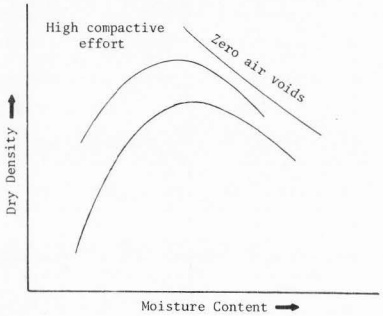

Figure III-6. Moisture density relationship typical of cohesive soils also showing the effect of increased compaction effort.

For a cohesionless soil the maximum dry unit weight is not as well related to moisture content and may be similar to the plot shown in Figure III-7. For a clean cohesionless material the maximum dry unit weight is obtained when the sample is air dry or completely saturated. At low moisture contents the rearrangement of particles is probably resisted by capillary forces, thus, resulting in lower unit weights (Lambe and Whitman, 1969).

The field tests of in-place unit weights of the material were determined by the sand cone method, ASTM-D 1556-64. The sand cone apparatus is shown on Figure III-8 (see page 24). The tests were conducted by determining the weight of a test sand required to fill a small hand-dug hole. The density of the sand was known and, therefore, the volume of the small hole could be determined. The weight of dry soil removed from the holes was then determined and the in-place dry unit weights were calculated. Field moisture tests were performed according to the laboratory determination of moisture content method, D-2216-63T. Moisture content is defined as the weight of water in a soil volume divided by the oven dry weight of soil. The soil is dried at a temperature of 110 ± 5 degrees centigrade.

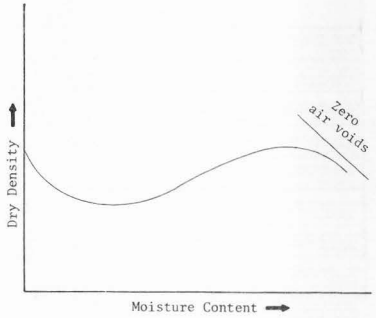

Figure III-7. Moisture density relationship typical of clean cohesionless soils.

Permeability tests

The rate at which water flows through a soil influences the shear strength, consolidation and erosion properties of the material as well as the infiltration and water holding capacity of the soil. Permeability tests were performed on several samples using constant head permeameters (Lambe and Whitman, 1969). The samples were prepared at various degrees of relative compaction to simulate various field conditions. Figure III-9 (see page 24), shows the constant head permeameters used in this study.

Percolation tests were also conducted in chert material on the north wing of the fill being placed at the South Maybe Canyon Dump. The tests were conducted at an elevation of about 125 ft (38 m) above the base of the dump. Two test sites were selected. At each site a four ft (1.2 m) diameter test area was created by hand shoveling a small dike into the shape of a circle. A two-in throat Parshall flume was placed through the dike and used to measure the flow rate of water into the test area. Water was supplied from a water truck. The tests were conducted for the purpose of estimating the capacity of the french drain currently being constructed at the South Maybe Canyon Dump.

Compression tests

Compression tests were performed on samples of chert and waste shale material. The testing apparatus consisted of a standard 2.50 in (63.5 mm) diameter fixed ring consolidometer as shown on the schematic of Figure III-10. The consolidometer was placed in a loading frame as shown on Figure III-11 (see page 24). A 4.44 in (112.7 mm) diameter fixed ring consolidometer was used on some of the waste shale samples. Loads were applied to the samples in increments for which each increment doubled the previous load on the sample. The maximum load produced a pressure of about 32,000 lb/ft^2 (1532.1 kPa). The materials could be saturated through a small hole in the side of the consolidometer.

The compression tests were used to evaluate the relative compressibility of the spoil material, and to predict post construction settlement.

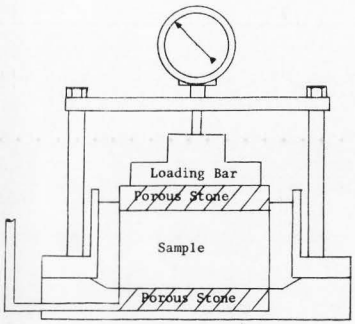

Figure III-10. Schematic diagram of compression test.

Shear strength tests

Evaluating the shear strength parameters of the spoil material was accomplished by conducting several triaxial shear and direct shear strength tests.

Triaxial shear tests. Triaxial shear tests were conducted on cylindrical soil samples. These samples were placed in rubber membranes and subjected to an all round confining pressure in the apparatus shown in Figure III-12 (see page 25). An axial load or deviator stress was then applied through a proving ring until the sample failed. Several samples were tested at different confining pressures.

Direct shear tests. Direct shear tests were conducted on samples placed in the cylindrical shear box shown in Figure III-13 (see page 25). A normal load was placed on the sample. The sample was then subjected to a horizontal shearing load until it failed.

Results from the triaxial shear and direct shear tests were used to plot Mohr's failure envelopes for various conditions. The values of the friction angles (ϕ) and the cohesive strengths (c) were determined from these failure envelopes. The values of ϕ and c are useful in determining the structural behavior of the soil for various conditions. Mohr's failure envelope is based on Mohr's failure theory and is discussed in the next section.

Mohr's failure theory. A Mohr's failure envelope can be established from the results of either direct shear or triaxial shear strength tests. In a direct shear test a normal load is applied to the sample which is then subjected to a horizontal shearing load as shown on Figure III-14. The shearing load is increased until the sample fails. The normal stress and shearing stress are then determined and represent the stress conditions on a horizontal plane at the time of failure. The horizontal plane is the plane of failure. The normal stress and shearing stress on the failure plane are then plotted on a coordinate grid and represent a point on Mohr's failure envelope. The normal stress is plotted along the horizontal axis and the shearing stress is plotted on the vertical axis. The vertical axis actually represents the shear strength of the soil once the failure envelope has been constructed. The failure envelope is approximately a straight line which connects several points established from a series of direct shear tests conducted at different normal loads, see Figure III-15. All points on the envelope represent a critical combination of shearing and normal stress that constitute failure. A point which falls above the failure envelope such as point F in Figure III-15 represents a condition which is not possible since the shear stress associated with this condition is greater than the shear strength the soil can exhibit under this particular normal stress. A point which falls below the failure envelope such as point E in Figure III-15 has a shearing stress less than the actual strength of the soil at this particular normal stress and, therefore, represents a safe condition.

Mohr's failure envelope can also be obtained from a series of triaxial tests. The failure envelope is constructed tangent to a series of Mohr's stress circles which represent the stress

Figure III-5. Proctor cylinder (1/30 ft^3 volume (9.40×10^{-4} m^3)) and 5.5 lb (24.47 N) hammer.

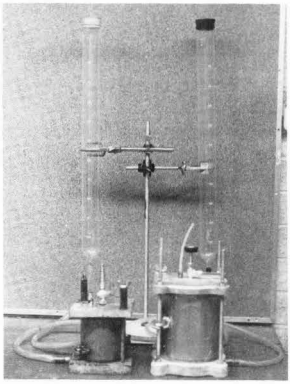

Figure III-9. Constant head permeameters.

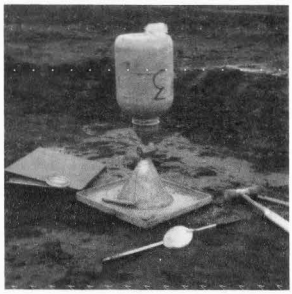

Figure III-8. Sand cone apparatus for determining the in-place dry unit weight.

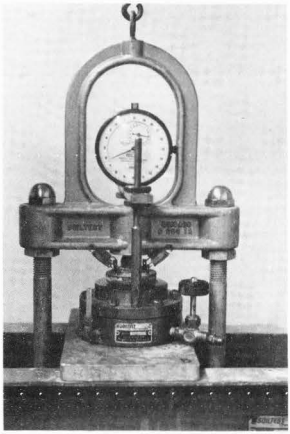

Figure III-11. 4.4 in (1.12×10^{-1} m) diameter fixed ring consolidometer and loading frame.

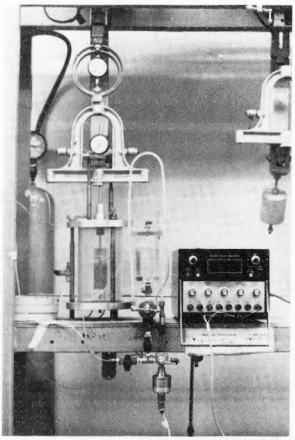

Figure III-12. Triaxial testing apparatus also showing back pressure device.

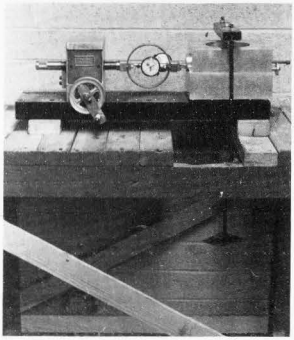

Figure III-13. Direct shear testing apparatus.

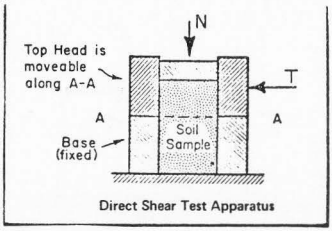

Figure III-14. Illustration of the direct shear test (after Dunn, Anderson and Kiefer, 1976).

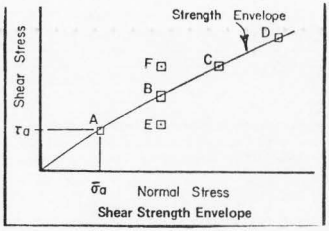

Figure III-15. Failure envelope established from direct shear testing (after Dunn, Anderson, and Kiefer, 1976).

condition at failure during triaxial tests conducted on samples at different all around confining pressures as shown in Figure III-16. Again, the vertical axis represents shearing strength and the horizontal axis represents the normal stress. Each Mohr's circle is established by measuring the major and minor principal stresses, σ_1 and σ_3, respectively, at failure. In a triaxial test the vertical and horizontal planes are the principal planes (no shear stresses exist on these planes) and, therefore, the principal stresses are the confining

pressure (σ_3) and the confining pressure plus the additional applied axial stress at failure (σ_1).

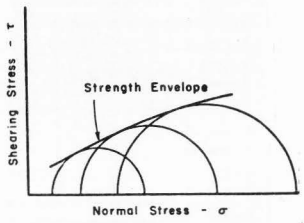

Figure III-16. Failure envelope shown tangent to Mohr's circles from three triaxial shear tests (after Dunn, Anderson and Kiefer, 1976).

The angle at which the failure envelope is inclined relative to the horizontal axis is the angle of internal friction (ϕ) of the soil and the intersection of the envelope with the vertical axis represents the cohesive strength of the soil.

Three types of drainage conditions are generally associated with triaxial testing and are used to simulate different field conditions. These drainage conditions include unconsolidated undrained, consolidated undrained, and consolidated drained.

The unconsolidated undrained test. The unconsolidated undrained test (UU) is used to simulate a short-term or end of construction condition. The sample is placed in the pressure chamber and subjected to an all round confining pressure without allowing the sample to drain. Directly after the confining pressure is applied, an axial load is applied. No drainage is allowed during testing. Several tests are conducted at various confining pressures and the failure envelope is constructed. The resulting strength is called the undrained strength. These strength parameters are used in a total stress stability analysis.

The consolidated undrained test. The consolidated undrained test (CU) generally is used to simulate a long-term condition. The sample is placed in a pressure chamber and subjected to an all round confining pressure. The sample is then allowed to completely consolidate under the influence of the confining pressure. When the sample has consolidated, the drain lines are closed and an axial load is applied until failure. The test is repeated for several different confining pressures and the strength envelope can be developed on the basis of total stresses. This is a total stress envelope. When the drain lines remain closed during the application of the axial load, pore pressures build up in saturated samples. These pore pressures can be effectively measured by means of a pressure transducer connected to porous stones at the end of the soil specimen. The pore pressure at the time of failure can then be subtracted from the total pressures and the effective stresses are obtained. Mohr's stress circles can then be plotted in terms of effective stresses. This shear strength envelope is an effective strength envelope and the resulting effective strength parameters can be used in an effective stress analysis. A typical example of both total and effective strength envelopes as determined from a CU test with pore pressure measurements are shown on Figure III-17.

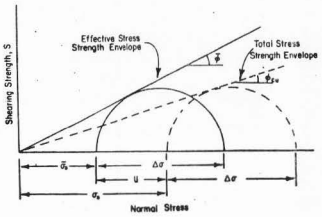

Figure III-17. Total and effective strength envelopes from CU triaxial shear tests on a normally consolidated clay (after Dunn, Anderson, and Kiefer, 1976).

The consolidated drained test. The consolidated drained test (CD) is conducted similar to the consolidated undrained test except that the sample is allowed to drain upon application of the axial load. To obtain meaningful results the load must be applied slow enough to allow for complete drainage (i.e., no build-up in excess pore pressure. The test is repeated for several different confining pressures and the resulting strength envelope is an effective stress envelope. Because fine-grained soils such as clays and silts drain very slow the CD test can be very time consuming and, therefore, is not always practical to perform.

Back pressure saturation. Performing a consolidated undrained test with pore pressure measurements requires the test specimens to be completely saturated. Saturation can normally be achieved by applying a back pressure to the soil specimen. The back pressure dissolves air which is entrapped in the samples pore spaces. The degree to which the sample is saturated is checked by increasing the cell pressure and measuring the corresponding increase in pore pressure. When the ratio of the increase in pore pressure (Δu) to the increase in cell pressure ($\Delta\sigma_3$) is equal to one the sample is 100 percent saturated. The ratio of $\Delta u/\Delta\sigma_3$ is known as the "B" value. A "B" value of 0.95 was accepted as adequate saturation for the middle waste shale samples. Figure III-12 shows the back pressure apparatus used to saturate samples during triaxial testing. The back pressure device is incorporated as part of the triaxial testing machine. The back pressure and cell pressure are increased in increments until the specimen is sufficiently saturated. The sample is then sheared.

Nutrient tests

The nutrient analysis is used to determine the deficiencies in the fertility of the soil. Fertilization recommendations are made based on the known fertilizer needs. Nutrient tests on spoil samples were performed by the Soils Testing Laboratory, Utah State University.

Results of the Field and Laboratory Tests

Classification tests

Grain size distributions were determined for 17 samples. Fifteen of the samples were taken from the Wooley Valley erosion study plots and two samples were obtained directly from surface spoil material at the North Maybe Canyon Dump. Particles larger than approximately 3.0 in (75 mm) in diameter, were discarded upon visual inspection during sampling. The results of the grain size tests are shown in Figures III-18, III-19, and III-20 and summarized in Table III-2. The material classifies as a silty-clayey gravel according to the Unified Soil Classification System. Typically, the material is composed of 30 to 50 percent gravel, 27 to 37 percent sand and 26 to 40 percent silt and clay.

Atterberg Limits were determined for 17 samples. Fifteen samples were obtained from the Wooley Valley erosion study plots and two samples from spoil material at the North Maybe Canyon Dump. The results are shown in Table III-2 and summarized on the plasticity chart of Figure III-21. The plasticity chart is a plot of liquid limit on the horizontal axis and plasticity index (liquid limit minus plastic limit) on the vertical axis. The chart is divided into regions. Inorganic clays lie above the A-line (see chart) and inorganic and organic silts lie below the A-line. The fine-grain soils are slightly plastic. The plasticity index ranges from one to nine. Low plasticity soils have liquid limits less than 50 percent and high plasticity soils have liquid limits greater than 50 percent.

The results of specific gravity tests are shown in Table III-3. These tests were conducted on 17 samples from both the Wooley Valley and Maybe Canyon mines. The value of specific gravity ranged from 2.60 to 2.77.

X-ray diffraction tests were conducted by the Department of Geology at Humboldt State University. These tests were conducted on samples of soft chert material obtained from the active Wooley Valley Mining area. In addition, the rock specimens were examined under the petrographic microscope. The rock appeared to be very fine-grained consisting of angular to subangular quartz with traces of illite. Very minor amounts of chlorite and muscovite were also present. The quartz grains are contained in an irregulatory shaped gray, presumably organic matrix. The rock specimen was classified as an organic siltstone. Although there are large quantities of chert material at both mines it is believed that some of the material referred to as chert, particularly the softer chert materials, are actually siltstones.

Relative compaction tests

The results from the in-place unit weight and field moisture tests are summarized in Tables III-4 and III-5. Table III-4 summarizes the values of field unit weights, field moistures, maximum dry unit weights, optimum moisture contents, degrees of relative compaction, and field methods of compaction for samples recovered from the surface of the Wooley Valley Dump Six and the North Maybe Canyon Dump. Table III-5 provides additional information regarding the optimum moisture and maximum dry unit weights for samples from both Wooley Valley and Maybe Canyon. Figure III-22 shows a typical moisture versus dry unit weight relationship for the waste shale material. The relative compaction of the waste shale material is very sensitive to the molding water content and changes in the molding water content result in substantial changes in the degree of relative compaction for the same compaction effort. Changes in the molding water content of the waste shales are likely to occur and will depend on the time of year as well as other geophysical conditions. Therefore, the values of relative compaction presented in Table III-4 for various compaction methods represent only reasonable estimates of compaction achieved for general placement conditions.

The relative compaction varied depending on the remolding moisture content and compaction effort. The compaction effort depends on the type of construction method in use. The end-dumped (free flowing) method results in a fairly uniform loosely deposited fill where as the scraper

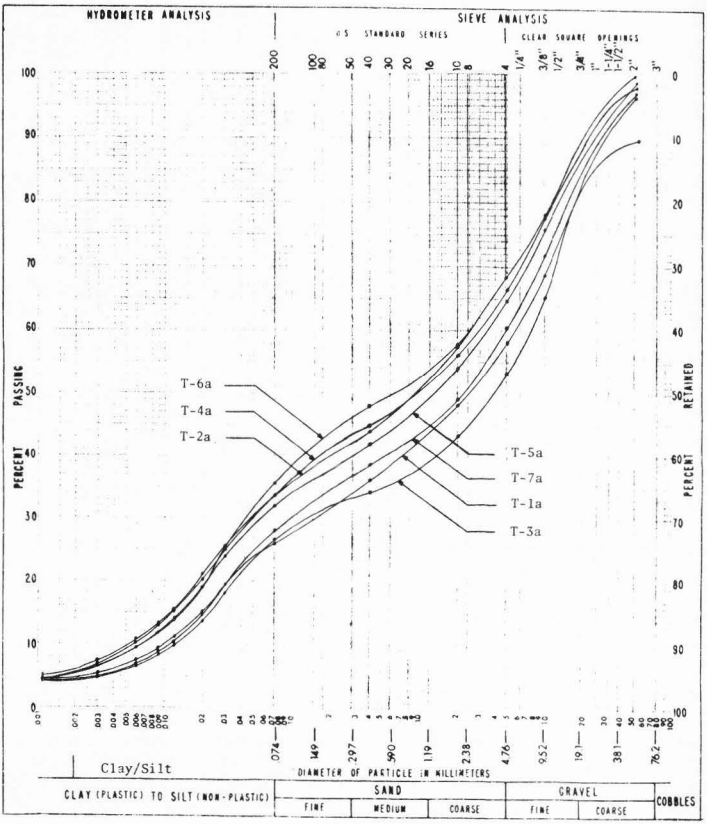

Figure III-18. Grain size curves for top soil material obtained from the Wooley Valley erosion study plots, October 1975.

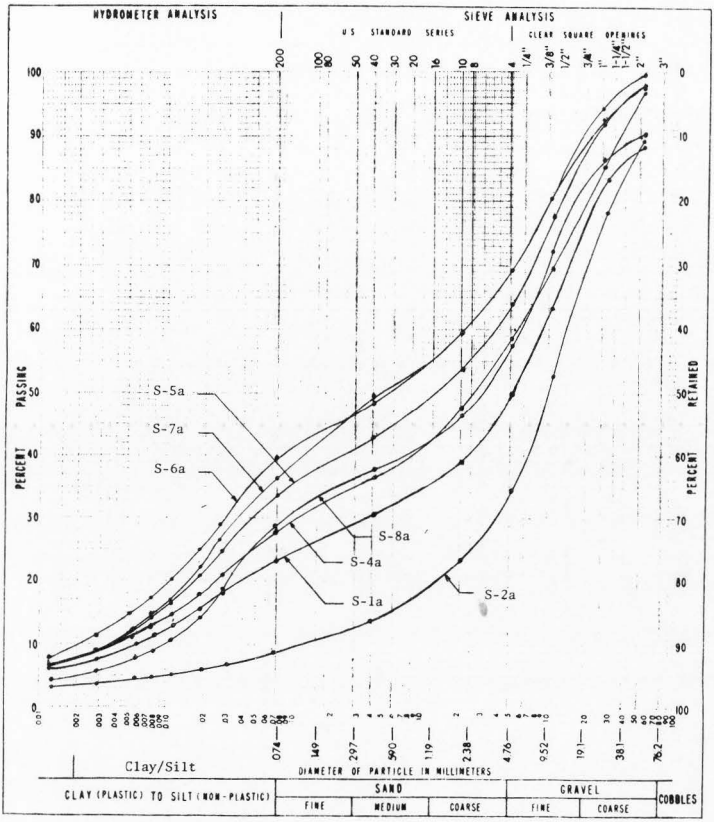

Figure III-19. Grain size curves for waste shale material obtained from the Wooley Valley erosion study plots, October 1975.

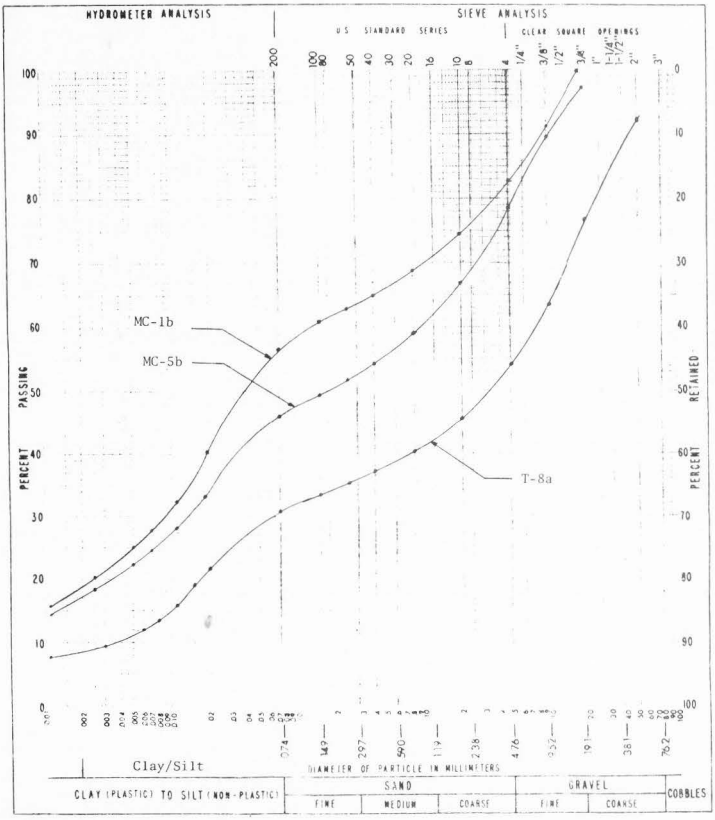

Figure III-20. Grain size curves for material obtained from the North Maybe Dump, April 13, 1976, and sample T-8a.

Table III-2. Common indexes of grain size distributions.

Sample No.	Diameter of 10% Finer Effective Size, D_{10} mm	Liquid Limit	Plastic Limit	Percent Passing #200 Sieve	Classification Unified System
S-1a	0.0070	27	22	22.78%	GM-GC
S-2a	0.1490	24	22	8.44%	GM
S-4a	0.0050	23	20	28.02%	GM
S-5a	0.0040	23	17	33.45%	GM-GC
S-6a	0.0033	24	22	39.70%	GM
S-7a	0.0045	25	15	36.23%	GC
S-8a	0.0119	18	17	27.79%	GM
T-1a	0.0088	29	23	26.24%	GM
T-2a	0.0072	27	25	33.72%	GM
T-3a	0.0135	33	27	26.67%	GM
T-4a	0.0062	27	23	33.55%	GM
T-5a	0.0060	26	26	32.26%	GM
T-6a	0.0059	26	26	35.83%	GM
T-7a	0.0105	30	25	27.82%	GM
MC-1b	less than 0.001	24	20	56.13%	ML
MC-5b	less than 0.001	27	21	45.00%	GM-GC
T-8a	0.0045	29	20	29.64%	GC

Table III-3. Summary of specific gravities.

Sample No.	Specific Gravity	Sample No.	Specific Gravity
S-1a	2.68	T-4a	2.71
S-4a	2.70	T-5a	2.68
S-5a	2.64	T-6a	2.70
S-6a	2.68	T-7a	2.68
S-7a	2.75	T-8a	2.77
S-8a	2.77	MC-1b	2.73
T-1a	2.71	MC-3b	2.72
T-2a	2.71	MC-5b	2.60
T-3a	2.66		

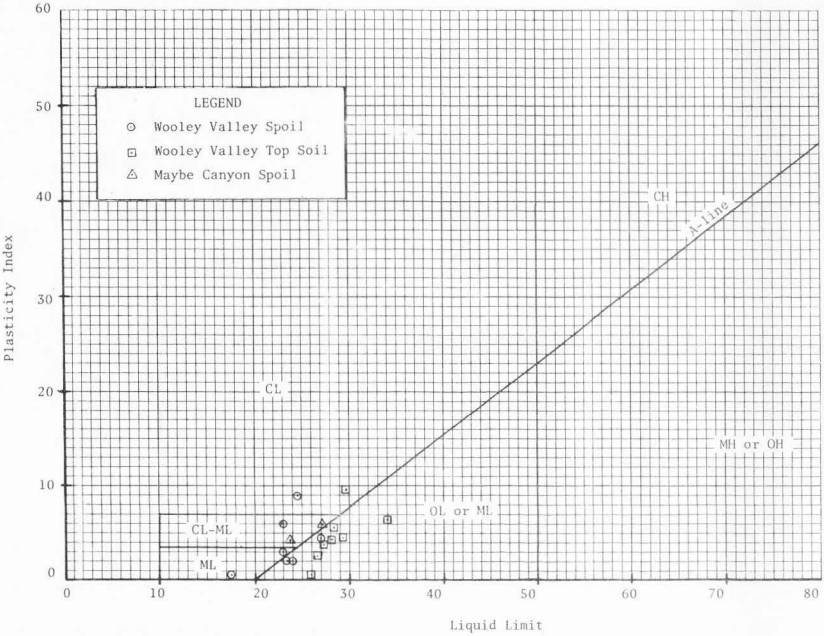

Figure III-21. Plasticity chart.

Table III-4. Summary of in-place unit weight tests.

Sample No.	Field Test ASTM-D 1556-64		Compaction Test ASTM-D 698-64T		Field Compaction Method	Relative Compaction
	γ_d $\frac{lb}{ft^3}$	w %	γ_{max} $\frac{lb}{ft^3}$	w_{op} %		
MC-1b	98.9	20.3	110.0	18.0	End-Dumped Wheel Compacted	89.9%
MC-2b	97.2	19.6	103.0	21.5	End-Dumped Wheel Compacted	94.6%
MC-3b	112.7	18.2	109.0	17.5	End-Dumped Wheel Compacted	102.8%
MC-5b	99.4	16.9	108.5	19.5	End-Dumped Wheel Compacted	92.0%
MC-1c	87.4	16.9	110.0	18.0	End-Dumped No Compaction	79.4%
MC-4c	96.8	17.9	108.5	19.0	Scraper Dumped Wheel Compacted Finished Area	89.2%
MC-5c	103.4	22.5	109.5	20.9	Scraper Dumped Wheel Compacted	94.5%
WV-2c	107.6	15.2	115.0	16.5	Scraper Dumped Wheel Compacted Finished Area	93.6%
WV-3c	99.5	18.4	105.5	22.0	Scraper Dumped Wheel Compacted Finished Area	94.3%
WV-4c	80.5	17.1	111.5	18.5	Scraper Dumped No Compaction	72.9%
WV-5c	98.6	5.3	112.0	16.0	Scraper Dumped Wheel Compacted - 1 Pass	88.0%
WV-1d	109.9	9.9	131.4	12.4	Scraper Dumped Wheel Compacted	83.4%
WV-2d	89.3	8.4	122.5	13.2	Scraper Dumped No Compaction	72.9%
WV-3d	95.3	10.9	114.0	14.0	Scraper Dumped Wheel Compacted	83.6%
WV-4d	104.4	10.8	114.5	14.8	Scraper Dumped Wheel Compacted - 1 Pass	91.2%
WV-5d	106.4	12.8	115.5	16.5	Scraper Dumped Wheel Compacted	92.1%

NOTE: 1 lb/ft^3 = 0.157 $\frac{kN}{m^3}$

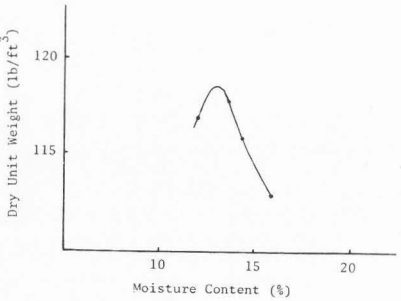

Figure III-22. Typical unit weight moisture content relationship for waste shale material (sample S-1a) as determined by ASTM-D 698-64T, Method C (1 lb/ft^3 = 0.157 kN/m^3).

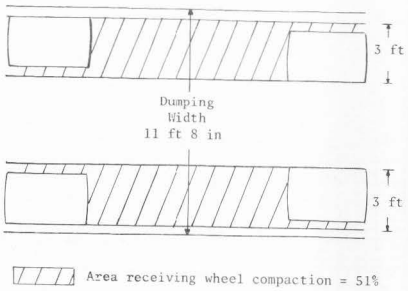

Figure III-23. Illustration of percent area receiving wheel compaction assuming drivers use same tracks for every dumping pass (1 ft = 0.305 m).

dumped method results in a fill with varying ranges of relative compaction. To provide some insight into the average relative compaction achieved by the scraper dump method relative compaction tests were conducted in areas receiving no compaction and in areas receiving some wheel compaction. The magnitude of area which would receive wheel compaction from earth moving equipment was based on measurements of the equipment and is shown on Figure III-23 (Caterpillar Corp, 1969). The average relative compaction was then evaluated. The results of these evaluations are discussed below.

Hauling and placing earthfill at the Wooley Valley Mine is done principally by 657-B push-pull type caterpillar rubber-tire scrapers. The fill material is placed in horizontal lifts approximately one to two ft (.3 to .6 m) thick. The resulting dump receives a substantial amount of wheel compaction. The scraper tire width is about 2 ft 9 in (6.84 m). The wheel base width on the scraper is 11 ft 8 in (3.6 m). A fully loaded 657-B scraper carries about 44 yd^3 (34 m^3) of material. For a lift thickness of 1.5 ft (.45 m) the dumping length would be about 68 ft (21 m). The length of a spoil dump generally exceeds 1000 ft (305 m) and, therefore, the placement of an 11 ft 8 in (3.6 m) wide section over the entire length of the dump can take over ten full loads. If the scraper operators are instructed to split wheel tracks during the dumping operation, nearly 100 percent of the area could receive some wheel compaction. If, however, the scraper drives over the same wheel tracks during the placement of a single row, the area receiving wheel compaction is reduced substantially. The exact amount of area is illustrated diagramatically on Figure III-23 and is approximately 51 percent of the total area.

This would represent the minimum amount of area which could be covered during spoil placement. The results of in-place dry unit weight tests show that scraper dumped areas receiving no wheel compaction have an average relative compaction of approximately 72.5 percent and areas receiving some wheel compaction have a relative compaction of 89 percent. A relative compaction of 89 percent was typical of areas receiving only one wheel pass as well as areas receiving several wheel passes. Based on this data the minimum average relative compaction for a scraper filled spoil dump would be approximately 81 percent. The maximum relative compaction would result when the entire dump receives wheel compaction and would equal nearly 89 percent. The actual relative compaction of spoil material at the Wooley Valley Dump is, therefore, likely to be somewhere between 81 percent and 89 percent. A reasonable estimate would be approximately 85 percent.

Hauling and placing earthfill at the Maybe Canyon Mine is done almost entirely by end-dumping material with off-highway end-dump trucks. The only areas receiving wheel compaction are finished areas and haul roads. These areas represent a small fraction of the entire dump. The resulting in-place unit weights average approximately 79 percent relative compaction. Areas receiving wheel compaction have substantially increased degrees of relative compaction as shown on Table III-4. However, these areas are small and constitute only a minor portion of the entire volume of the dump material. The average

Table III-5. Summary of compaction tests (ASTM-D 698-64T, Method C).

Sample Number	Optimum Moisture Content	Maximum Dry Unit Weight
S-1a	13.5%	117.5 lb/ft^3
S-4a	13.5%	117.0 lb/ft^3
S-5a	16.0%	113.2 lb/ft^3
S-6a	16.0%	111.8 lb/ft^3
S-7a	16.0%	113.0 lb/ft^3
S-8a	12.0%	117.5 lb/ft^3
T-2a	17.2%	110.0 lb/ft^3
T-4a	18.4%	108.0 lb/ft^3
T-5a	16.2%	112.5 lb/ft^3
T-6a	18.5%	108.5 lb/ft^3
T-7a	18.0%	109.0 lb/ft^3
MC-1b	18.0%	110.0 lb/ft^3
MC-2b	21.5%	103.0 lb/ft^3
MC-3b	17.5%	104.0 lb/ft^3
MC-5b	19.0%	108.0 lb/ft^3
MC-1c	18.0%	110.0 lb/ft^3
MC-4c	19.0%	108.5 lb/ft^3
MC-5c	20.9%	109.5 lb/ft^3
WV-2c	16.5%	115.0 lb/ft^3
WV-3c	22.0%	105.5 lb/ft^3
WV-4c	18.5%	111.5 lb/ft^3
WV-5c	16.0%	112.0 lb/ft^3
WV-1d	12.4%	131.-4 lb/ft^3
WV-2d	13.2%	122.5 lb/ft^3
WV-3d	14.0%	114.0 lb/ft^3
WV-4d	14.8%	114.5 lb/ft^3
WV-5d	16.5%	115.5 lb/ft^3

NOTE: 1 lb/ft^3 = 0.157 $\frac{kN}{m^3}$

in-place relative compaction at the North Maybe Canyon Dump is estimated at 79 percent.

The Bureau of Reclamation specifies relative compactions of 95 to 98 percent of standard proctor for earth dam design. Comparing the degrees of relative compaction achieved by the above two construction methods with the Bureau's specifications provides insight as to how well the spoil material is compacted upon placement.

Permeability tests

Results from constant head permeability tests were obtained using material from samples MC-1b, MC-2b, MC-5b, and S-7a. The samples were prepared at a moisture content 2 percent dry of optimum moisture and at relative compactions ranging from 86.4 percent to 94.8 percent. The results of these tests are presented in Table III-6. The average permeability for these samples was 32 ft/yr (3×10^{-5} cm/sec). The average permeability probably is representative of the permeability of waste shales within the dump. However, the effects of surface compaction, weathering and siltation from surface erosion could substantially reduce the permeability at the dump surface. This low permeability at the dump surface could then lead to ponding on top of the dump.

Percolation tests were conducted on the north wing of the South Maybe Dump currently being constructed. These tests were performed for the purpose of determining the flow capacity of a french drain that is being constructed in the bottom of the dump. The top surface of the test sites selected were essentially horizontal and approximately 125 ft (38 m) above the valley floor. The infiltration rates were monitored over a 20 minute time period. At both sites the flow reached a constant rate very rapidly (less than 30 seconds). The infiltration rates were calculated by dividing the measured flow rates by the surface area of the corresponding test site. At test site one the steady-state infiltration rate was $I_1 = 4.23 \times 10^{-3}$ ft/sec (0.13 cm/sec) and at test site two $I_2 = 5.53 \times 10^{-3}$ ft/sec (0.16 cm/sec). The hydraulic conductivities at sites one and two will also equal the values of I given above because the hydraulic gradients during testing were equal to unity.

An estimation of the capacity of the french drain was subjected to a number of assumptions. The most crucial assumptions were probably associated with estimating the permeability of the much coarser materials in the bottom of the fill which constitute the french drain and assuming that flow through the french drain will be laminar (i.e., that Darcy's law applies). It was estimated that the hydraulic conductivity at the bottom of the fill was about 100 times the material tested. A number of other assumptions were made and include:

1. The permeability of the french drain varies linearly from K = 0.50 ft/sec (15.0 cm/sec) at the bottom to 0.50×10^{-2} ft/sec (0.15 cm/sec) at a position 100 ft (30.48 m) from the bottom.

2. The hydraulic gradient (i) is constant along the entire length of the drain.

3. The same quantity of water is flowing through all cross-sections of the french drain at the depths given and the water movement is one-directional.

4. The cross-sections of the french drain do not vary and are equal to the average values given in Table III-7.

Under these assumptions the capacities of the french drain were determined as a function of water depth and hydraulic gradients (i) and are given in Table III-8 as flow rates.

Table III-6. Summary of permeabilities.

Sample No.	Dry Unit Weight (lb/ft^3)	Relative Compaction	Permeability (cm/sec)
MC-2b	90.0	86.4%	2.55×10^{-5}
MC-1b	101.7	92.5%	4.59×10^{-5}
MC-5b	102.4	94.8%	1.92×10^{-5}
S-7a	103.2	91.3%	3.32×10^{-5}
		AVERAGE	3.10×10^{-5}

NOTE: 1 cm/sec = $1.03 \times 10^6 \frac{ft}{yr}$

$1\ lb/ft^3 = 0.157 \frac{kN}{m^3}$

Table III-7. Cross-sectional areas of french drain for various assumed depths of water.

Assumed depth of Water (ft)	Area (ft^2)			
	Section #1	Section #2	Section #3	Average
5	248	124	140	171
10	888	368	512	589
15	1640	752	1132	1175
20	2980	1240	1884	2035
25	4368	1792	2792	2984
30	5980	2588	3764	4111
40	9324	4472	6744	6847
50	13460	7040	10648	10383

NOTE: 1 ft = 0.305 m

$1\ ft^2 = 0.093\ m^2$

Table III-8. Estimates of flow rate that the french drain might be expected to pass for various depths and hydraulic gradients (i). Values given in the table are in ft^3/sec.

Depth (ft) \ i	0.07	0.14	0.21
0	0	0	0
5	5.0	10	15
10	19.	38	57
15	36	72	108
20	56	112	168
30	105	210	315
40	161	322	
50	220	440	
100	420		

NOTE: $1\ \frac{ft^3}{sec} = 0.028\ \frac{m^3}{sec}$

1 ft = .305 m

Compression tests

An evaluation of the settlement characteristics of spoil material was based on the results of confined compression tests performed on samples of both chert and waste shales.

Chert material. Two grades of chert material were tested, a hard resistive chert and a soft chert (more appropriately classified as a silt stone). The material was crushed in the laboratory to obtain the desired particle size. The hard chert material broke down into angular shaped particles and the soft chert material broke down into platey shaped particles. The crushed particles were screened and the material retained between a number 4 and 20 sieve was used in the compression tests. This particle size produced a 6:1 ratio between the diameter of the consolidometer and the maximum particle size. Sowers et al. (1965) recommended this ratio for compression tests on crushed rock.

The compression tests were conducted on samples subjected to three different moisture treatments. These included dry samples, samples receiving continual cycles of wetting and drying, and dry samples which were saturated after reaching various stress levels. Load increments were applied to the samples and maintained constant for periods of 3 to 4 days. The loads resulted in normal stresses on the sample of 250 lb/ft^2 (11.97 kPa) to 32,000 lb/ft^2 (1532.1 kPa). The cycles of wetting and drying were applied on an alternating basis and each cycle was maintained for a period of one day. The results of these tests were plotted as strain log time and strain log pressure curves. A typical strain log time curve is shown in Figure III-24. Strain log time curves for all other chert samples tested are contained in Appendix A. The strain log pressure curves are shown in Figures III-25 through III-32. The strain was computed as the settlement divided by the original sample height. The strain versus log of time curves indicated that both the hard and soft cherts experienced nearly instantaneous initial settlement followed by a continuing gradual settlement approximating the shape of a straight line on semi log paper.

The shape of the strain versus log of pressure curves also approximated the shape of straight lines. Steep strain versus log pressure curves indicate a compressible material and flat curves indicate material of low compressibility. Hard and soft samples of chert showed similar compression characteristics when tested dry. Samples of hard chert showed no significant increases in compressibility when treated with cycles of wetting and drying, however, substantial increases in compressibility were measured for samples of soft chert subjected to cycles of wetting and drying. The log of stress versus strain curves were nearly twice as steep for soft chert samples treated with wet and dry cycles. Large increases in settlement were also measured for soft cherts when saturated after reaching various stress levels. Dry samples of soft chert material were saturated after reaching stress levels of 16,000 lb/ft^2 (766.1 kPa) and 32,000 lb/ft^2 (1532.3 kPa). An increase in strain of about 67 percent occurred at 16,000 lb/ft^2 (766.1 kPa) while the amount of strain more than doubled at a stress of 32,000 lb/ft^2 (1532.3 kPa). This increase in settlement occurred immediately after the samples were saturated. For a given stress level the ultimate vertical strain after saturation was approximately equal to the vertical strain which occurred during cycles of wetting and drying (see Figure III-33). The effect that moisture has on the magnitude of vertical strain in soft chert materials seems to be independent of the nature in which it is applied, that is, if water surrounds soft chert material the magnitude of strain for a given load is likely independent of whether previous cycles of wetting and drying occurred. Samples of hard chert material were maintained saturated for over 24 hours while at stress levels of 32,000 lb/ft^2 (1532.3 kPa) and no significant change in settlement occurred.

The substantial increases in settlement of soft chert material when treated with water either by saturation or cycles of wetting and drying is not completely understood. Close examination of this material through x-ray powder diffraction revealed traces of the clay mineral illite. It is believed that the illite reacts with water to reduce the strength of the soft chert. One possible explanation is that the illite may soften upon contact with water resulting in crushing near particle contact points.

Clay chemistry and the double layer theory provide additional insight concerning the softening of the illite. The lack of free water within the colloidal system results in tension forces in the double layer water. The clay particles, therefore, are held together by large capillary forces. The addition of free water by saturation or cycles of wetting and drying eliminates the negative pore water pressures in the double layer and thus, the capillary forces are reduced. The material looses strength and crushing proceeds until the contact areas increase and an equilibrium stress condition is reached.

Waste shale material. Samples of middle waste shale material were tested to determine their compression characteristics. The material was passed through a number ten sieve and the larger material was discarded. To simulate moisture placement conditions the samples were prepared at approximately 2 percent dry of optimum moisture content. Samples were prepared at relative compaction ranging from 82.4 percent to 96.4 percent. A number of these samples were saturated at various stress levels. Load

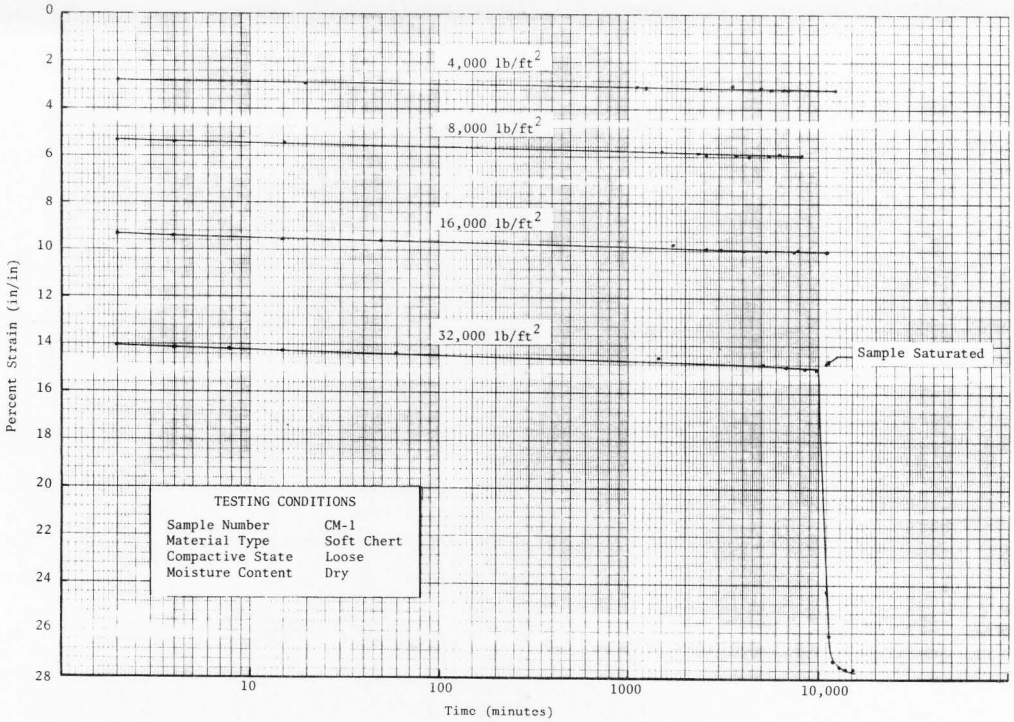

Figure III-24. Time versus compression characteristics of soft chert showing effect of saturation after reaching a stress level of 32,000 lb/ft^2 (lb/ft^2 = .0479 kPa).

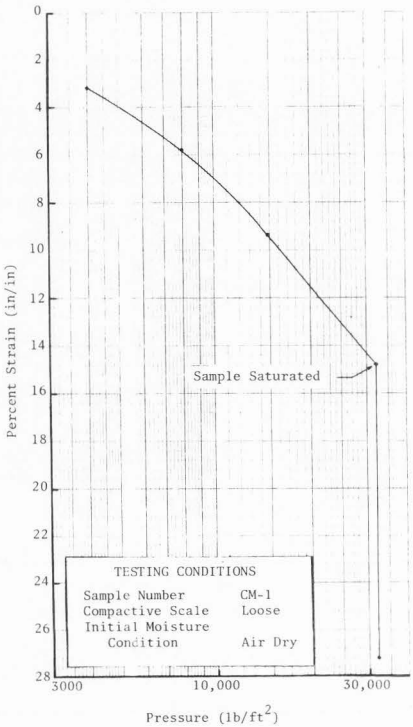

Figure III-25. Strain log pressure relationship for soft chert showing effects of saturation at a stress level of 32,000 lb/ft^2 (1 lb/ft^2 = .0479 kPa).

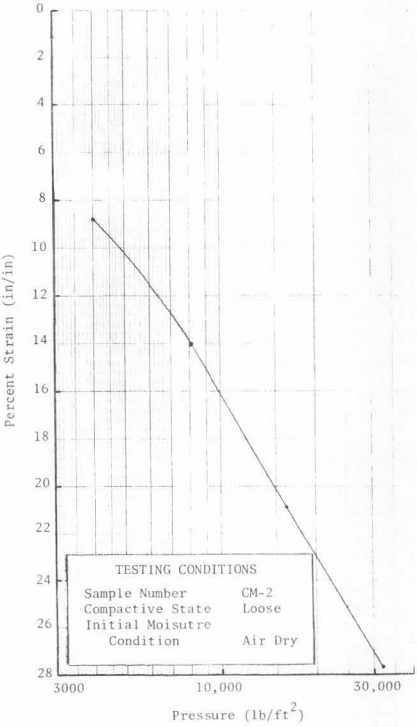

Figure III-26. Strain versus log pressure relationship for soft chert subjected to cycles of wetting and drying (1 lb/ft^2 = .0479 kPa).

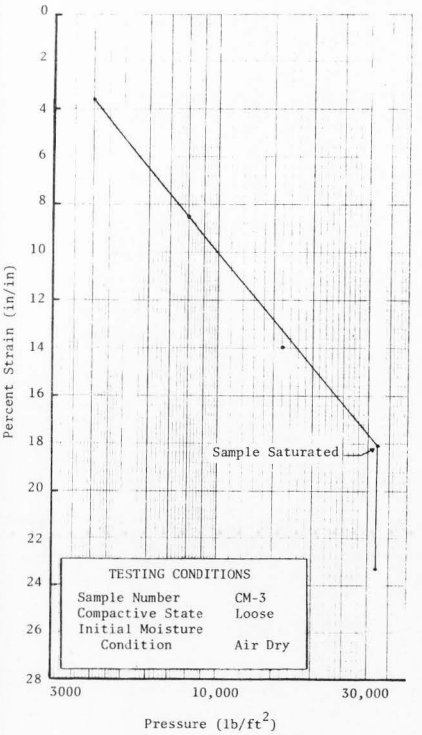

Figure III-27. Strain versus log pressure relationships for soft chert showing effects of saturation at a stress level of 32,000 lb/ft^2 (1 lb/ft^2 = .0479 kPa).

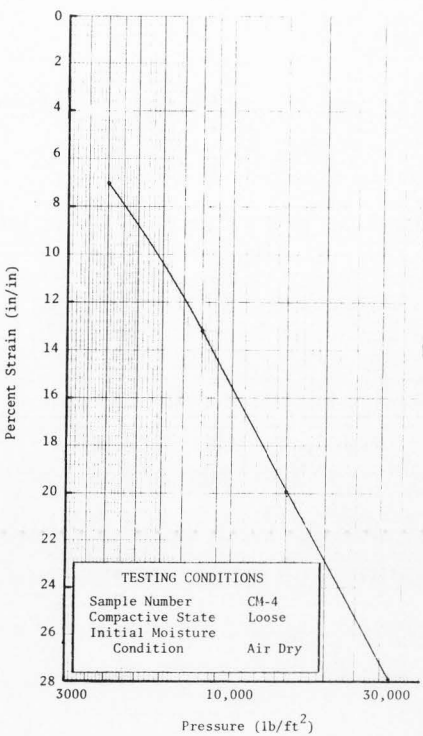

Figure III-28. Strain versus log pressure relationship for soft chert subjected to cycles of wetting and drying (1 lb/ft^2 = .0479 kPa).

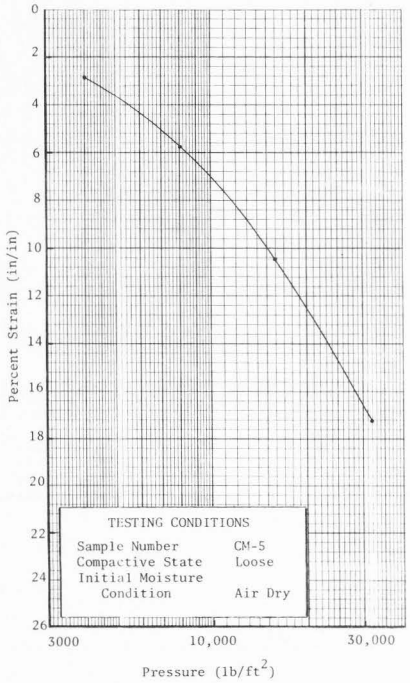

Figure III-29. Strain versus log pressure relationships for soft chert (1 lb/ft^2 = .0479 kPa.

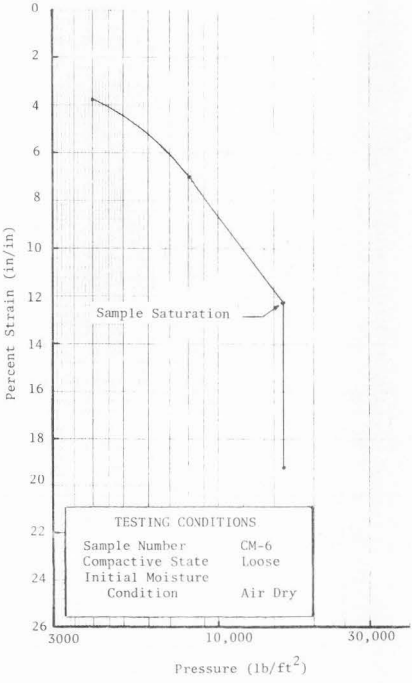

Figure III-30. Strain versus log pressure relationship for soft chert showing effect of saturation at a stress level of 16,000 lb/ft^2 (1 lb/ft^2 = .0479 kPa).

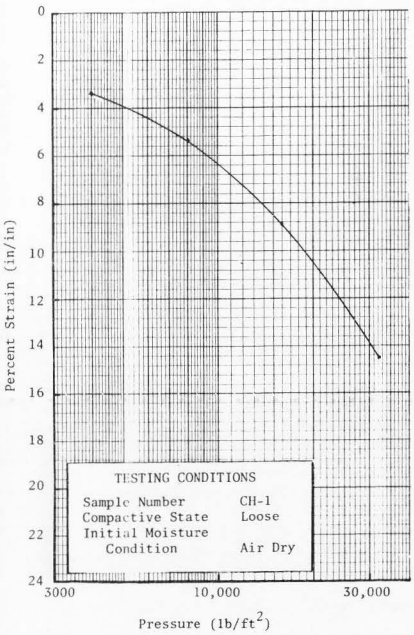

Figure III-31. Strain versus log pressure relationship for hard chert material subjected to cycles of wetting and drying (1 lb/ft^2 = .0479 kPa).

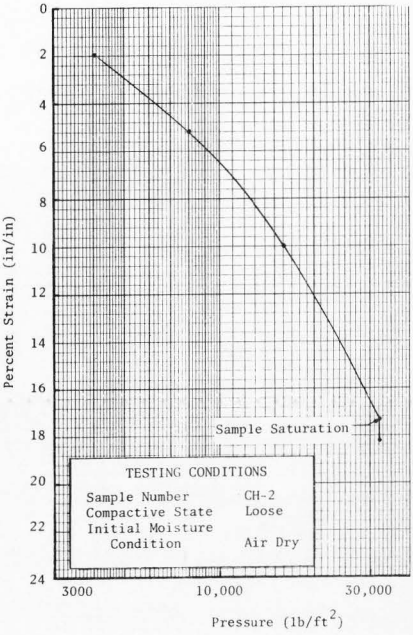

Figure III-32. Strain versus log pressure relationship for hard chert showing effect of saturation at a stress level of 32,000 lb/ft^2 (1 lb/ft^2 = .0479 kPa).

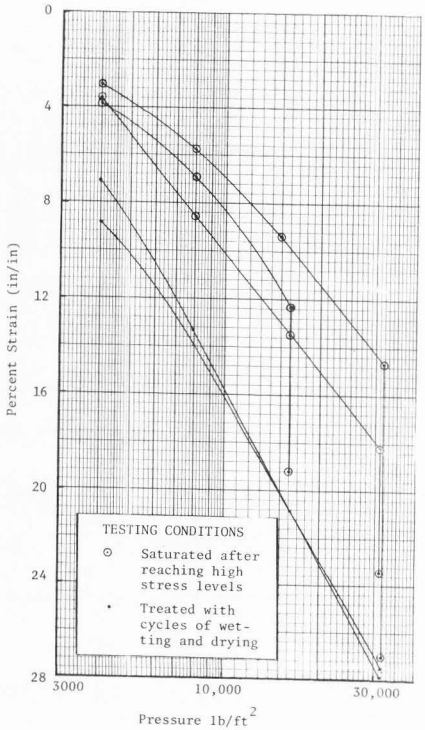

Figure III-33. Strain versus log pressure relationships for soft chert showing effects of moisture treatments (1 lb/ft^2 = .0479 kPa).

increments were applied to the samples each day and resulted in normal stresses ranging from 500 lb/ft (23.94 kPa) to 32,000 lb/ft (1532.10 kPa). The results are summarized on strain versus log time and strain versus log pressure curves. The strain versus log time curves are contained in Appendix A. A typical strain versus log time curve is shown on Figure III-34. The strain versus log pressure curves are given in Figures III-35 through III-41.

The effect of compaction on the compressibility of waste shale material is illustrated by the strain versus log pressure curves of Figures III-39 through III-41. Increased compaction significantly reduces the compressibility of the middle waste shale material.

The effect that an increase in moisture has on the compressibility of the middle waste shale material is shown on Figures III-35 through III-38. The waste shales are sensitive to water. Increases in compression occur not only upon saturation but upon small increases in the moisture content. The strain versus log pressure curves, Figures III-37 and III-38, show increased compressibility at low stress levels as a result of the addition of minor amounts of water. The water was added to prevent these samples from drying out. A minor amount of additional compression occurred upon saturation of these two samples at high stress levels. Figures III-35 and III-36 show increases in compression for waste shales upon saturation at low stress levels. Any increase in the moisture content appears to induce compression of the waste shale material.

Much of the compression occurring in the middle waste shale samples takes place almost immediately after the application of a load. This nearly instantaneous compression is followed by a slow compression which is linear with the log of time much like the rate of compression for chert material. Complete saturation of relatively dry samples of middle waste shales causes an immediate increase in compression (collapse settlement). If the moisture content is increased by a small amount, the rate of increased compression is much slower as compared to the rate upon saturation.

Additional compression upon increases in moisture content is probably caused by a collapse of the soil structure resulting from a reduction in capillary stresses. Compression resulting from a reduction in capillary stresses has been described previously. Collapse settlement is explained by Mitchell (1976). The middle waste shales may collapse when the clay particles become weaker as a result of swelling caused by increases in moisture.

Shear strength tests

To evaluate the mass stability of spoil dumps it was necessary to determine the strength characteristics of the different spoil materials. The strength parameters depend on various physical factors some of which are subject to changes. These factors include the dry unit weight and moisture content at the time of placement, the existing pore water pressure conditions, the existing moisture content and the degree of consolidation or compression which has taken place as the result of the overburden pressures. Both triaxial shear and

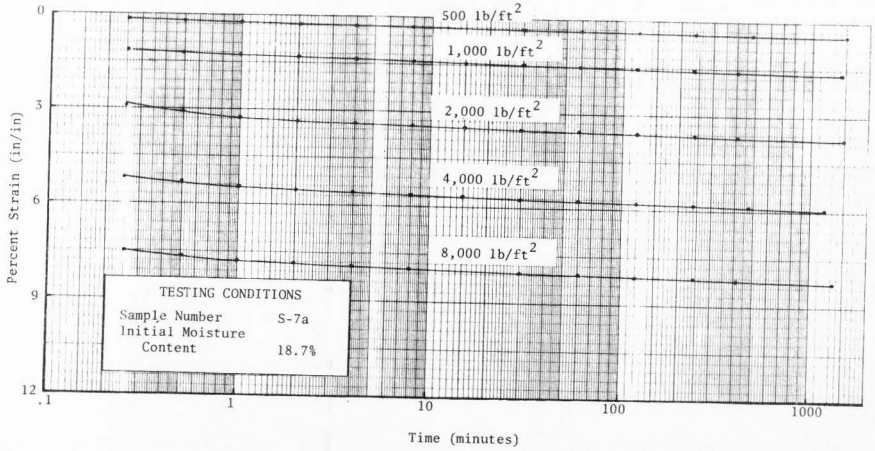

Figure III-34. Time-compression characteristics of waste shale material compacted to 82.4% R.C.

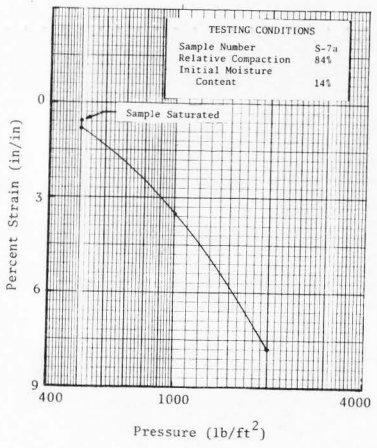

Figure III-35. Strain versus log pressure relationship for waste shale showing effect of saturation at a stress level of 500 lb/ft^2 (1 lb/ft^2 = .0479 kPa).

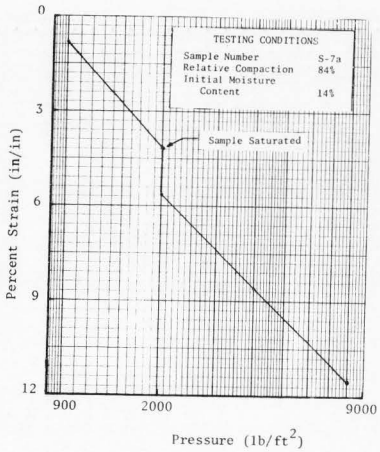

Figure III-36. Strain versus log pressure relationship for waste shale showing effect of saturation at a stress level of 2000 lb/ft^2 (1 lb/ft^2 = .0479 kPa).

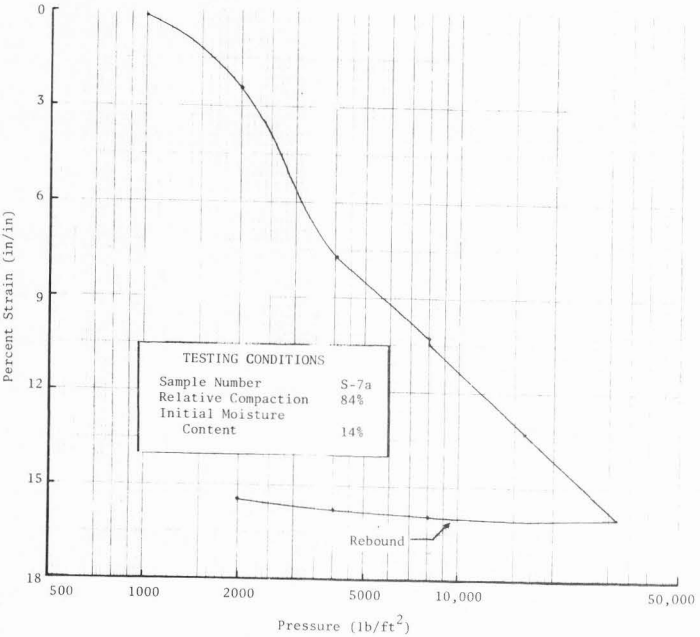

Figure III-37. Strain versus log pressure relationship for waste shale material showing effect of increasing the moisture content at low pressures (1 lb/ft^2 = .0479 kPa).

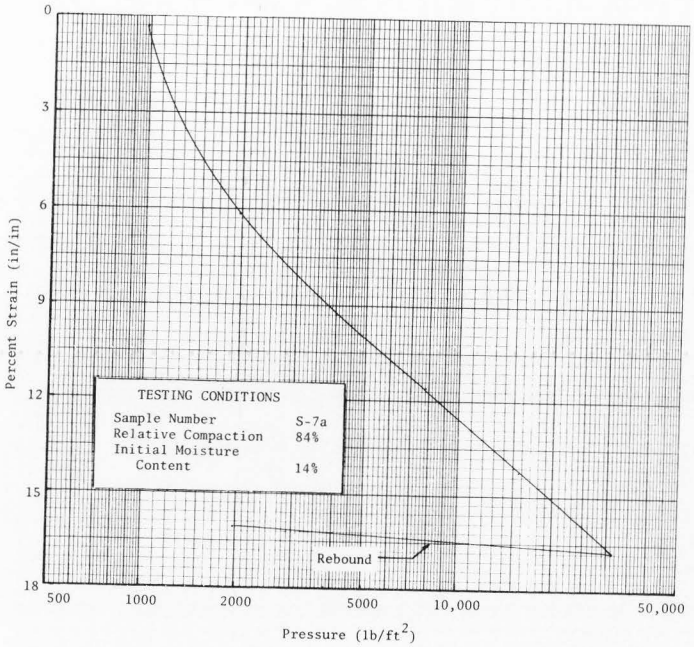

Figure III-38. Strain versus log pressure relationship for waste shale showing effect of increasing the moisture content at low pressures (1 lb/ft^2 = .0479 kPa).

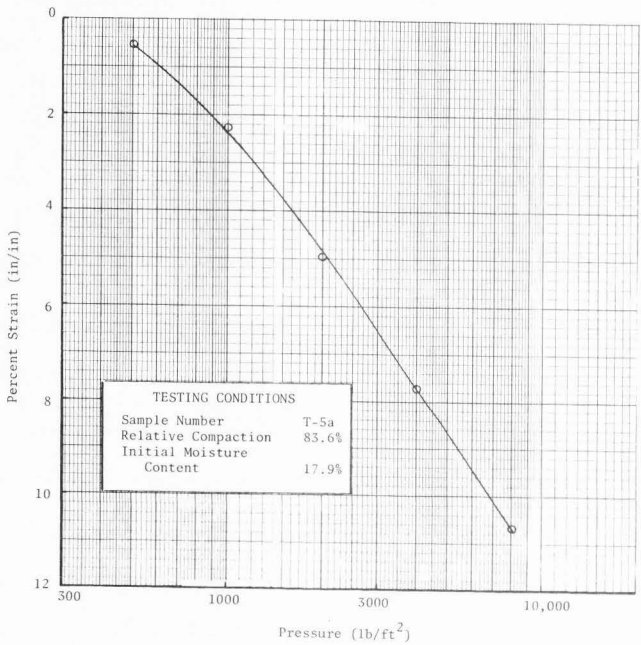

Figure III-39. Strain versus log pressure relationship for top soil material compacted at 83.6% RC (1 lb/ft^2 = .0479 kPa).

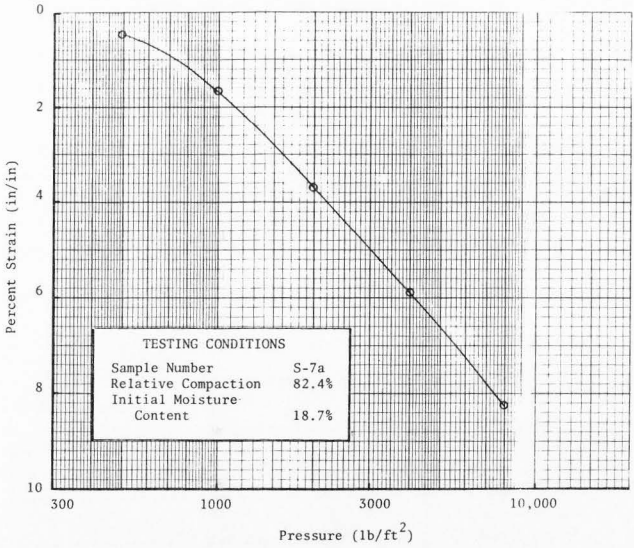

Figure III-40. Strain versus log pressure relationship for waste shale material compacted at 82.4% RC (1 lb/ft^2 = .0479 kPa).

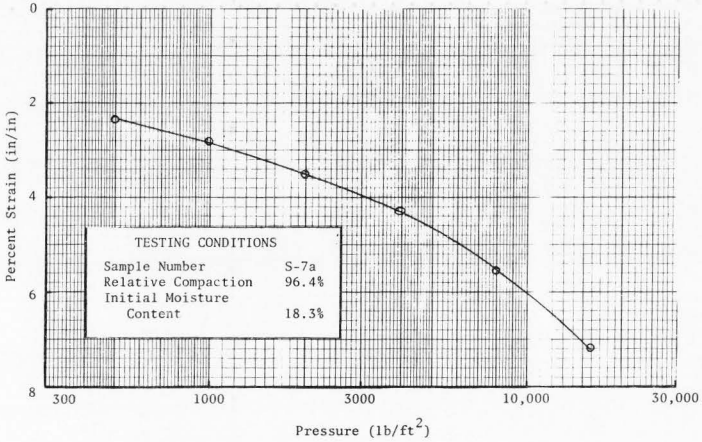

Figure III-41. Strain versus log pressure relationship for waste shale compacted at 96.4% RC (1 lb/ft^2 = .0479 kPa).

direct shear tests were, therefore, performed on specimens prepared under various conditions. These tests were conducted on samples of crushed chert and middle waste shales.

Crushed chert. Direct shear tests on samples of both soft and hard crushed chert were performed. Tests were conducted on both loose and dense dry samples, and on saturated samples which were soaked for over 24 hours. The loose samples were prepared by pouring the material into the apparatus without compaction. The dense samples were prepared by vibrating the apparatus while pouring in the chert material. The apparatus was vibrated by tapping the sides with a rubber mallet. The saturated samples were soaked after placement and application of the normal load. These samples were prepared in a dense state. The results of the direct shear tests are summarized by stress versus strain curves and Mohr's failure envelopes, Figures III-42 through III-51. The friction angles for soft chert ranged from 48 degrees to 54 degrees for loose and dense states respectively. Hard cherts exhibited friction angles of 44 degrees and 48 degrees for loose and dense states respectively.

Densifying the chert material increases the friction angle for both the soft and hard chert material. The soft cherts exhibited greater friction angles of both loose and dense states than did the hard chert. Saturation had no appreciable effect on the value of the friction angle for either the soft or hard chert material.

Middle waste shale. Twenty triaxial shear tests were performed on samples of middle waste shale material. The test results are summarized on the stress versus strain curves and on Mohr's failure envelopes, Figures III-52 through III-67.

To provide useful results the test specimens were prepared to simulate conditions likely to occur during construction and possible long-term conditions. A number of factors were considered when attempting to prepare specimens to simulate these conditions. The results from field testing indicated that during construction the waste shale is typically placed at moisture contents approximately 2 percent dry of optimum. Because of the different construction methods used to dispose of the waste shale material the dry unit weight upon placement also varies from site to site. Therefore, triaxial specimens were initially prepared at moisture contents 2 percent dry of optimum and at dry unit weights corresponding to 80, 90, and 100 percent relative compactions. As additional waste shale materials are placed in the disposal area, the lower portions of the embankment begin to compress under the influence of the overburden load. The rate at which this compression takes place is of crucial importance. Test specimens were observed to compress very rapidly when subjected to the all round chamber pressures. The waste shale material in the field is also likely to compress rapidly during construction. It is believed that the waste shales have sufficient time to fully compress during embankment construction. Therefore, all test specimens were allowed to completely compress under the all round chamber pressure prior to shear.

The shear strength parameters corresponding to the during construction condition were determined from tests conducted on specimens prepared by the method described above. The results show the material behaves essentially as a cohesionless material except at low pressures where the failure envelopes change shape (see Figures III-55 and III-57) and intersect the vertical axis indicating a small value of cohesive strength. This cohesion is probably due to capillary forces (negative pore pressures) developing in the sample at these low pressures. This cohesion can only be mobilized at very shallow depths. The values of the friction angles for the during construction condition as simulated from these tests were 31.0 degrees, 37.9 degrees and 47.5 degrees for relative compactions of 80, 90, and 100 percents respectively, see Table III-9. However, assuming saturation occurs is reasonable and represents a condition which might result from extreme flooding or the continual melting of large snow masses which become buried near embankment slopes. These samples were initially prepared at relative compaction of 80, 90, and 100 percent and at moisture contents of 2 percent dry of optimum to simulate field placement. The samples were then saturated through a porous stone connected to both the specimens and a small reservoir. Water was allowed to percolate up through the sample and out to the top of a second porous stone connected at the top of the specimen and to a drain line. After several hours of percolation the drain valve was closed and any remaining entrapped air was dissolved with back pressure. After achieving complete saturations the specimens were subjected to all round confining pressures and allowed to consolidate completely. The axial load on the specimens were then increased until failure. During application of the axial load the pore water pressures were measured and both total and effective strength parameters were determined. The results are summarized on the stress versus strain curves and Mohr's failure envelopes of Figures III-50 through III-67. Both total and effective friction angles are given in Table III-9. The saturated samples exhibited no cohesive strength.

Increased compaction improved the shearing resistance of both partially saturated and fully saturated samples. For partially saturated samples the friction angle increased from 31.0 degrees at 80 percent relative compaction to 47.5 degrees at 100 percent relative compaction. Saturated samples tested under identical conditions showed an increase from 15.0 degrees at 80 percent relative compaction to 37.5 degrees at 100 percent relative compaction for the values of the total

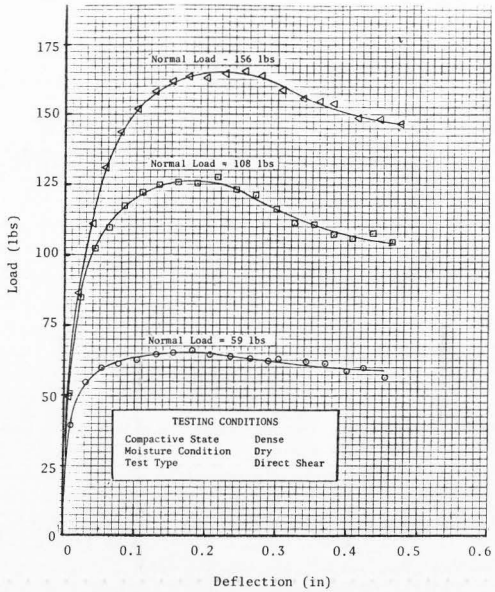

Figure III-42. Load versus deflection curves from direct shear tests on hard chert (1 lb = 4.45 N).

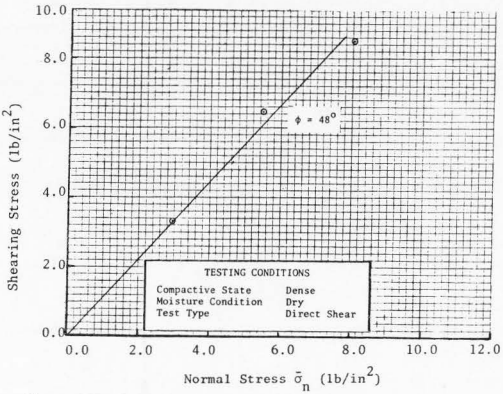

Figure III-43. Mohr's failure envelope from direct shear tests on hard chert (1 lb/in^2 = 6.9 kPa).

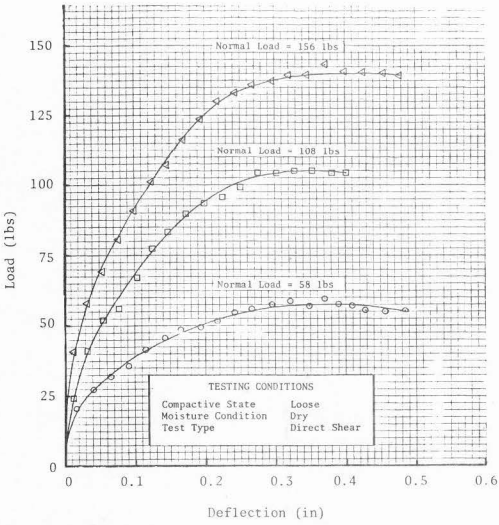

Figure III-44. Load versus deflection curves from direct shear tests on hard chert (1 lb = 4.45 N).

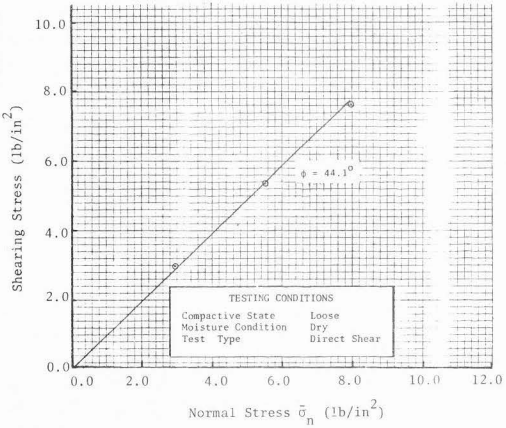

Figure III-45. Mohr's failure envelope from direct shear tests on hard chert (1 lb/in^2 = 6.9 kPa).

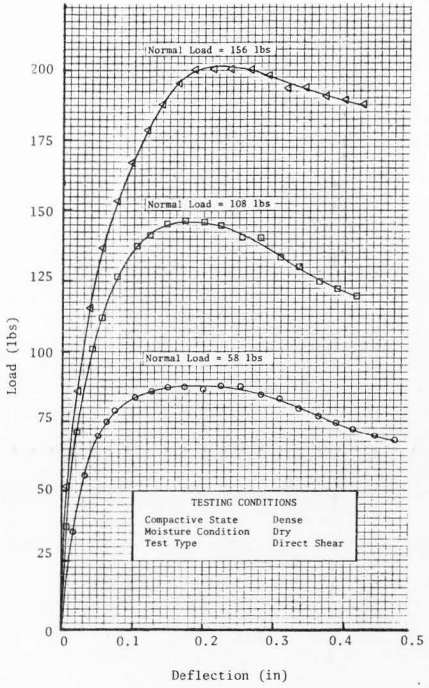

Figure III-46. Load versus deflection curves from direct shear tests on soft chert (1 lb = 4.45 N).

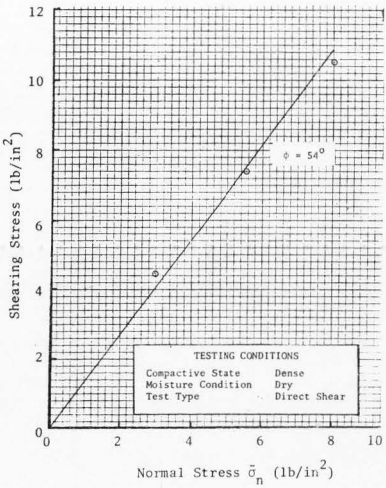

Figure III-47. Mohr's failure envelope from direct shear tests on soft chert (1 lb/in^2 = 6.9 kPa).

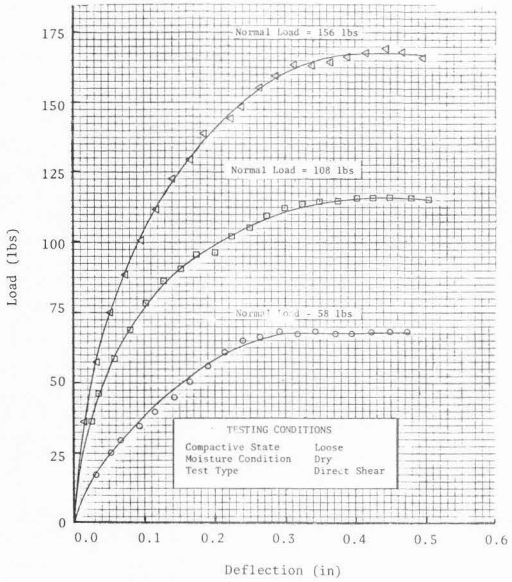

Figure III-48. Load versus deflection curves from direct shear tests on soft chert (1 lb = 4.45 N).

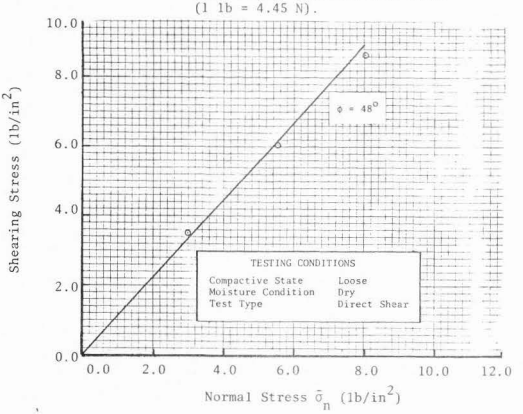

Figure III-49. Mohr's failure envelope from direct shear tests on soft chert (1 lb/in^2 = 6.9 kPa).

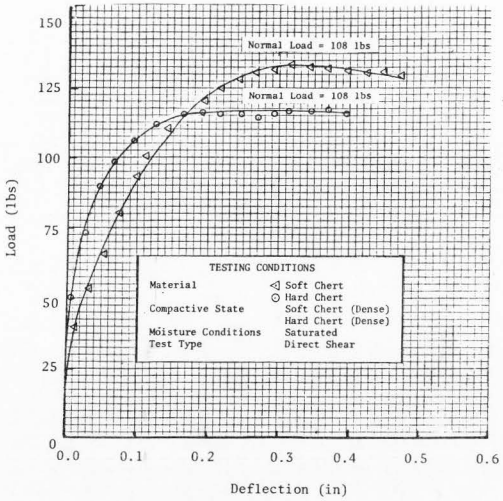

Figure III-50. Load versus deflection curves from direct shear tests on saturated samples of hard and soft cherts (1 lb = 4.45 N).

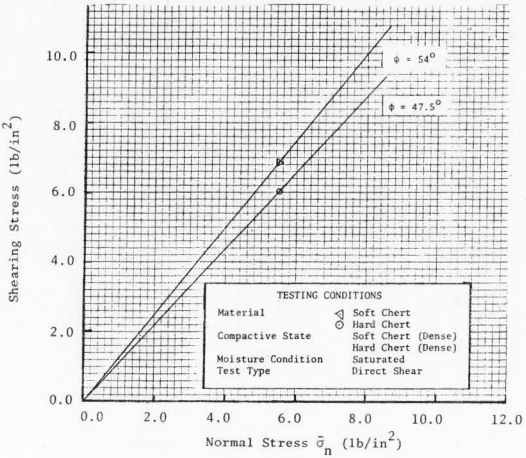

Figure III-51. Mohr's failure envelope from direct shear tests on saturated samples of hard and soft chert (1 lb/in^2 = 6.9 kPa).

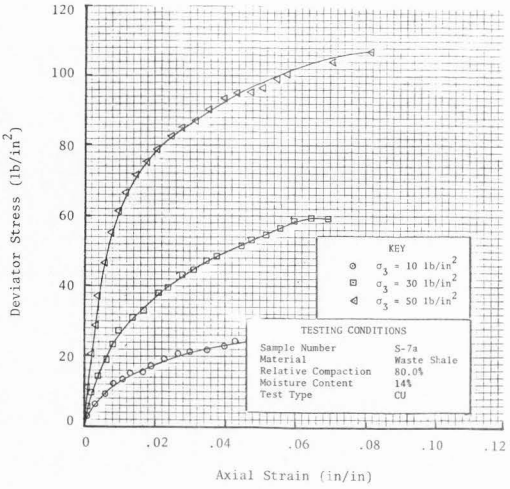

Figure III-52. Consolidated-undrained triaxial shear test stress-strain curves for partially saturated samples (1 lb/in^2 = 6.9 kPa).

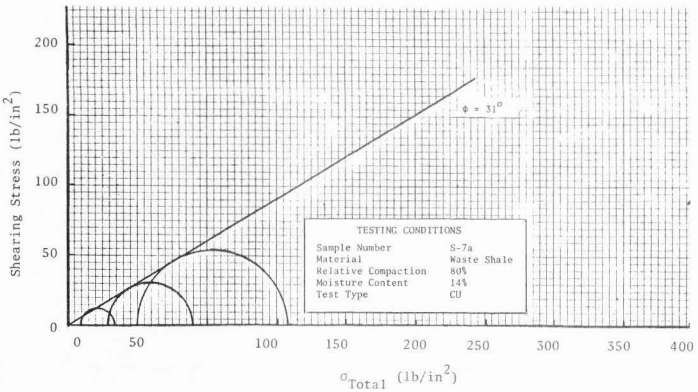

Figure III-53. Mohr's total stress failure envelope from consolidated-undrained triaxial shear tests on partially saturated samples (1 lb/in^2 = 6.9 kPa).

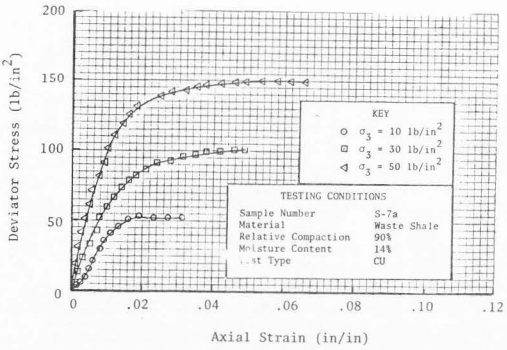

Figure III-54. Consolidated-undrained triaxial shear test stress-strain curves for partially saturated samples (1 lb/in^2 = 6.9 kPa).

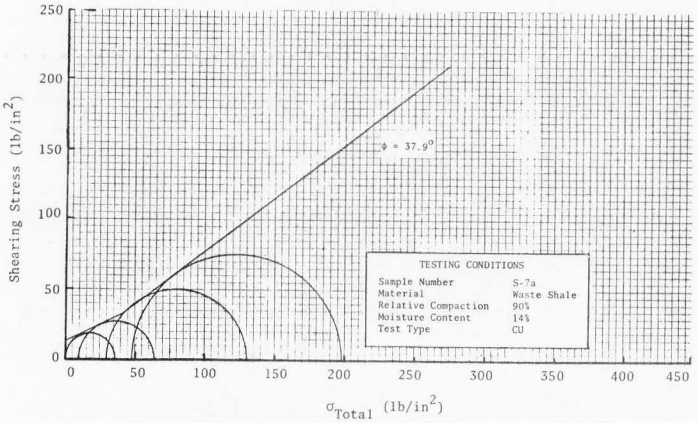

Figure III-55. Mohr's total stress failure envelope from consolidated-undrained triaxial shear tests on partially saturated samples (1 lb/in^2 = 6.9 kPa).

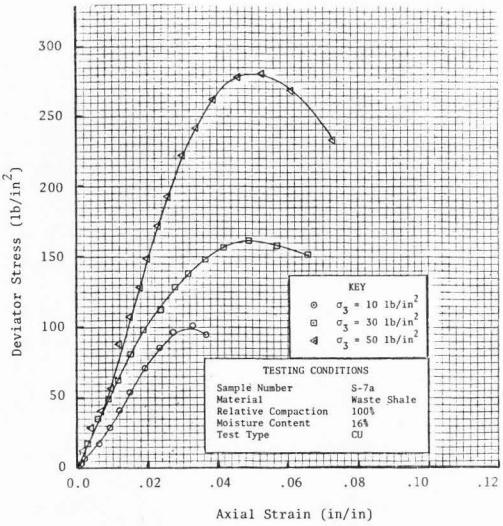

Figure III-56. Consolidated-undrained triaxial shear test stress-strain curves for partially saturated samples (1 lb/in^2 = 6.9 kPa).

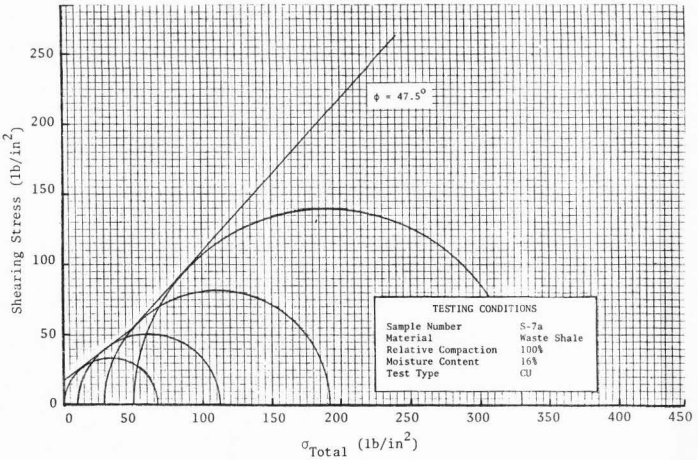

Figure III-57. Mohr's total stress failure envelope from consolidated-undrained triaxial shear tests on partially saturated samples (1 lb/in^2 = 6.9 kPa).

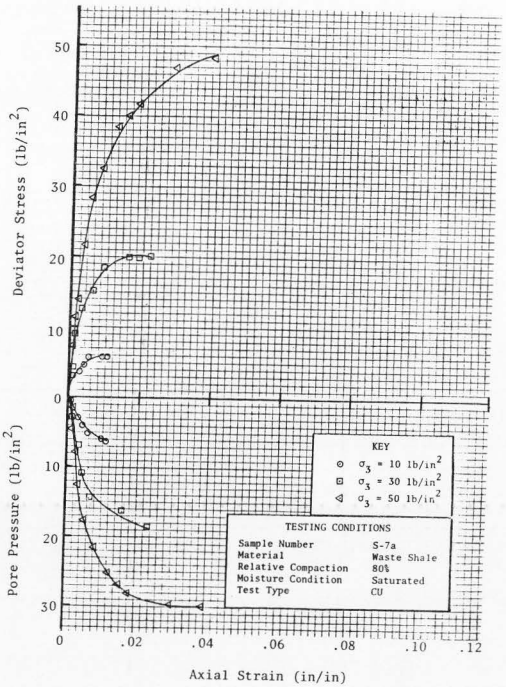

Figure III-58. Consolidated-undrained triaxial shear test stress-strain curves with pore pressure measurements (1 lb/in^2 = 6.9 kPa).

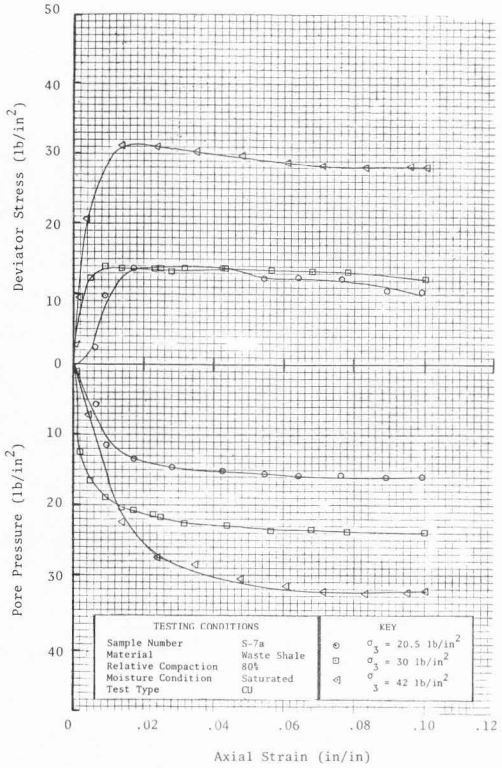

Figure III-59. Consolidated-undrained triaxial shear test stress-strain curves with pore pressure measurements (1 lb/in^2 = 6.9 kPa).

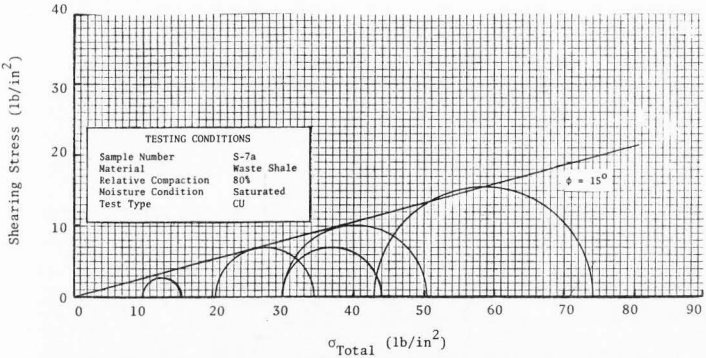

Figure III-60. Mohr's total stress failure envelope from consolidated-undrained triaxial shear tests with pore pressure measurements (1 lb/in^2 = 6.9 kPa).

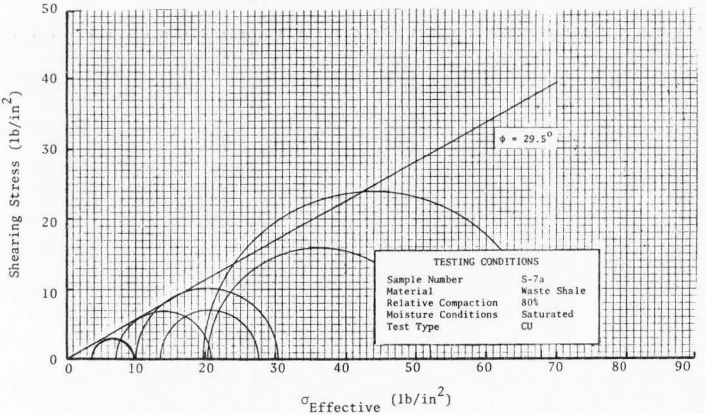

Figure III-61. Mohr's effective stress failure envelope from consolidated-undrained triaxial shear tests with pore pressure measurements (1 lb/in^2 = 6.9 kPa).

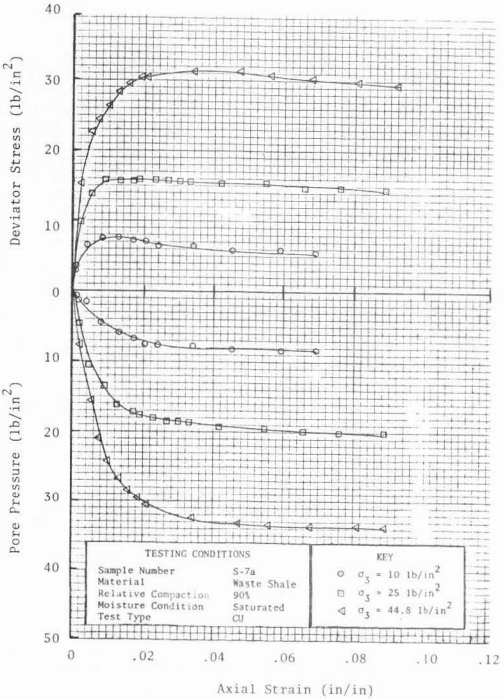

Figure III-62. Consolidated-undrained triaxial shear test stress-strain curves with pore pressure measurements (1 lb/in^2 = 6.9 kPa).

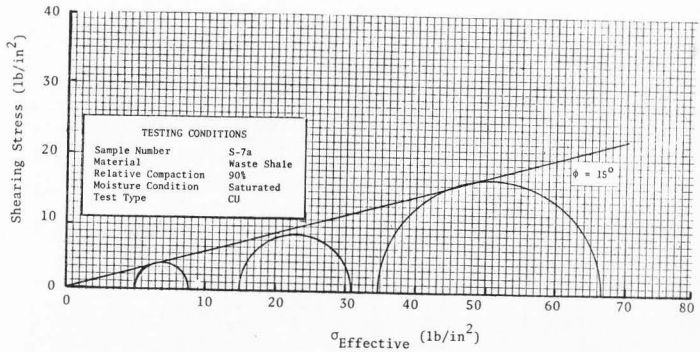

Figure III-63. Mohr's total stress failure envelope from consolidated-undrained triaxial shear tests with pore pressure measurements (1 lb/in^2 = 6.9 kPa).

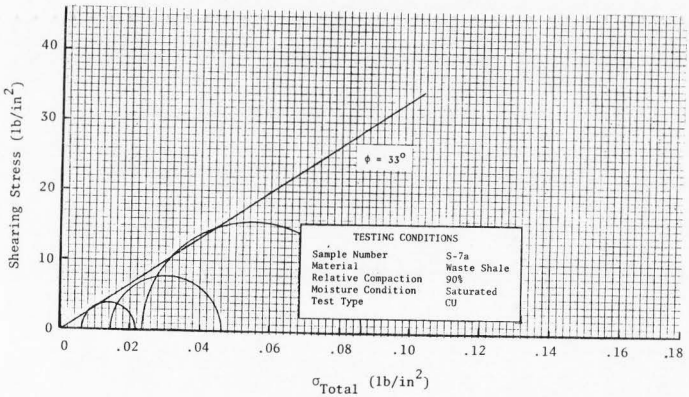

Figure III-64. Mohr's effective stress failure envelope from consolidated-undrained triaxial shear tests with pore pressure measurements (1 lb/in^2 = 6.9 kPa).

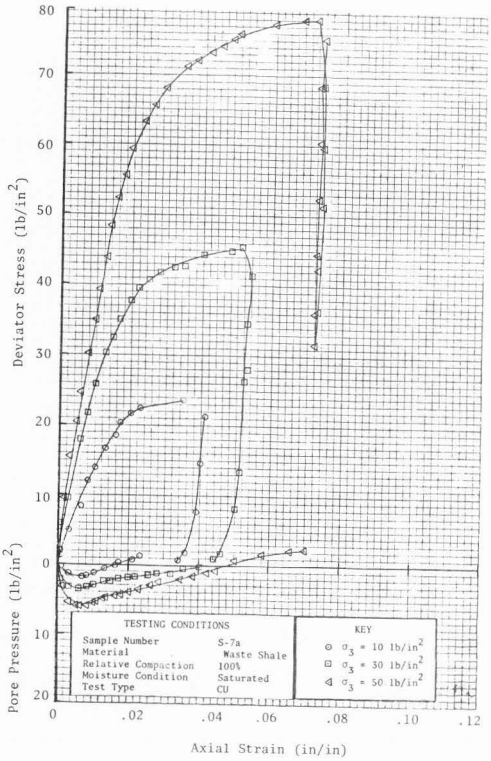

Figure III-65. Consolidated-undrained triaxial shear test stress-strain curves with pore pressure measurements also showing unloading curve (1 lb/in^2 = 6.9 kPa).

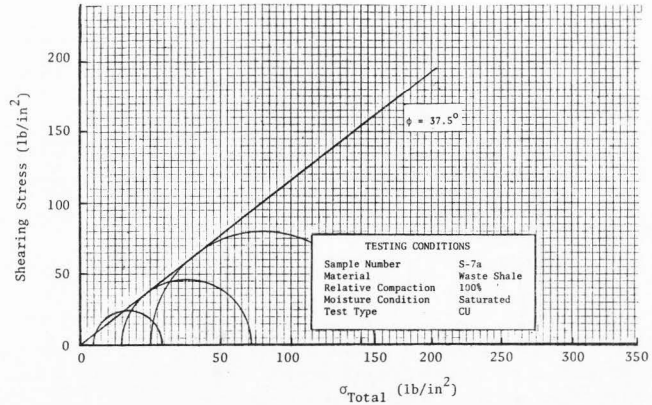

Figure III-66. Mohr's total stress failure envelope from consolidated-undrained triaxial shear tests with pore pressure measurements (1 lb/in^2 = 6.9 kPa).

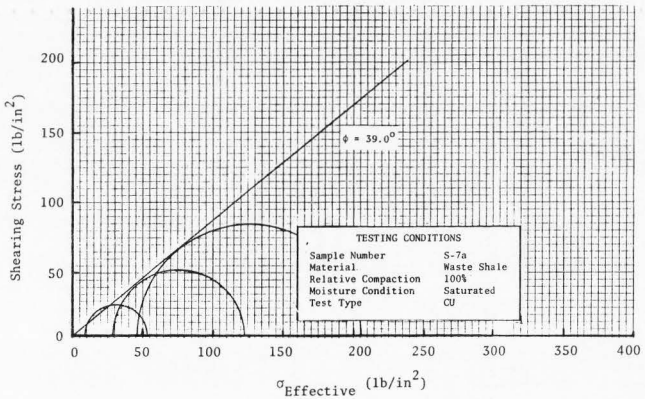

Figure III-67. Mohr's effective stress failure envelope from consolidated-undrained triaxial shear tests with pore pressure measurements (1 lb/in^2 - 6.9 kPa).

Table III-9. Friction angle versus compaction and moisture content for waste shale material.

Percent Relative Compaction	Percent Water Content	Total Friction Angle ϕ	Effective Friction Angle $\bar{\phi}$
80	14%	31.0^{o}	
90	14%	37.9^{o}	
100	14%	47.5^{o}	
80	Saturated	15.0^{o}	29.5^{o}
90	Saturated	15.0^{o}	33.0^{o}
100	Saturated	37.5^{o}	39.0^{o}

strength friction angles and the effective strength friction angles increase from 29.5 degrees to 39.0 degrees for the same specimens.

The waste shale material is very sensitive to changes in the moisture content. Table III-9 shows that both the total and effective angles of internal friction were less for saturated samples then partially saturated samples.

Nutrient tests

Nutrient contents from 15 samples of material from the Wooley Valley erosion study plots and two samples from the North Maybe Canyon Dump were determined by the Utah State University Soil Testing Laboratory. The results are given in Table III-10.

Table III-10. Summary of nutrient analysis.

Sample No.	% 72 mm	PH	Soluble Salts EC_e	P ppm	K ppm	T Texture	Lime[a]	Fe ppm	Zn ppm
S-1a	80.3	6.6	0.3	27	117	Loam	0	22.0	45.0
S-2a	92.3	7.4	0.4	25	100	Sandy Loam	+	21.4	33.0
S-3a	80.8	6.9	0.2	14	82	Sandy Loam	+	13.4	12.0
S-4a	81.0	7.7	0.3	35	78	Silt Loam	+	17.0	93.0
S-5a	69.7	7.6	0.4	37	70	Silt Loam	++	19.6	126.0
S-6a	68.6	7.5	0.3	26	64	Silt Loam	+	15.0	135.0
S-7a	65.6	7.3	0.3	21	60	Silt Loam	+	9.6	159.0
S-8a	75.6	7.7	0.4	22	70	Silt Loam	++	13.4	84.0
T-1a	70.5	6.8	0.4	49	112	Silt Loam	0	37.0	90.0
T-2a	74.1	6.7	0.3	91	190	Silt Loam	+	57.0	93.0
T-3a	69.4	6.6	0.3	104	245	Silt Loam	+	93.0	96.0
T-4a	67.5	7.4	0.4	34	117	Silt Loam	++	25.4	96.0
T-5a	83.5	7.5	0.4	47	140	Silt Loam	+	43.6	87.0
T-6a	78.7	6.5	0.8	72	160	Silt Loam	0	75.0	99.0
T-7a	73.1	6.8	0.7	60	140	Silt Loam	0	56.0	96.0
MC-1b	--	7.6	--	--	--	----	0	--	--
MC-2b	--	6.9	--	--	--	----	0	--	--

[a] 0 = none
+ = same
++ = high

CHAPTER IV

SLOPE STABILITY

Identification of Problem

Establishing a successful land rehabilitation scheme requires waste disposal areas to be free of landslide failures. The earthfill embankments containing the spoil material as well as the natural sloping surfaces upon which they are placed must be stable during construction and indefinitely thereafter. The stability of waste spoil embankments for dumps in the mountainous terrain of Southeastern Idaho is the topic of this chapter.

Analyzing embankment slopes and natural sloping surfaces is very complex due to the number of variable conditions which might occur in combination with one another. The parameters used in every slope stability investigation are site dependent; each dump location has unique characteristics which must be accounted for in the stability analysis. Predicting stability under the most adverse conditions likely to occur requires a knowledge of basic principles but also judgment.

It is the intent of this chapter to (1) develop useful relationships as aids in the construction of waste spoil embankments and to (2) illustrate that the foundation is an important component of the stability of the embankment. In order to accomplish these objectives stability analyses were conducted for a number of hypothetical conditions. While these examples are called hypothetical because they do not necessarily depict a given embankment in Southeastern Idaho they are intended to be representative of the spoil dumps existing in the phosphate mines. The angle of internal friction and other strength parameters are those determined from a number of field and laboratory tests conducted on samples of material taken from the spoil dumps. The slopes are also representative of those currently used for the overburden dumps.

As discussed in the Review of Literature chapter, numerous methods for analyzing slope stability exist. The Simplified Bishop method was used principally in this study. This method assumes that failure occurs along a circular failure surface. The failure mass is divided into a number of slices and the vertical side forces on each slice are assumed to cancel. Studies have confirmed the accuracy of this method (Morgenstern, 1965). Detailed discussions concerning the Simplified Bishop method are given by Jeppson, Hill and Israelsen (1974) and in most soil mechanics textbooks (Lambe and Whitman, 1969).

A computer program based on the Simplified Bishop method was used to perform the stability computations. This program, LEASE I, was developed at the M.I.T. Civil Engineering Systems Laboratory (Bailey and Christian, 1969). The program includes sufficient logic to search for the most critical failure surface. In addition to the LEASE I program a slope stability computer program developed by the Harza Engineering Company (Baker, 1967) was used to analyze non-circular failure surfaces. The program uses the Harza stacked polygon method. A wedge method of analysis, which considers the freebody of the failure mass as a whole, was also used.

General Foundation Considerations

Every stability analysis requires an assessment of the foundation conditions. Unless the foundation material is included in the stability investigation the overall stability of a spoil dump can not be evaluated. Waste spoil embankments which appear adequately safe against slope failures can fail when the foundation is not properly prepared or when the foundation material cannot adequately support the weight of the overlying spoil material. A recent example of the influence of the foundation on slope stability was the slope failure at the South Maybe Canyon Dump (1977). Although the failure occurred during construction and the results were not catastrophic it did require considerable modifications to the dump construction plans.

Field investigations

The data provided by a field investigation is required to properly design any significant disposal facility (D'Appolonia, undated). A field investigation can include both surface and subsurface investigations. In some cases a surface investigation will provide sufficient information to properly design the facility. The following two sections briefly discuss both surface and subsurface investigations.

Surface investigation. The extent of a surface investigation is site dependent and should be based on the complexity of the disposal facility and site conditions. Any available physical, geologic, and geophysical information about the site should be acquired prior to the field work. Sources of information include topographic maps, agricultural soil survey maps, aerial photographs,

and past site investigation. Walking over the proposed dumping site and observing the general geologic conditions, soil types, relative cover, spring discharge, topographic details, or any other information which may be useful in the slope stability analysis can be considered appropriate (D'Appolonia, undated). The study of surface features associated with a proposed dump site can reveal the existance of old landslides or creeping landslides which can present potential hazards. Surface cracks, bulging ground, and depressions are signs of ground movement. Typically, tension cracks are observed near the crown, or head, of a slide. These are generally accompanied by diagonal cracks (en echelon cracks) along the flanks and bulging near the toe (see Figure IV-1).

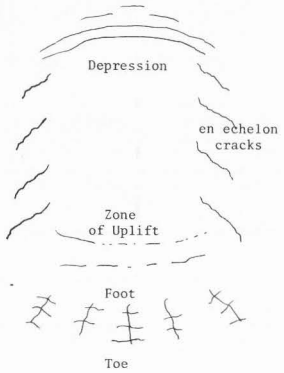

Figure IV-1. Crack patterns associated with ground movement in cohesive material (after Ritchie, 1958).

Geologic rock type and structure will also influence slope stability. The presence of discontinuities such as bedding planes, joints, and faults as well as the stratographic sequence should be noted when possible. Pore water pressures can develop in pervious beds bounded by relatively impervious soils resulting in a decrease in the shear strength. Natural slip planes can develop near bedding planes, faults and joints. The location of bedrock often serves as a lower limit through which failure of the residual soil mass might pass. The information provided by a surface investigation can be used to determine the necessity and extent of a subsurface investigation. The surface investigation is a vital component of the design and analysis of every disposal facility.

Subsurface investigation. Subsurface investigations are useful in determining the physical characteristics of foundation materials. Such investigations provide data about groundwater elevation, seepage conditions and the shear strength of the soil. All of this information is required to perform a slope stability analysis. Boreholes and backhoe test pits provide subsurface profiles and water surface elevations. Boreholes are generally expensive and therefore, these locations should be selected so that the maximum amount of information can be learned from minimal boring (D'Appolonia, undated). Test pits provide information over larger areas than boreholes and are generally less expensive. They also provide large amounts of soil to be observed in the field and also sampled for laboratory testing (D'Appolonia, undated). Sample retrieval and laboratory testing are used to determine the compaction characteristics, shear strength, compressibility and permeability of the soil.

A surface investigation conducted prior to the design of all spoil dumps would provide valuable design information and would likely prevent many foundation failures. Depending on the conditions observed in the field the necessity and extent of a required subsurface investigation can be determined. Performing a stability analysis requires data on the surface topography, surface conditions, groundwater information and soil strength. A field investigation can provide this data.

Weak foundations

Embankment failures can often extend into the material underlying a fill (Terzaghi and Peck, 1967). Such a failure occurs when the foundation material is unable to support the weight of the overlying fill material. A disposal dump may appear to be safe from failure through the embankment, however, slope stability cannot be guaranteed unless the foundation material can adequately support the weight of the spoil dump above. Embankments on weak foundation soils are especially susceptible to this type of failure If weak soils are encountered where a disposal facility is planned special care must be taken in designing the dump and in planning its placement operations.

The following hypothetical example problem is presented to illustrate that failure through the foundation can be critical.

Example:

A 300 ft. (91.5 m) high disposal dump is placed on a horizontal foundation with finish slopes of $2\frac{1}{2}$ horizontal to 1 vertical as shown on Figure IV-2.

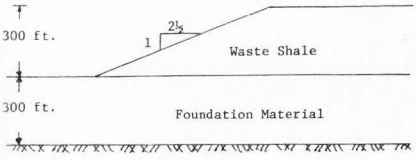

Figure IV-2. Cross-section of example problem illustrating the effect of weak foundation soils (1 ft = 0.305 m).

The stability of the dump was evaluated for the following foundation conditions: (1) the foundation material consists of a fairly stiff competent granular soil, and (2) the foundation material consists of a rather low strength clay soil. The strength properties of the dump material are ϕ = 35 degrees and c = 0.0 lb/ft^2. These values are representative of the dump material of the Southeastern Idaho phosphate mines. The strength properties of the foundation material for case one are identical to those of the fill material. The strength properties of the foundation for case two were ϕ = 0 degrees and c = 2500 lb/ft^2 (29.9 kPa) (typical of a stiff clay).

The results of this example are summarized in Table IV-1 along with the results from other example problems. The stability of the dump is adequate in case one. However, the foundation is inadequate for case two. The factor of safety for case two is 0.61.

Embankment failures caused by failure through the foundation generally occur during or immediately after construction because thereafter the foundation gradually gains strength as a result of consolidation. In a stability analysis it is common to represent the strength of the clay in terms of the undrained strength (ϕ = 0 condition). The ϕ = 0 conditions are satisfied when permeabilities are low and the water content of the soil does not change appreciably for a significant time after application of the load; such conditions can exist in saturated clays and silts. The ϕ = 0 concept implies nothing about the internal mechanism of shear but has considerable practical importance. The ϕ = 0 condition was used to describe the strength parameters of the foundation for case two. Some shear tests on the foundation material at the South Maybe dump indicated that the average undrained strength is approximately 2500 lb/ft^2 (29.9 kPa). Weak foundations may or may not exist at a given disposal site. The adequacy of the foundation can be determined by subsurface investigations.

Foundation preparation

Embankment foundation preparation is often necessary to minimize embankment slope failures. Proper preparation of the foundation becomes especially important when disposal sites are located in mountainous terrain.

Cutting and removal of trees, brush and other vegetative matter can generally be considered appropriate for most waste disposal sites. If not removed, the decay of such vegetative matter over a long period of time can result in a weak layer of thin soil. This thin soil layer can then provide a natural slip plane at a critical location. Placing very wet material at the bottom of a dump or placing spoil material on a foundation covered with snow can also result in a thin layer of weak soil through which failure might occur. The removal of snow and or extremely wet soils located at the embankment-foundation interface can generally be considered appropriate. Keying can provide additional protection against slope failure occurring at the embankment-foundation interface when foundation conditions are poor and/or when there is a heavy vegetative cover. Keying will be of little value if the keyways are backfilled with weak material. D'Appolonia (undated) recommends keying a hillside or an existing refuse embankment when coal waste is to be placed as structural fill. "This removes surface material which may not be at structural density, permits compaction at the construction interface and reduces the tendency for a natural slip plane to develop" (D'Appolonia, undated).

To illustrate the influence of weak foundation layers the following hypothetical example is presented:

Example:

> A dump approximately 300 ft (91.5 m) high is placed on a hillside as shown in Figure IV-3. Near the toe of the dump the hill slope is 4 horizontal to 1 vertical and near the upper portion of the fill the natural surface is bedrock which dips at about 40 degrees to the horizontal. The fill has finish grades of 2½ horizontal to 1 vertical.

The internal friction angle and cohesive strength of the dump material are Φ = 35 degrees and c = 0.0 lb/ft^2 respectively. These values reflect those of the spoil material for phosphate spoil dumps in the Southeastern Idaho area. The foundation material for this example was assigned

Table IV-1. Results of stability analysis for various hypothetical foundation conditions.

Example Problem Number	Foundation Conditions	Strength Parameters of Foundation		Safety Factor
		Friction (ϕ) degrees	Cohesion (c) lb/ft^2	
1.	Horizontal foundation competent granular soil	35^o	0	1.78
2.	Horizontal foundation weak soil	0^o	2500	0.61
3.	Sloping foundation competent soil prepared by clearing	20^o	2500	1.86
4.	Sloping foundation competent soil left covered with vegetative matter resulting in thin layer of peat	5^o	1000	0.86

NOTE: 1 lb/ft^2 = 0.0479 kPa

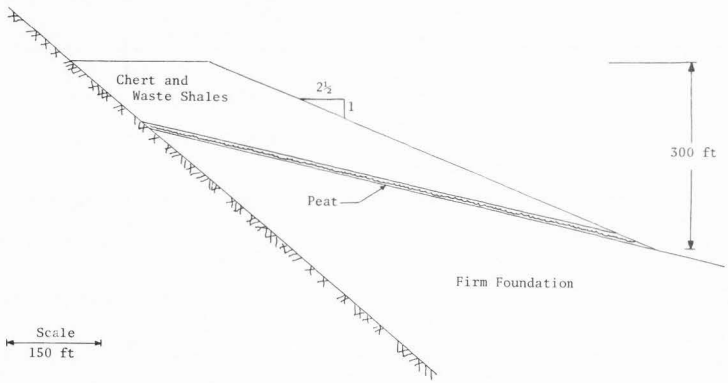

Figure IV-3. Cross-section of example problem (surface foundation preparation) (1 ft = 0.305 m).

strength values of ϕ = 20 degrees and c = 2500 lb/ft^2 (299 kPa). The results of a stability analysis using these strength parameters is given in Table IV-1 as example 3. The lowest factor of safety was found to be 1.86. Suppose, however, that prior to the placement of the disposal material the vegetative matter (trees, brush, roots, dead leaves) was not removed. Over an extended period of time this vegetative matter would begin to decay and eventually a thin layer of soft organic peat could develop. This layer of peat would create a weak plane at the dump-foundation interface through which failure could occur. The values of ϕ = 20 degrees and c = 2500 lb/ft^2 (29.2 kPa) would not longer represent the strength characteristics of the soil at the construction interface. Tests conducted on peat show that the angle of internal friction (ϕ) is generaly less than 5 degrees and that the cohesive strength can be as low as 200 lb/ft^2 (2.4 kPa), (Hanraham, 1954) and (Samson, 1972). For the purpose of illustration values of ϕ = 5 degrees and c = 1000 lb/ft^2 (12 kPa) were selected to represent the strength parameters of the thin layer located at the construction interface. These values could also be representative of a thin layer of extremely wet soil existing at this location resulting from either placement of such wet material or from neglecting to remove snow from the embankment-foundation interface.

A simple wedge stability analysis with failure assumed along the layer of weak organic material was performed to evaluate the long-term stability of this hypothetical dump. The results are summarized in Table IV-1 as example 4. The factor of safety was found to be equal to 0.86 indicating failure. It is clearly evident that for this case the ultimate result of inadequate foundation preparation would be instability of the dump.

Failure to clear disposal sites of vegetative matter before placing spoil dump material will not always lead to a failure condition because so much depends on the original topography as well as the final dump geometry. However, in mountainous terrain many disposal facilities will warrant clearing of the foundation to provide adequate safety against embankment failures.

Summary of foundation considerations

Much of the research concerning embankment stability in the past has been devoted to failures passing only through the embankments. Failures resulting from inadequate foundations, either deep failures through weak foundations or failures along the embankment-foundation interface have received little attention. The hypothetical examples in the previous sections illustrate the importance of foundation considerations. It is imperative to access the adequacy of the foundation conditions early in the planning stages of proposed waste disposal facilities.

Embankment Considerations

The stability of embankment slopes constructed from spoil material similar to that on phosphate mines in Southeastern Idaho were analyzed for a number of hypothetical conditions. Several factors which effect the stability of embankment slopes are subject to change. These changes include the moisture content of the spoil material, the density of the spoil material, and the elevation of a phreatic surface within the embankment. These conditions effect not only the shear strength but also the driving forces within the embankment. To provide meaningful information the embankments must be analyzed for conditions likely to occur both during and after construction and for unfavorable conditions which might possibly occur during periods of heavy rain and snow melt. The strength parameters used in the stability computations were determined from triaxial testing of representative samples of the overburden middle waste shales. The safety factors were determined by the Simplified Bishop slope stability method and compared with the infinite slope case.

Acceptable factors of safety

Theoretically an embankment will be safe against a slope failure for any condition with a factor of safety greater than one. However, because of uncertainties in the methods of analysis, in the reliability of strength parameters and in the prediction of pore pressures some acceptable margin of safety must be established. Recognizing the uncertainties involved in performing a slope stability analysis, the acceptable minimum factor of safety should reflect the consequences of failure.

The design of most earth dams in the United States is based on extensive field and laboratory testing. A minimum factor of safety of 1.5 is generally considered acceptable for the steady-state seepage condition (full reservoir) (U.S. Department of the Army, 1970; Sherard et al., 1963). The consequences of failure for an earth dam with a full reservoir can be catastrophic and, therefore, a high factor of safety (1.5) is justified. For the other critical conditions that must be considered in the design of an earth dam

a lower factor of safety can be considered acceptable. These other conditions include during and immediately after construction, and sudden draw down. Since the reservoir would not be full during these states a lower minimum factor of safety is considered acceptable. The U.S. Department of the Army (1970) recommends minimum factors of safety of 1.2 for sudden draw down from normal pool, 1.0 for sudden draw down from maximum pool and 1.3 for the end of construction state. However, for dams over 50 ft (15 m) high on weak foundations the minimum factor of safety for the end of construction state is recommended to be 1.4

The consequences of failure of a spoil dump would not be catastrophic in terms of lives lost or the cost of damage. Therefore, factors of safety lower than 1.5 should be considered adequate. The minimum acceptable factor of safety for a particular spoil dump should be based on the accuracy and completeness of knowledge about the spoil material, shear strength, pore pressure conditions and the driving forces within the embankment. In general, the minimum acceptable factor of safety for spoil dumps should probably be on the order of 1.15 for the during and end of construction condition and 1.3 for long-term stability. When many uncertainties exist and a number of assumptions are made regarding material strength and driving forces a higher factor of safety should be used. The minimum acceptable values should be established by the appropriate control agencies.

Short-term stability

During construction and immediately after construction the spoil material will generally contain no water table within the fill. Strength parameters for this case can be determined best from the results of a series of consolidated undrained triaxial shear tests on partially saturated samples prepared to represent the condition of the spoil material during placement in the dump. Field tests indicate that the spoil material is generally placed approximately two percent dry of optimum moisture content. The laboratory test specimens were observed to consolidate rapidly under its own weight during placement. Consolidated undrained strength parameters on partially saturated samples accurately represent the conditions during construction and shortly thereafter. The triaxial tests indicate that the angles of internal friction of typical waste shale material are 31 degrees, 37.9 degrees and 47.5 degrees for initial compaction to 80 percent, 90 percent, and 100 percent of the standard proctor maximum dry unit weight respectively. The shear strength parameters and partially saturated unit weights used in the stability analysis are summarized in Table IV-2. The waste shale material also exhibited cohesive strengths of 403 lb/ft^2 (19.3 kPa) and 1457 lb/ft^2 (69.8 kPa) at both 90 and 100 percent relative compactions respectively. This cohesive strength was probably due to negative pore pressures and could only be mobilized at depths less than about 50 ft (15.2 m). At depths greater than 50 ft (15.2 m) the waste shales should behave normally consolidated. Therefore, the existence this additional cohesive strength has been ignored during the short-term stability analysis. Relationships between slope angle, relative compaction and safety factor for the short-term case are presented in Figure IV-4. The embankment slopes considered were 2, 2½, and 3 horizontal to 1 vertical. The results of the stability analyses indicate that for the temporary condition of during construction embankment slopes of 2, 2½ and 3 horizontal to 1 vertical are all safe for dumps constructed using both the scraper filled method (relative compaction is approximately 85 percent) and the end-dump method (relative compaction is approximately 79 percent). The lowest safety factor would occur in middle waste shale embankments having slopes of 2 horizontal to 1 vertical constructed using the free flowing (end-dumped) method, however, this safety factor is adequate and approximately equal to 1.2

Long-term stability

The stability of waste shale embankments was analyzed for two possible long-term conditions. First, analyses were conducted on embankments which utilized the effective friction angles for saturated material. Laboratory tests showed that the waste shale material exhibited less frictional strength after saturation even when no pore pressures existed. For these analyses the unit weight of the bulk material also includes the weight of the water in the pores. Second, stability analyses were performed on saturated waste shale embankments having a phreatic surface in the fill near the top of the slope as shown on Figure IV-5.

Saturation of the fill material resulting from surface infiltration is not likely because of the low permeabilities of the waste shale material (see Chapter III). Saturation is possible, however, from a combination of the following: (1) placing the fill material at high moisture contents so that as it compresses under its own weight the degree of saturation increases, (2) placing the fill over an area where groundwater emerges to the surface, or (3) by burying large masses of snow near the slope of the fill where upon subsequent melting will transmit the ground water into the surrounding unsaturated material. When buried snow exists in chert materials the permeability is likely sufficiently large to prevent positive pore pressure. In the shale materials, however, the transfer of energy through the material to melt masses of snow can cause melt rates in excess of the rate at which the water is transferred from the melt area, thus, causing pore pressure.

Table IV-2. Summary of parameters used in short-term stability analysis of waste shale embankments.

Percent Relative Compaction	Void Ratio (e)	Porosity (η)	Typical Placement Total Unit Weight (lb/ft^3)	Unsaturated Moisture Content (percent)	Friction angles (ϕ)	Cohesion (c) (lb/ft^2)
80%	0.90	0.47	103	14.0	31^o	0
90%	0.69	0.41	116	14.0	37.9^o	0
100%	0.52	0.34	131*	16.0	47.5^o	0

*Sample prepared at optimum moisture content

NOTE: 1 lb/ft^3 = 0.157 $\frac{kN}{m^3}$

1 lb/ft^2 = 0.0479 kPa

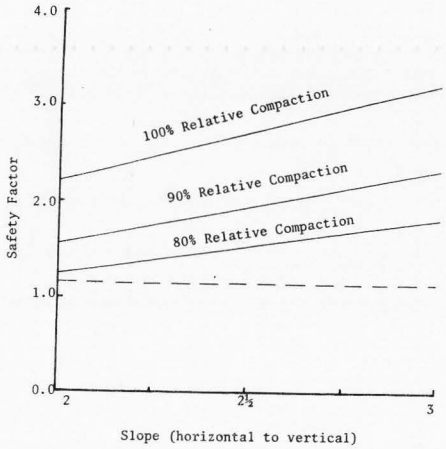

Figure IV-4. Slope angle, relative compaction, and safety factor relationships for waste shale embankments during and immediately after construction.

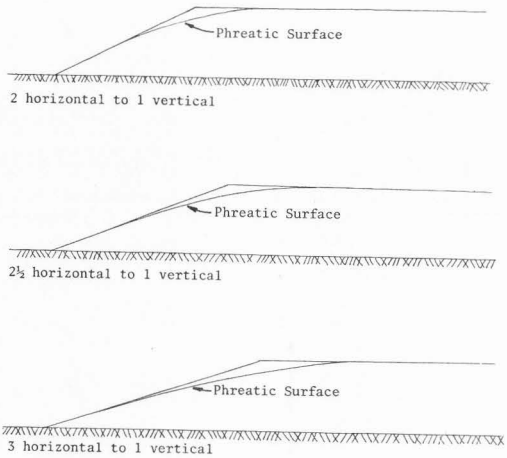

Figure IV-5. Location of phreatic surface used in stability analysis (long-term case 2) for various embankment slopes in waste shales.

Results for no phreatic surface. The shear strength parameters used in this analysis were determined from consolidated undrained triaxial shear tests with pore pressure measurements conducted on saturated samples. The saturated unit weights of the waste shales were also determined and used in the analysis. The unit weights and corresponding values of the effective angle of internal friction for relative compactions of 80, 90, and 100 percent of standard proctor are summarized in Table IV-3. The triaxial test results indicated that in a saturated state the waste shales behave as a cohesionless material.

Results from the stability analysis using the Simplified Bishop method showed that the critical failure surfaces are located at very shallow depths (see Figure IV-6) as would be expected for cohesionless material. Deep failures show higher values of factors of safety. For slopes of cohesionless materials a shallow failure could also be appropriately analyzed using the infinite slope method. For cohesionless material the factor of safety using the infinite slope method is determined from the expression:

$$FS = \frac{\tan i}{\tan \phi}$$

where,

FS = the factor of safety

i = the external slope of the embankment in degrees

ϕ = the friction angle of the material

The results from the infinite slope analyses showed safety factors nearly identical to those determined by the Simplified Bishop method. A shallow failure in a spoil dump would likely manifest itself in the form of sloughing along the surface of the embankment. This sloughing would have an undesirable effect on the erosional characteristics of the embankment and also retard rehabilitation. Even shallow failures, therefore, cannot be tolerated. The safety factors corresponding to these shallow failures represent the critical values to be used for this long-term condition. Since the critical surfaces are shallow and the factors of safety seem to increase with depth rather low factors of safety and justified because the consequences of failure are not great. The relationships between embankment slope angle, relative compaction and safety factors for this case are shown in Figure IV-7.

Table IV-3. Summary of parameters used in long-term stability analysis of waste shale embankments.

Percent Relative Compaction	Void Ratio (e)	Porosity (η)	Saturated Unit Weight lb/ft^3	Values of Internal Friction		Cohesion (c) lb/ft^2
				(ϕ)	($\bar{\phi}$)	
80%	0.90	0.47	120	15^o	29.5^o	0
90%	0.69	0.41	127	15^o	33^o	0
100%	0.52	0.34	134	37.5^o	39^o	0

NOTE: 1 lb/ft^3 = 0.157 $\frac{kN}{m^3}$

1 lb/ft^2 = 0.0479 kPa

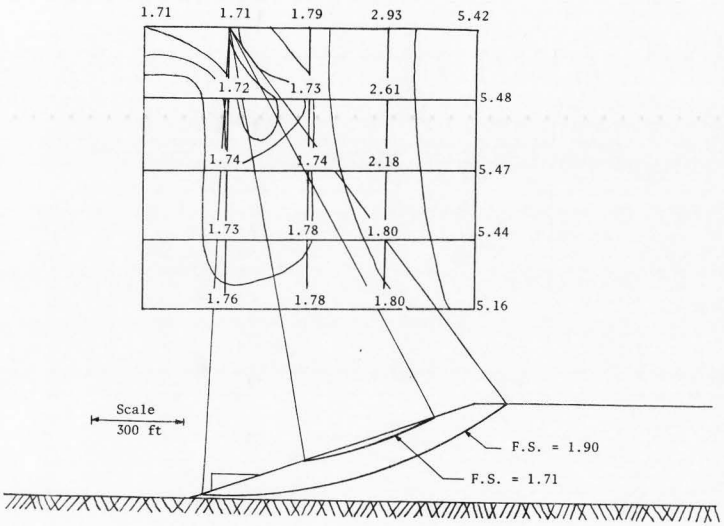

Figure IV-6. Contours of safety factors showing deep and shallow failures in waste shale embankments. (1 ft = 0.305 m)

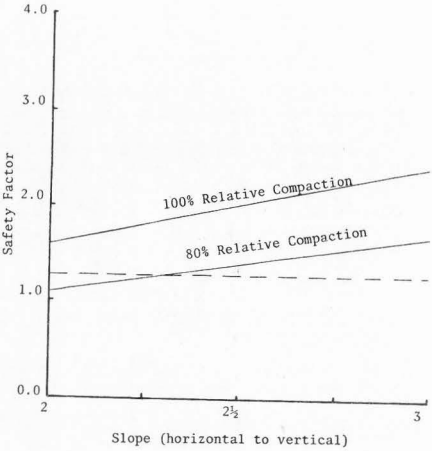

Figure IV-7. Slope angle, relative compaction and safety factor relationships for waste shale disposal facilities for long-term condition with no phreatic surface in the fill.

The stability of an embankment with a slope of 2 horizontal to 1 vertical compacted to 80 percent of standard proctor or less appears extremely marginal (FS $\leq$ 1.1). At 85 percent relative compaction slopes of 2 horizontal to 1 vertical would also be only marginally safe (FS $\leq$ 1.3). Embankment slopes of 2½ horizontal to 1 vertical and flatter appear adequately safe for relative compaction of 80 percent of standard proctor and greater (FS > 1.4). The free flowing (end-dump) method of construction results in middle waste shale compacted to approximately 79 percent of standard proctor. It is believed that waste shales compacted to this degree (79 percent) would also be adequately safe for slope angles of 2½ horizontal to 1 vertical and flatter (FS = 1.35). Middle waste shales in scraper filled dumps are typically compacted to approximately 85 percent of standard proctor and therefore, embankment slope angles of 2½ horizontal and 1 vertical and flatter will again provide adequate safety against slope failure (FS = 1.6). It is, therefore, recommended that for embankments containing only middle waste shale material, the final slopes should not be steeper than 2½ horizontal to 1 vertical when constructed using either the free flowing or the scraper filled methods.

In order to access the stability of embankments which are zoned a separate individual analysis would be required. The free flowing method of construction results in a naturally graded embankment which typically consists of large rock material at the lower elevations and finer-grained soils near the top of the fill. This in effect is a somewhat zoned embankment. In order to perform a meaningful stability analysis it can be considered appropriate to divide the dump into zoned layers with each layer having different strength parameters. For spoil dumps in Southeastern Idaho constructed by the free flowing method, the lower zones can contain principally large boulders while the upper layers consist primarily of middle waste shales. Although the densities are lower, as compared to a scraper-filled dump the material is naturally graded which places the coarser more permeabile and higher strength material in the lower portions of the embankment. The large, grained material near the bottom eliminates stability problems associated with excessive pore pressures and also enhances stability because of its greater strength qualities as compared to the fine-grained middle waste shales near the top of the dump. If the embankment slope guidelines discussed above are adhered to, then failures in these types of embankments are not likely to occur. The factors of safety will apply to the top parts of the dump containing middle waste shales.

When a free flowing (end-dumped) embankment is homogeneous and consists entirely of middle waste shale material then the relationships for embankment slopes, relative compaction and safety factors discussed previously apply.

Results for phreatic surface condition

Long-term stability of waste shale embankments was also analyzed for the case in which a phreatic surface within the fill existed. As was shown in Figure IV-5, the phreatic surface is located near the top of the embankment and emerges as a seepage face along the embankment slope at approximately one-third (1/3) the height of the embankment. A phreatic surface located within the disposal embankment such as the one just described is a condition which might occur during a period of extreme rain accompanied by massive snow melt within the fill.

Effective stress analyses were used to determine the safety factors for various embankment slopes and degrees of relative compaction. The effective strength parameters and saturated unit weights were determined as discussed for case one above and are summarized in Table IV-3. Relationships between embankment slopes, relative compaction, and safety factors for this hypothetical case are summarized on Figure IV-8. For embankments compacted to 80 percent of standard proctor or less and with slopes of 3 horizontal to 1 vertical and steeper the factors of safety against failure indicate these slopes are unstable (FS < 1.1).

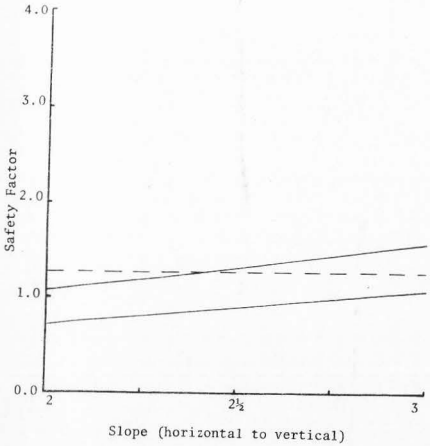

Figure IV-8. Slope angle, relative compaction, and safety factor relationships for waste shale disposal facilities for long-term severe condition with a phreatic surface near the surface of the embankment.

For embankments compacted to 90 percent of standard proctor only slope grades of 3 horizontal to 1 vertical or flatter are safe from failure (FS = 1.35). Embankments compacted to 100 percent of standard proctor are safe for slopes graded to 2½ horizontal to 1 vertical and flatter (FS $\geq$ 1.35). The free flowing method of construction results in relative compactions of only about 79 percent of standard proctor. Therefore, embankment slopes flatter than 3 horizontal to 1 vertical would be necessary to provide an adequate factor of safety for this extreme condition. This is also the case of scraper-filled embankments in which the degree of relative compaction is 85 percent of standard proctor.

Achieving the necessary compaction in spoil dumps constructed using either the free flowing method or scraper-filled method to provide adequate safety against slope failure when a phreatic surface exists near the top of the slope would require the use of a compaction device such as a sheeps foot roller. This may not be practical. It is, therefore, mandatory that large masses of snow be removed from the dump site prior to waste disposal. Also, proper drainage must be provided in areas where groundwater emerges to the surface or where cross-valley filling interrupts a natural drainage channel. When drainage is properly provided and snow masses are removed prior to waste disposal the relationships between embankment slope, relative compaction and safety factors discussed for long-term stability without a phreatic surface are adequate and should be used as guidelines for waste shale spoil dump construction.

The South Maybe Dump Landslide

The South Maybe Dump Landslide serves as an example of a foundation failure. This type of failure could be used as a large scale field test to develop strength properties of the foundation materials. The geometry of the original ground and the dump at the time of failure can be used to evaluate the slope stability for various strength parameters along the assumed failure surface. The strength parameters that yield a safety factor of one can then be used to predict the stability of other dump configurations. In order to carry out this type of stability analysis the following information is required:

1. Location of the failure arc
2. Geometry of the dump at the time of failure
3. Physical properties of the various dump materials
4. General stratifications of dump materials

A stability analysis of the South Maybe Dump failure was performed to attempt to evaluate the strength properties of the foundation soils. The results of this analysis were inconclusive, however, primarily because the location of the failure arc was unknown. A factor of safety of one (indicating a failure condition) could be obtained by using several different probable combinations of the failure arc location and values for the foundation strength parameters.

The location of the failure arc could have been determined by installing slope meters in the slide area. Location of the failure surface would have allowed a reasonable estimate of the foundation strength parameters to be made. These parameters could have then been used for analysis purposes to evaluate various alternative dump operation plans for stopping the slide movement.

CHAPTER V

POST CONSTRUCTION SETTLEMENT

Identification of the Problem

Post construction settlement in spoil dumps can result from (1) consolidation of the foundation and (2) compression of the middle waste shale and chert dump materials. In order to have a dump conform to specified geometry for a long period of time its ultimate settlement needs to be predicted. The final grade of a dump is generally crowned to accomodate long-term settlement. If the crown is not sufficient, there will be depressions in the dump surface and poor surface drainage. This could cause water to pond on the dump surface. Ponding introduces seepage into the fill material which may induce a mass stability failure of the dump. A lack of proper surface drainage can also lead to excessive embankment erosion which delays rehabilitation. Total rehabilitation can not be successful unless surface drainage is controlled. Predictions of post construction settlement are, therefore, needed to allow proper rehabilitation.

A first step in predicting post construction settlement requires an evaluation of the compression characteristics of the spoil dump materials. Stress strain relationships for both chert and waste shale materials were determined and are discussed in Chapter III. A technique to predict the magnitudes of post construction settlements is presented in this chapter. This technique is based on the compression characteristic of the chert and waste shale materials for both saturated and dry conditions.

Settlement in Spoil Dumps

Settlement in spoil dumps results from consolidation of the foundation and from compression of the waste shale and chert layers in the dump. Settlement of the foundation material is caused by the weight of the dump material. The magnitude and rate of foundation settlement can be determined using generally accepted soil mechanics principles, but it requires a description of the foundation soil profile and the compression properties of the foundation material. Settlement of the foundation material probably constitutes only a small portion of the total post construction settlement in spoil dumps.

Settlement of the spoil dump material is caused principally by (1) compression as a result of the added weight from continual placement of additional overburden and from (2) collapse settlement when the moisture content of the dump material is increased. The increase in moisture content may be the result of percolating surface water, natural springs, melting snow buried in the dump and/or flow from natural or artificial drainage channels.

Compression from added fill weight

The compression associated with the weight of the added fill probably results from particle movement and particle crushing. The rearrangement of particles seeking a more compact structure results in a decrease in the void ratio and consequently, compression of the waste shale and chert layers. Most of the settlement of layers within the spoil dump that is caused by the weight of the added fill occurs during the construction period. However, after completion of dump construction there will still be some settlement that will occur from the weight of the fill. This settlement will occur almost indefinitely at a gradually decreasing rate. This slow process is responsible for some of the post construction settlements in spoil dumps and will be referred to in subsequent discussions as creep settlement.

Saturation collapse settlement

As discussed in Chapter III the compression characteristics of waste shale materials and soft chert materials are highly sensitive to increases in moisture contents. Increases in the moisture content within a spoil dump embankment will undoubtedly cause additional settlements. The compression resulting from the flow of water through dry layers of soft chert and waste shales probably constitutes the major portion of post construction settlement occurring in spoil dumps. This type of settlement will be referred to as saturation collapse settlement. Complete saturation of a spoil dump is not likely to occur, however, the magnitude of settlement caused by saturation of laboratory samples might occur in the field over a long period of time due to particle weathering and the gradual reduction of capillary forces from increased moisture contents. In other words, the rate of saturation collapse settlement measured in the laboratory may not model the field conditions but the relative magnitude of saturation collapse settlement that was measured in the laboratory is probably indicative of the settlement that will eventually occur in the field from this process.

Predicting Post Construction Settlement

In order to evaluate the magnitude of post construction settlement a method was developed which predicts the amount of creep settlement which will occur over a given time period after the construction of the dump is complete and also the magnitude of saturation collapse settlement. The saturation collapse settlement will occur from increases in the moisture content of dry layers of soft chert and waste shales. The method was developed to give estimates of the magnitude of post construction settlements and can not be used to predict rates of settlement. A number of curves are used to evaluate various soil parameters which are required in the settlement computations. The curves were developed from laboratory strain versus log stress and strain versus log time relationships for waste shales and cherts. The method can be applied to both scraper filled and end-dump (free flowing) disposal facilities.

Creep settlement

The first step requires subdividing the dump into several vertical layers. The thickness of each layer should be approximately 25 ft (7.6 m) or less to provide accurate estimates of the average stress condition used to determine the α_c parameters used in the analysis. The α_c parameters represent the slopes of strain versus log time curves and are used to predict creep settlement. The value of α_c is related to the strain (ε_c) by the expression:

$$\varepsilon_c = \alpha_c \log \frac{t_2}{t_1}$$

where t_1 and t_2 are the initial and final times for the period over which the strain (ε_c) is desired. The value of α_c for each layer varies somewhat with depth because the pressure increases with depth. An average value of α_c should, therefore, be used for each layer and assumed constant throughout the layer. The value of α_c can be determined by computing the vertical pressure in the middle of each layer and choosing the appropriate value for α_c from Figures V-1 and V-2. These curves were developed from the results of the laboratory compression tests presented in Chapter III. The vertical pressure is the product of the unit weight of the overburden material and the depth to the middle of the layer from ground surface, or

$$\sigma_i = \gamma_t y_i$$

where,

σ_i = the stress in the middle of the layer i

γ_t = the total unit weight of the overburden material

y_i = the depth from ground surface to the middle of the layer i

If several different materials processing different unit weights lie above the layer considered then the stress in the middle of the layer is determined by summing the vertical pressure resulting from the various materials. The creep settlement for each layer can then be evaluated by determining the strain in each layer and multiplying the original height of the layer by the strain:

$$\Delta h_{ci} = \varepsilon_{ci} h_{oi}$$

The strain for each layer (ε_{ci}) can be obtained from the expression:

$$\varepsilon_{ci} = \alpha_{ci} \log t_2/t_1$$

As stated previously, the value of α_c corresponds to the vertical stress in the middle of the layer considered and can be evaluated from the curves in Figures V-1 and V-2.

The values of t_1 and t_2 must be referenced from a given starting time, t'_o. Each layer has its own value of t'_o which represents when placement of that layer began relative to the beginning of dump construction. The beginning of dump construction will be referred to as time zero or t_o. The value of t_1 is the end of construction time minus t'_o. The value of t_2 is expressed as t_1 plus the elapsed time from the end of construction to the date at which the post construction settlement is desired. For example, if the magnitude of post construction creep settlement is desired 15 years after the dump has been completed then the value of t_2 is equal to t_1 plus 15 years. The value of t_1 has little effect as t_2 becomes large. The suggested method for establishing the values of t_1 and t_2 is subject to some question. However, it appears to be a rational method for the construction periods typical of phosphate mines in Southeastern Idaho. The total amount of post construction creep settlement is determined by summing the individual settlements (Δh_{ci}) for all layers, or;

$$\Delta H_c = \sum_{i=1}^{n} \Delta\varepsilon_{ci} \times h_{oi}$$

Saturation collapse settlement

Saturation collapse settlement can be obtained from the stress versus saturation strain curves on Figures V-3 and V-4. These curves were developed from the results of laboratory compression tests. The saturation collapse strain represents the strain which occurs in a spoil dump due to saturation of the spoil material or due to constant weathering at particle contact points as a result of changes in the moisture content. To obtain the saturation collapse settlement the percent of saturation collapse strain must

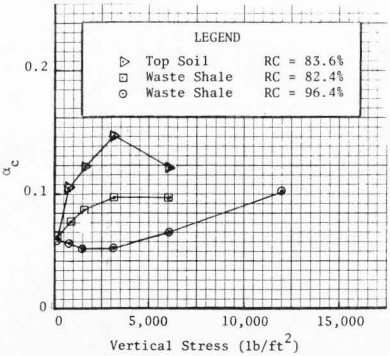

Figure V-1. Relationships between α_c and vertical stress for dry middle waste shale and top soil material (1 lb/ft^2 = .0479 kPa).

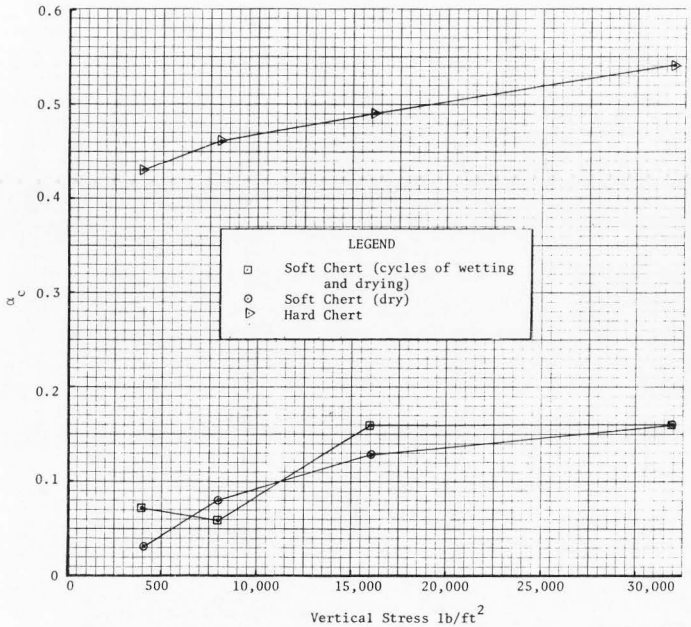

Figure V-2. Relationships between α_c and vertical stress for chert material (1 lb/ft^2 = .0479 kPa).

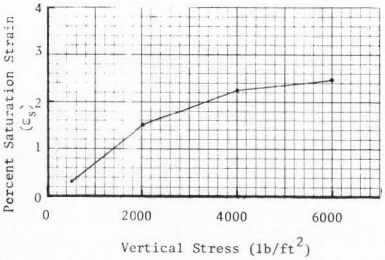

Figure V-3. Saturation collapse settlement versus vertical stress for middle waste shale material (1 lb/ft^2 = 0.0479 kPa).

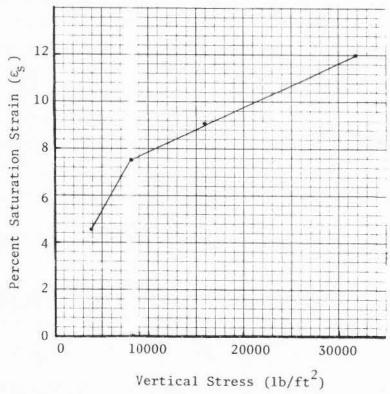

Figure V-4. Saturation collapse settlement versus vertical stress for soft chert material (1 lb/ft^2 = 0.0479 kPa).

first be determined for each layer. Collapse strain can easily be obtained by selecting the value of ε_s which corresponds to the vertical stress condition for the particular layer considered (see Figures V-3 and V-4). The percent saturation collapse strain for each particular layer is then multiplied by the original height of the corresponding layer; this yields the saturation collapse settlement for each layer. The total amount of saturation collapse settlement is then computed by summing the individual magnitudes of settlement for each layer. The total magnitude of post construction settlement is the sum of the creep and saturation settlements, or:

$$\Delta H = \Delta H_c + \Delta H_s$$

Example problem

The following example problem illustrates the technique developed for predicting the magnitudes of post construction settlement.

> The cross-section of a hypothetical proposed dump facility is shown in Figure V-5. The magnitude of post construction settlement is to be predicted at ten years and one hundred years after completion of the facility. The following dump construction sequence was assumed.
>
> The dump construction was completed three years after placement of the fill material began. The free flowing method of construction was used. The material was end-dumped over a 200 ft (61 m) high embankment across the valley floor. The completion of this portion of the embankment took approximately two years. A second portion was then placed on top of the 200 ft (61 m) section and extended an additional 85 ft (26 m) in elevation. This portion was completed approximately one year later. The types of spoil material and construction times are shown on the cross-section, Figure V-5 and on Table V-1. The upper 85 ft (26 m) portion includes 75 ft (23 m) of waste shale material and a 10 ft (3.1 m) layer of top soil at the surface.

First divide the entire cross-section into 25 ft (7.6 m) layers and then determine the stress at the middle of each layer (see Figure V-5 and Table V-1). The corresponding values of α_c for each layer can then be obtained from the curves on Figures V-1 and V-2. These values of α_c are listed in Table V-1. A value of t'_o can then be determined for each layer according to the estimated construction schedule. Layer number one will have a value of t'_o equal to zero. Since the

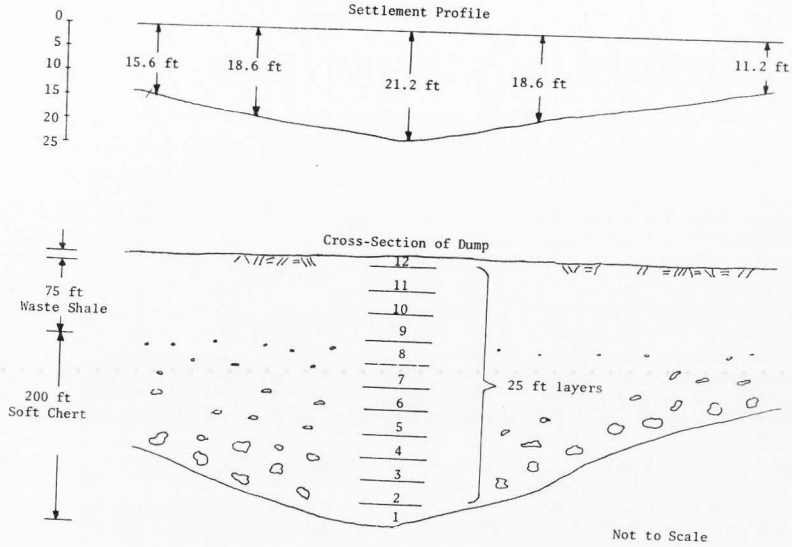

Figure V-5. Typical cross-section used as example problem also showing predicted settlement profile (1ft = 0.305 m).

Table V-1. Summary of example problem.

Layer Number	Material	Unit Wt lb/ft^3	Stress in the Middle of Layer lb/ft^2	α_c	t'_o yrs	t_1 yrs	t_2 yrs	% $\varepsilon_c = \alpha_c \log \frac{t_2}{t_1}$	Δh_{ci} ft	Δh_{si} ft
1	Chert	100	29375	0.16	0	3	13	0.10	0.02	2.68
2	Chert	100	26875	0.16	0	3	13	0.10	0.04	2.60
3	Chert	100	24375	0.16	0	3	13	0.10	0.02	2.55
4	Chert	100	21875	0.16	0	3	13	0.10	0.02	2.50
5	Chert	100	19375	0.16	0	3	13	0.10	0.02	2.45
6	Chert	100	16875	0.16	0	3	13	0.10	0.02	2.12
7	Chert	100	14375	0.14	0	3	13	0.09	0.02	2.12
8	Chert	100	11875	0.11	0	3	13	0.07	0.02	2.01
9	Waste Shale	125	9063	0.11	2	1	11	0.12	0.03	0.62
10	Waste Shale	125	5938	0.11	2	1	11	0.12	0.03	0.62
11	Waste Shale	125	2812	0.11	2	1	11	0.11	0.03	0.45
12	Top Soil	125	625	0.13	2	1	11	0.14	0.01	0.04
								TOTAL	0.28	20.76

NOTE: $1 \frac{lb}{ft^3} = 0.157 \frac{kN}{m^3}$

$1 \frac{lb}{ft^2} = 0.048$ kPa

1 ft = 0.305 m

free flowing or end-dump method of construction was proposed for this example the entire lower 200 ft (61 m) portion of the dump began at time zero relative to the beginning of dump construction and, therefore, layers one through eight all have a value of t'_o equal to zero. The values of t'_o for the layers in the upper 85 ft (26 m) portion all equal two because the construction of the entire upper portion all began two years after the beginning of the initial construction. The values of t_2 for each layer can next be determined by adding 10 years to the corresponding values of t_1 for each layer. The values of t_1 and t_2 for each layer are summarized in Table V-1. The percent creep strain for each layer can now be determined from the expression:

$$\varepsilon_c = \alpha_c \log \frac{t_2}{t_1}$$

These values are also summarized in Table V-1. The settlement in feet is calculated for each layer and summed to give the total magnitude of post construction creep settlement. For this example the creep settlement is approximately 0.3 ft (0.09 m) for 10 years after construction and 0.7 ft (0.21 m) for 100 years after construction.

The magnitude of saturation collapse settlement must now be determined for the lower 200 ft (61 m) layer of soft chert and upper 85 ft (26 m) of waste shales. The percent saturation collapse strain for each layer can be obtained from the curves on Figure V-3 and V-4. The vertical stress in layer one is equal to 29,375 lb/ft^2 (1407 kPa). The corresponding value of percent vertical strain is 11.5% from Figure V-4. This process is repeated for each layer. The saturation collapse settlement for each layer can then be calculated from the formula,

$$\Delta h_{si} = \varepsilon_{si} \times h_{oi}$$

The values for Δh_{si}, the saturation collapse settlements for each layer, are shown in Table V-1. The total saturation collapse settlement is then determined by summing the values of Δh_{si}. The magnitude of saturation collapse settlement for this example is 20.9 ft (6.4 m). Much of this settlement may occur before the ten year period and some may occur during the construction period depending on how moisture changes occur during and after construction and before the end of the ten year period. The total magnitude of post construction settlement is the sum of the creep settlement and saturation settlement and is equal to 21.2 ft (6.5 m).

Because of the cross-sectional geometry of the dump the largest magnitudes of settlement will occur near the center where the fill depth is greatest. Using the procedures discussed above a settlement profile was developed and is shown on Figure V-5. The settlement profile illustrates that depressions can occur near the center of the dump. The final grade of the dump could now be crowned to accommodate settlements and thus, eliminate these depressions. Proper rehabilitation could then be established.

Additional settlements may occur from compression of the foundation material. For example, if there is 50 ft (15.3 m) of a fairly stiff-clay material between bedrock and the original ground surface than a reasonable estimate of the foundation settlement would be about 1.6 ft (0.51 m). This settlement could be much greater for softer and/or deeper foundation soil deposits. Only a portion of this settlement would occur after construction of the dump was complete.

Summary of Post Construction Settlement

Post construction settlement is caused by creep settlement and saturation collapse settlement. Creep settlement contributes very little to the total magnitudes of post construction settlement. In the above example problem the creep settlement represented only about 1.4 percent of the total post construction settlement. For the accuracy required to properly crown a dump surface creep settlement can be neglected when the dump materials are similar to those sampled in the Southeastern Idaho mines. In some cases, foundation settlement may be significant. Predicting the magnitude of foundation settlement will require a knowledge of subsurface conditions. Settlement profiles can be developed for various dump cross-sections using the technique described in this chapter. The final dump configuration can be based on the estimated settlement profile. Although various alternatives for reducing settlement exist, such as sluicing the material during placement, they do not appear to be economically justified. Crowning the final dump grade is probably the most practical method for accommodating settlement.

CHAPTER VI

CONCLUSIONS AND RECOMMENDATIONS

The principal goals of this study were as follows:

1. Determination of the engineering properties of spoil materials from phosphate mines of Southeastern Idaho.

2. Development of relationships between safety factor of the dump fills against mass failure and their physical features such as relative compaction and embankment slopes. As a second goal regarding mass stability, the importance of the foundation and its effect on stability were studied.

3. Development of a method for estimating magnitudes of post construction settlement in spoil dumps.

The conclusions reached in this study are summarized below under three headings: (1) classification and engineering properties, (2) slope stability, and (3) post construction settlement. Specific recommendations are also summarized below.

Classification and Engineering Properties

The spoil materials were classified and the permeability, compressibility and shear strength properties were determined.

Spoil classification

Phosphate mining in Southeastern Idaho generates essentially two types of spoil material. These spoil materials are called middle waste shale and chert.

1. The middle waste shales are classified as silty-gravels according to the unified soils classification system.

2. The chert material varies in its engineering properties and can be grouped into two general categories. These categories are hard chert and soft chert. The soft chert is more appropriately classified as an organic siltstone.

Engineering properties

1. The physical or engineering properties of the spoil material are significantly effected by the methods of dump construction.

2. The free flowing method of construction results in a relatively uniform placement of the waste material; the average relative compaction is approximately 79 percent.

3. The scraper filled method of construction results in a range of relative compactions with an average relative compaction of approximately 85 percent.

4. The middle waste shale materials are relatively impervious with an average permeability equal to 32 ft/yr (3×10^{-5} cm/sec). Compaction reduces the permeability of the middle waste shales.

5. The chert materials are free draining. Field tests showed the permeability of the chert material in end-dump embankments is about 1.5×10^{5} ft/yr (38 m) above the valley floor. The permeability will increase near the bottom of the dump because of the much coarser materials at this location, probably 100 times the above value.

6. The compression characteristics of both middle waste shales and soft cherts are significantly effected by increases in the moisture contents. Laboratory tests show saturation causes immediate additional compression in both soft chert and middle waste shale. Compression strain from saturation of laboratory samples was a high as 2.5% for the middle waste shale and 12% for the soft chert.

7. Increases in pressure in dry chert samples and relatively dry samples of middle waste shales are accompanied by nearly instantaneous compressions followed by slow gradual compressions which are linear with the log of time. The same characteristics were noted for moist samples.

8. Soft chert exhibits friction angles of 48 degrees and 54 degrees for loose and dense states, respectively.

9. Hard chert exhibits friction angles of 44 degrees and 48 degrees for loose and dense states, respectively.

10. Partially saturated samples of typical middle waste shale materials exhibit friction angles of 31, 37.9, and 47.5 degrees for relative compactions of 80, 90, and 100 percent.

11. The partially saturated samples of middle waste shales exhibit cohesive strengths of 403 lb/ft^2 (19.3 kPa) and 1457 lb/ft^2 (69.8 kPa) at relative compactions of 90 and 100 percent, respectively. This strength was apparent at low pressures and is probably due to capillary pressures. For the purpose of stability analyses this cohesive strength can be ignored.

12. Saturated samples of typical middle waste shale materials exhibit total stress friction angles of 15, 15, and 37.5 degrees for relative compactions of 80, 90 and 100 percent.

13. Saturated samples of typical middle waste shale materials exhibit effective stress friction angles of 29.5, 33, and 39 degrees for relative compactions of 80, 90 and 100 percent.

14. The angles of internal friction of middle waste shale materials are increased by compaction and reduced by increases in moisture content. The friction angles of both hard and soft cherts are increased by compaction. Increases in the moisture content has little effect on the friction angles of hard and soft chert.

Slope Stability

Conclusions regarding the stability of phosphate mine spoil dumps in Southeastern Idaho are presented below:

1. For both scraper filled and end-dumped embankments, finished slopes of 2½ horizontal to 1 vertical or flatter will provide adequate protection against slope failure in waste shale embankments provided that proper cautions against the development of a phreatic surface near the top of the embankment are taken.

2. To prevent the development of a phreatic surface, large snow masses near the embankment slopes must be removed from the dumping area. Also, when a fill is to be placed across a natural drainage channel or over an area where groundwater emerges to the surface, the area should be properly designed to provide adequate flow. However, this will not be necessary if it is determined through proper analysis that the flow of water from such sources is not of sufficient quantity to create a phreatic surface near the top of the embankment.

3. Because of the natural gradation which occurs during end-dumping, free flowing embankments containing significant amounts of coarse material will exhibit greater shearing resistance in the lower portions of the embankment. This greater shearing resistance can be attributed to the higher frictional strength and free draining characteristics of the coarse material. Therefore, additional protection against slope failure is provided in the lower portions of such dumps.

4. Inadequate preparation of the embankment foundation interface and/or the existence of weak foundation soils can cause slope failures of spoil dumps. This was shown to be the case for two hypothetical example problems based on what might be real situations in the phosphate mines. For both of these examples the factor of safety against failure was less than 1.0.

5. Keyways can provide additional protection against slope failures occurring at the foundation embankment interface when poor conditions exist at this location. Keyways will be of little value if they are backfilled with weak material.

6. A surface reconnaissance should be conducted prior to the design of all new disposal facilities. The minimum requirements of such a reconnaissance should include observing and recording information concerning the general geologic conditions, topographic details, soil types, vegetative cover and location of natural springs and drainage channels. This information should be evaluated specifically with dump design in mind. The results of a surface reconnaissance will aid in determining the necessity and requirements of a subsurface investigation.

Post Construction Settlement

Conclusions regarding post construction settlement of spoil dumps in Southeastern Idaho are summarized as follows:

1. The results of laboratory testing showed that post construction settlement in spoil dumps can be attributed to two factors:

   a. Creep settlement as described in Chapter V.

   b. Collapse of the soil and/or rock structure of middle waste shale and soft chert layers upon increases in moisture content.

2. The amount of post construction settlement caused by increases in moisture contents in layers of soft chert is typically 100 times greater than the amount of post construction settlement caused by creep settlement and 10 times greater in layers of middle waste shale.

3. The magnitude of saturation collapse settlement caused by increasing the moisture content in layers of middle waste shale and soft chert can be estimated from the strain versus log stress relationships presented in Chapter III. For example, for a fill height of 100 ft, the magnitude of saturation collapse settlement for waste shale material is about 2.5 ft (0.8 m) and for soft cherts is about 8 ft (2.5 m).

4. The rate of creep settlement is linear with the log of time and the magnitudes of such settlements can be reasonably estimated from laboratory strain log time relationships. However, the amount of settlement caused by creep is very small compared to saturation collapse settlement and it can generally be neglected.

5. A rationale method of predicting post construction settlement is presented in Chapter V. Settlement profiles can be determined using this method. These profiles can be used to design crowns at the finished surfaces of spoil dumps.

6. Because of the construction methods currently used in Southeastern Idaho, the use of a crown to accommodate post construction settlement appears to be the most economical alternative.

LITERATURE CITED

Bailey, W.A., and J.T. Christian. 1969. ICES LEASE-I -- A problem-oriented language for slope stability analysis-user's manual. Soil Mechanics Publication No. 235. Department of Civil Engineering, Massachusetts Institute of Technology, Cambridge, Mass. April.

Baker, L.E. 1967. Harza stability analysis computer program: HASTAN. Harza Engineering Company, Chicago, Ill. February.

bishop, A.W. and L. Bjerrum. 1960. The relevance of the triaxial test to the solution of stability problems. Presented at the June, ASCE Research Conference on Shear Strength of Cohesive Soils held at Boulder, Col.

Butner, D.W. 1949. Phosphate rock mining in Southeastern Idaho. Bureau of Mines Circular 7529, United States Department of the Interior.

Cowherd, D.C. 1977. Geotechnical characteristics of coal mine waste. Presented at the ASCE Speciality Conference held at Ann Arbor, Mich. June.

D'Appoionia, E., et al. (Undated). Engineering and design manual coal refuse disposal facilities. U.S. Department of the Interior Mining Enforcement and Safety Administration.

Doyle, F.J., et al. 1975. Investigation of mining related pollution reduction activities and economic incentives in the Monoangahelo River Basin. ARC-72-89/ RPC-707, Appalachian Regional Commission, Washington, D.C. April.

Dunn, I.S., L.R. Anderson and F.W. Kiefer. 1976. Fundamentals of geotechnical analysis. Utah State University, Logan, Utah.

Gibbs, H.J., et al. 1960. Shear strength of cohesive soils. Presented at the ASCE Research Conference on Shear Strength of Cohesive Soils held at Boulder, Col. June.

Hanrahan, E.T. 1954. An investigation of some of the physical properties of peat. Geotechnique, Vol. 4. pp. 108-123.

Hilf, J.W. 1973. Construction of embankments. Design of Small Dams, 2nd Edition. United States Department of the Interior, Bureau of Reclamation, Washington, D.C. pp. 619-644.

Hilf, J.W. 1975. Compacted fill. Foundation Engineering Handbook. H.F. Winterkorn and H.Y Fang, Editors. Van Nostrand Reinhold Company, New York, N.Y. pp. 244-311.

Huang, Y.H. 1977. Stability of mine spoil banks and hollow fills. Presented at the ASCE Speciality Conference held at Ann Arbor, Mich. June.

Jeppson, R.W., R.W. Hill and C.E. Israelsen. 1974. Slope stability of overburden spoil dumps from surface phosphate mines in Southeastern Idaho. Special Publication PRWG 140-1, Utah Water Research Laboratory, Utah State University, Logan, Utah. April.

Lambe, T.W. 1958. The engineering behavior of compacted clays. Journal of the Soil Mechanics and Foundation Division, Vol. 84, No. SM2. May. pp. 1655-1-1655-35.

Lambe, T.W. and R.V. Whitman. 1969. Soil mechanics. John Wiley and Sons, Inc. New York, N.Y.

Lee, K.L. and S.C. Haley. Strength of compacted clay at high pressure. Journal of the Soil Mechanics and Foundation Division, Vol. 94, No. SM6. November. pp. 1303.

Lee, K.L. and H.B. Seed. 1967. Drained strength characteristics of sands. Journal of the Soil Mechanics and Foundation Division, Vol. 93, No. SM6. November. pp. 117-141.

Marsal, R.J. 1973. Mechanical properties of rockfill. Embankment Dam Engineering Casagrande Volume. R.C. Hirchfeld and S.J. Poulos, Editors. John Wiley and Sons, Inc. New York, N.Y.

Mekelvey, V.E. 1959. The phosphoria, Park City, and Shedhorn Formations in the western phosphate fields. Geological Survey Professional Paper 313-4, U.S.G.S.

Mitchell, J.K. 1976. Fundaments of soil behavior. John Wiley and Sons, Inc., New York, N.Y.

Mitchell, J.K. 1977. Soil improvement methods and applications. University of California, Berkeley, Berkeley, California. January. pp. 5-24.

Morgensten, M.R. and V.E. Price. 1965. The analysis of the stability of general slip surfaces. Geotechnique, Vol. 15. pp. 79-93.

Ritchie, A.M. 1958. Recognition and identification of landslides. Special Report 29, National Research Council, Washington D.C. pp. 48-68.

Samson, L. and P.L. Rochelle. 1972. Design and performance of an ex-pressway constructed over peat by preloading. Canadian Geotechnical Journal, Vol. 9. pp. 447-466.

Sherard, J.L., et al. 1963. Earth and earth-rock dams. John Wiley and Sons, Inc., New York, N.Y.

Sowers, G.F., R.C. Williams and T.S. Wallace. 1965. Compressibility of broken rock and the settlement of rockfills. Presented at the Proceedings of the Sixth International Conference on Soil Mechanics and Foundation Engineering held at Montreal, Can. September.

Stefanko, R., R.V. Ramani and R.F. Michael. 1973. An analysis of strip mining methods and equipment. Interim Report 7. Coal Research Section College of Earth and Mineral Services, Pennsylvania State University, Pennsylvania, Pa. May.

Taylor, D.W. 1948. Fundamentals of soil mechanics. John Wiley and Sons, Inc., New York, N.Y.

Terzaghi, K. and R.B. Peck. Soil mechanics in engineering practice. 2nd Edition. John Wiley and Sons, Inc., New York, N.Y.

Unauthored. 1964. Procedures for testing soils. 4th Edition. ASTM, Philadelphia, Pa. December.

Unauthored. Caterpillar 657-B. Circular AE040520, Caterpillar Corporation, Salt Lake City, Utah. September.

Unauthored. 1976. Draft environmental impact statement. United States Department of the Interior, Vol. 1.

Unauthored. 1976. Draft environmental impact statement. United States Department of the Interior, Vol. 2.

Unauthored. 1977. Geotechnical practice for disposal of solid waste. ASCE Speciality Conference, Ann Arbor, Mich. June.

United States Army Corp of Engineers. 1953. Soil mechanics design settlement analysis. Manual EM-1110-2-1904, United States Army Corp of Engineers, Washington, D.C. January.

United States Army Corp of Engineers. 1970. Engineering and design stability of earth and rockfill dams. Manual EM-1110-2-1902, United States Army Corp of Engineers, Washington, D.C. April.

United States Department of the Interior, Bureau of Reclamation. 1960. Control of construction. Earth Manual, 1st Edition. Bureau of Reclamation, Washington, D.C. pp. 181-209.

United States Department of the Interior, Bureau of Reclamation. 1973. Design of small dams. 2nd Edition. Bureau of Reclamation, Washington, D.C.

United States Department of the Interior, Bureau of Reclamation. 1974. Soil as an engineering material. Report No. 17, Bureau of Reclamation, Washington, D.C.

Whitman, R.V. 1960. Shear strength of undisturbed cohesive soils. Presented at the ASCE Research Conference on Shear Strength of Cohesive Soils held at Boulder, Col. June.

Whitman, R.V. and W.A. Bailey. 1966. Use of computers for slope stability analysis. Stability and Performance of Slopes and Embankments. American Society of Civil Engineers, Berkeley, California.

Appendix A

STRAIN LOG TIME CURVES FOR CHERT AND WASTE SHALE MATERIAL

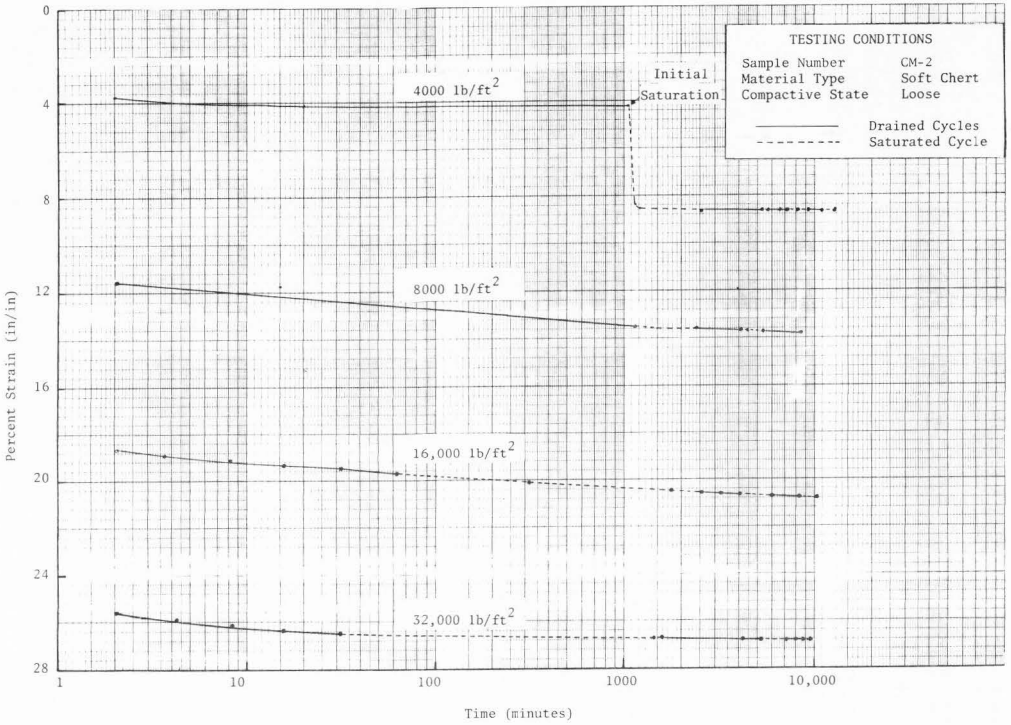

Figure A-1. Time-compression characteristics of soft chert subjected to cycles of wetting and drying. (1 lb/ft^2 = .0479 kPa).

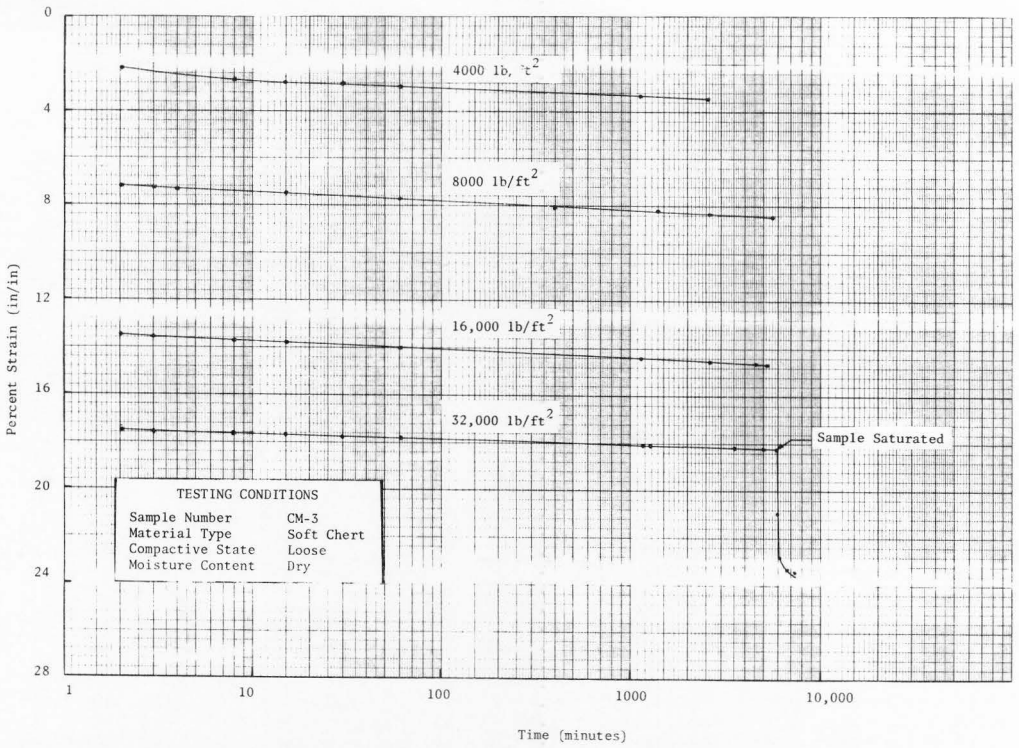

Figure A-2. Time-compression characteristics of soft chert showing effects of saturation after reaching a stress level of 32,000 lb/ft^2 (1 lb/ft^2 = .0479 kPa).

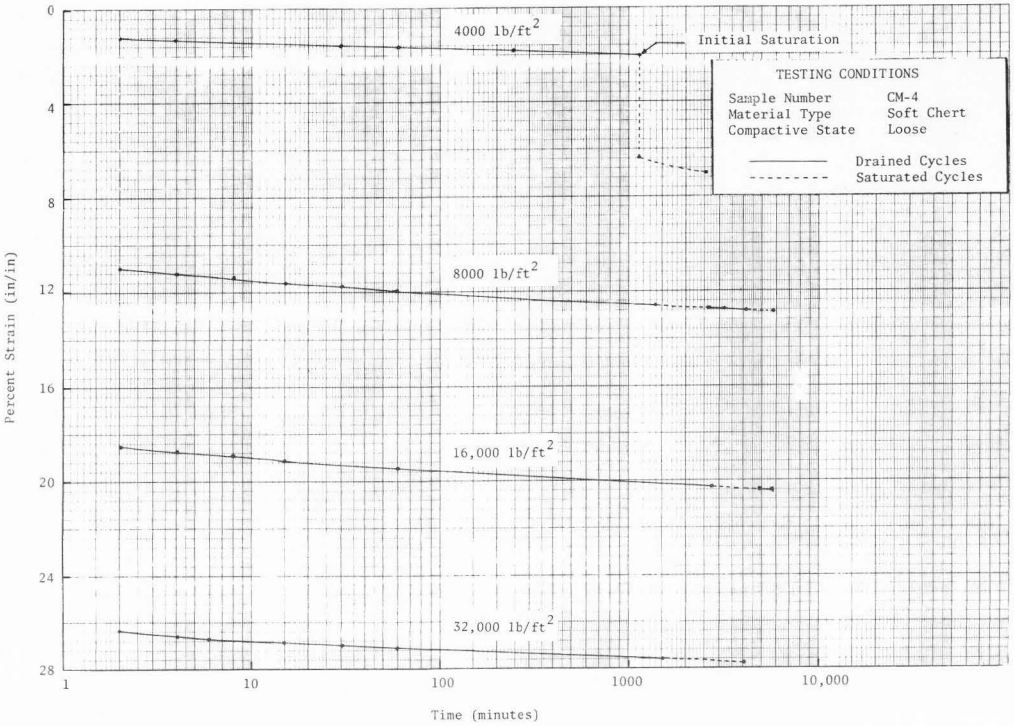

Figure A-3. Time-compression characteristics of soft chert subjected to cycles of wetting and drying (1 lb/ft^2 = .0479 kPa).

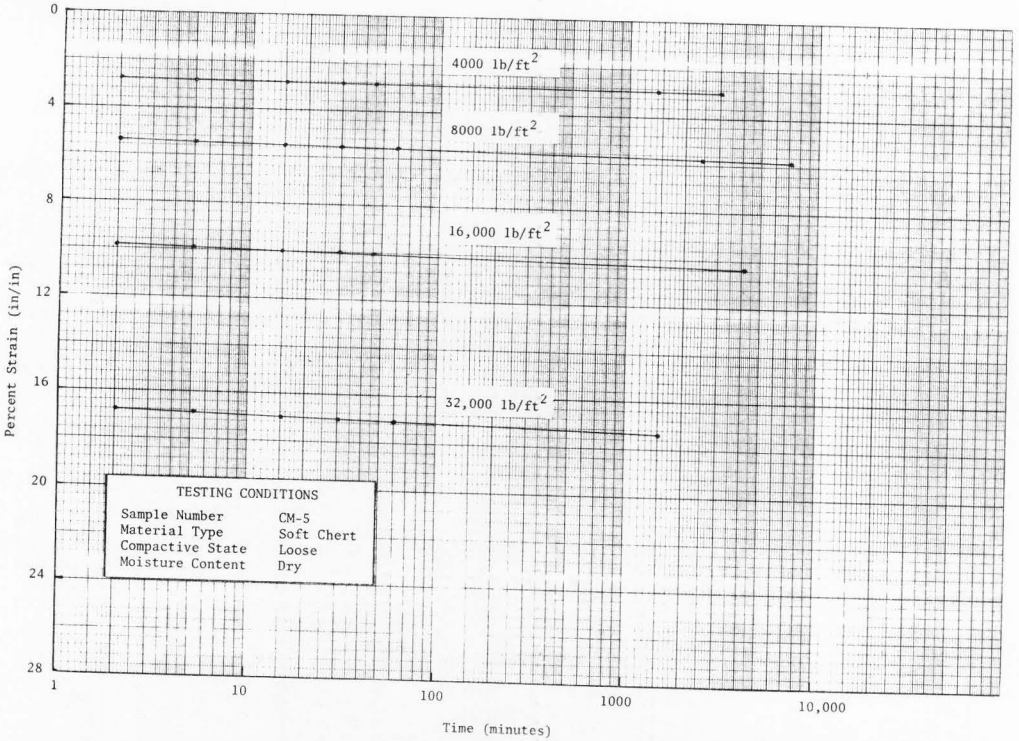

Figure A-4. Time-compression characteristics of soft chert (1 lb/ft^2 = .0479 kPa).

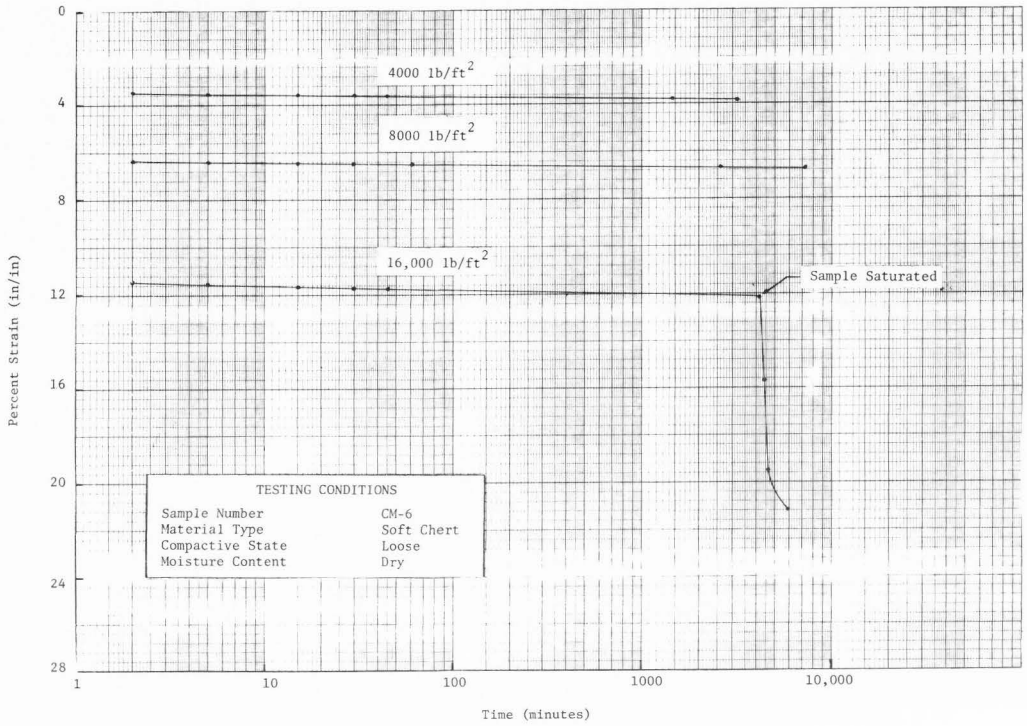

Figure A-5. Time-compression characteristics of soft chert showing effect of saturation after reaching of stress level of 16,000 lb/ft^2 (1 lb/ft^2 = .0479 kPa).

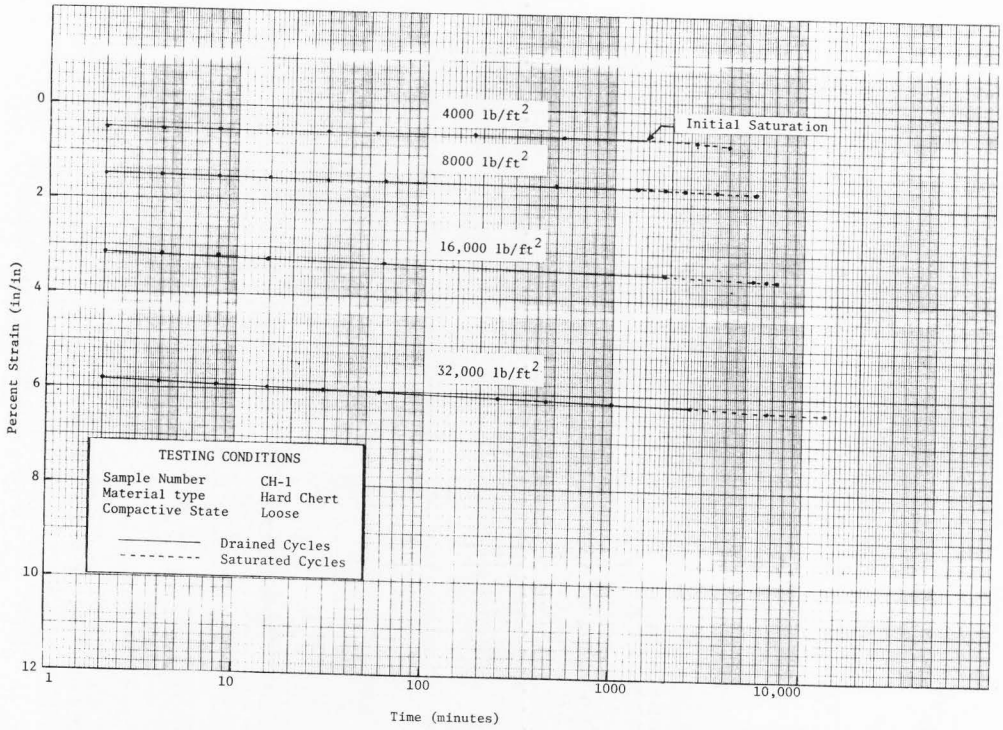

Figure A-6. Time-compression characteristics of hard chert subjected to cycles of wetting and drying (1 lb/ft^2 = .0479 kPa).

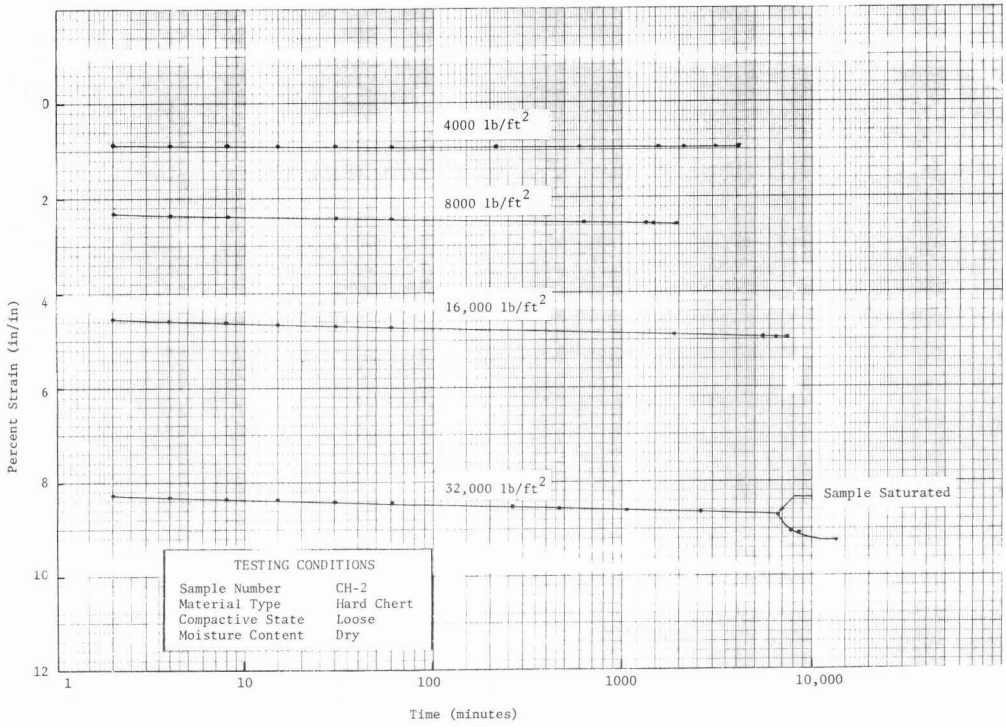

Figure A-7. Time-compression characteristics of hard chert showing effect of saturation after reaching a stress level of 32,000 lb/ft^2 (1 lb/ft^2 = .0479 kPa).

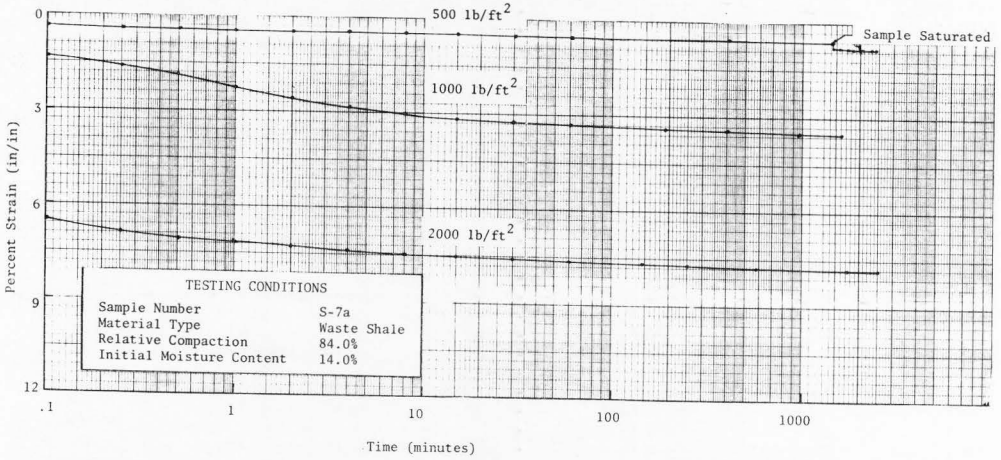

Figure A-8. Time-compression characteristics of waste shale material showing effect of saturation at a stress level of 500 lb/ft^2 (1 lb/ft^2 = .0479 kPa).

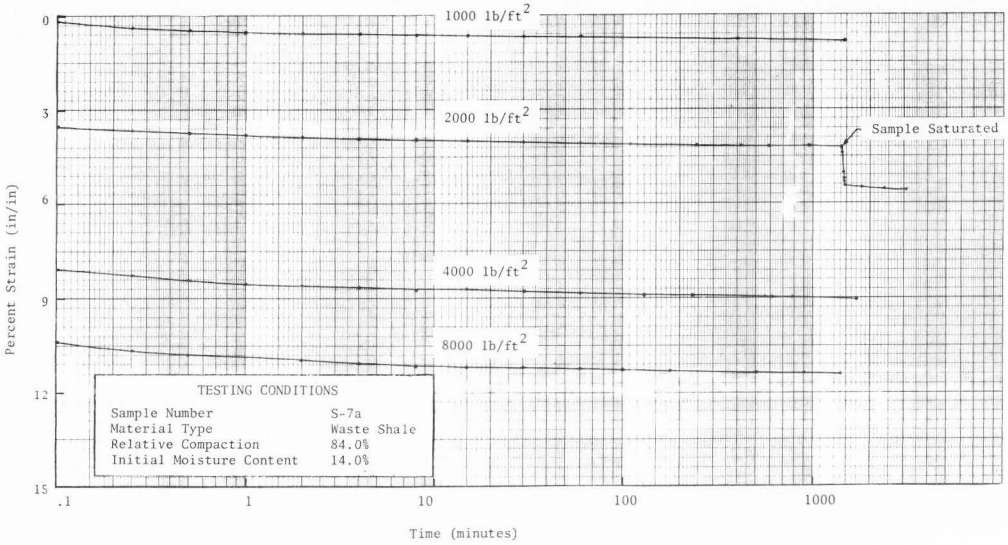

Figure A-9. Time-compression characteristics of waste shale showing effect of saturation at a stress level of 2000 lb/ft^2 (1 lb/ft^2 = .0479 kPa).

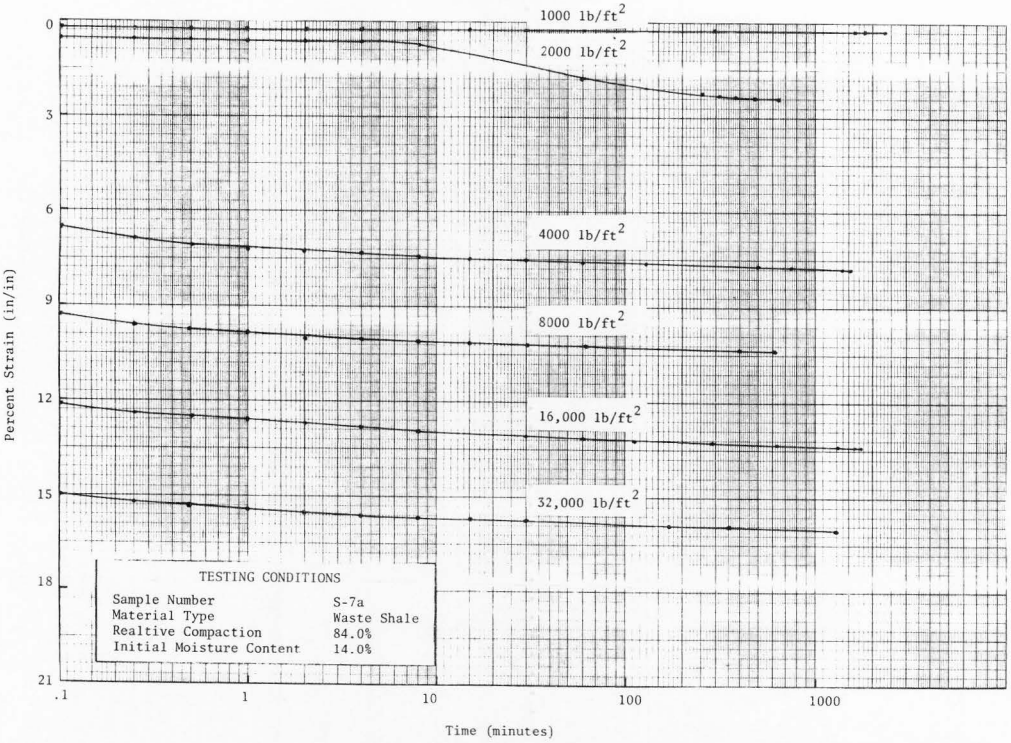

Figure A-10. Time-compression characteristics of waste shale showing effect of the addition of minor quantities of water at a stress level of 2000 lb/ft^2 (1 lb/ft^2 = .0479 kPa).

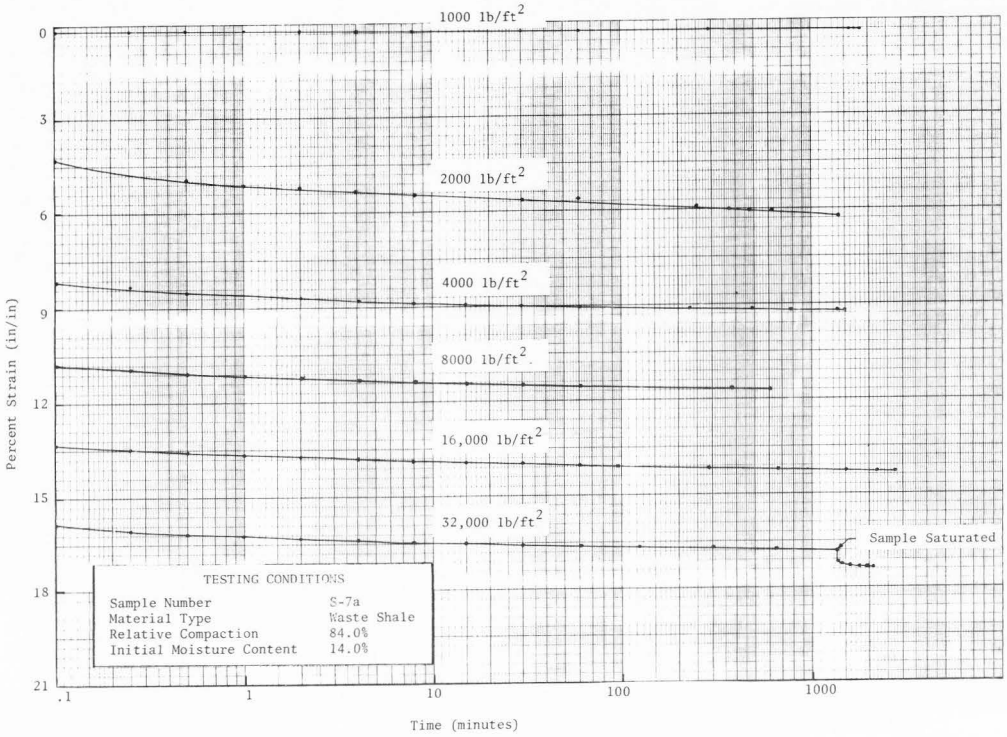

Figure A-11. Time-compression characteristics of waste shale showing the effect of the addition of minor quantaties of water at a stress level of 2000 lb/ft^2 (1 lb/ft^2 = .0479 kPa).